Functional characterisation of T329 phosphorylation in the tetramerisation domain of p53

Inaugural-Dissertation

zur Erlangung des Doktorgrades der Naturwissenschaften

- Dr. rer. nat. -

angefertigt am Biochemischen Institut

Fachbereich Medizin und dem Fachbereich Biologie und Chemie der Justus-Liebig-Universität Gießen

vorgelegt von

Maja Marilier Freiin Treusch von Buttlar-Brandenfels

Angefertigt:

September 2017 – Mai 2021

Vorgelegt:

Mai 2023

Dekan:	Prof. Dr. Thomas Wilke Tierökologie und spezielle Zoologie Fachbereich Biologie und Chemie Justus-Liebig-Universität Gießen
1. Gutachter	Prof. Dr. Michael U. Martin Professur für Molekulare Immunologie Fachbereich Biologie und Chemie Justus-Liebig-Universität Gießen
2. Gutachter	Prof. Dr. M. Lienhard Schmitz Biochemisches Institut Fachbereich Medizin Justus-Liebig-Universität Gießen

Eidesstattliche Erklärung

„Ich erkläre: Ich habe die vorgelegte Dissertation selbstständig und ohne unerlaubte fremde Hilfe und nur mit den Hilfen angefertigt, die ich in der Dissertation angegeben habe. Alle Textstellen, die wörtlich oder sinngemäß aus veröffentlichten Schriften entnommen sind, und alle Angaben, die auf mündlichen Auskünften beruhen, sind als solche kenntlich gemacht. Ich stimme einer evtl. Überprüfung meiner Dissertation durch eine Antiplagiat-Software zu. Bei den von mir durchgeführten und in der Dissertation erwähnten Untersuchungen habe ich die Grundsätze guter wissenschaftlicher Praxis, wie sie in der „Satzung der Justus-Liebig-Universität Gießen zur Sicherung guter wissenschaftlicher Praxis“ niedergelegt sind, eingehalten.“

Maja Marilier Freiin Treusch von Buttlar-Brandenfels

Bad Endbach, 02.05.2023

Table of content

ABBREVIATIONS

4NQO	4-nitrochinoline-1-oxide
53BP1	TP53-binding protein 1
6-4PP	pyrimidine photoproduct
ACN	acetonitrile
APC	allophyocyanin
APS	ammonium persulfate
ARF-BP1	E3 ubiquitin-protein ligase HUWE1
ASPP	ankyrin-repeat-SH-domain-and proline-rich-region-containing-protein
ATM	ataxia telangiectasia mutated
ATP	adenosine triphosphate
ATR	ataxia telangiectasia and Rad3 related
ATRIP	ATR-interacting protein
Bax	Bcl-2-associated X protein
BER	base excision repair
bp	base pairs
BSA	bovine serum albumin
C-abl	tyrosinekinase ABL1
cAMP	cyclic AMP
CBP	CREB binding protein
Cdc	cell division cycle protein
Cdc25	dual specificity phosphatase Cdc25
CDK	cyclin-dependent kinase
cDNA	complementary DNA
ChIP	chromatin immunoprecipitation
Chk1 & 2	checkpoint kinase
CK	casein kinase
Co-IP	co-immunoprecipitation
Cop-1	E3 ligases like Caspase recruitment domain-containing protein 16
CPDs	cyclobutane pyrimidine dimers
CPT	camptothecin
CREB	cAMP-responsive element-binding protein
CRISPR	clustered regularly interspaced short palindromic repeats

CSB	DNA excision repair protein ERCC-6
DAG	diacylglycerol
DBD	DNA binding domain
DDR	DNA damage response
DMSO	dimethyl sulfoxide
DNA	deoxyribonucleic acid
DNA-PK	DNA-dependent protein kinase
Dox	doxycycline
DREAM	multi-vulval class B complex
ds	double-stranded
DSB	double-strand breaks
DUSP26	dual specificity protein phosphatase 26
DYRK	dual-specificity tyrosine phosphorylation regulated kinases
E. coli	*Escherichia coli*
E2F	E2 factor
ECL	enhanced chemiluminescence
EHMT2	histone-lysine N-methyltransferase EHMT2
FACS	fluorescence-activated cell sorting
FAS	tumor necrosis factor receptor superfamily member 6
FDR	false discovery rate
G1 & G2 phase	gap 1 & gap 2 phase
Gadd45a	growth arrest and DNA damage protein
GFP	green fluorescent protein
GO	gene ontology
GOF	gain-of-function
HBx	hepatitis B virus protein
HDAC5	histone deacetylase 5
HIPK	homeodomain-interacting protein kinase
hMOF	histone acetyltransferase KAT8
HPV-16 E2	human papillomavirus type 16 E2 protein
HRP	horseradish peroxidase
Hzf	zinc finger protein 385A
iASPP	inhibitory ASPP
IgG	immunoglobolin G
kDa	kilo dalton
KEGG	Kyoto Encyclopedia of Genes and Genomes

Ku70	X-ray repair cross-complementing protein 6
Ku80	ATP-dependent DNA helicase 2 subunit KU80
LC3	microtubule-associated protein light chain 3
LMNB	lamin-B
LOF	loss-of-function
mAb	monoclonal antibody
MDC1	mediator of DNA damage checkpoint protein 1
MDM2	E3 ubiquitin-protein ligase Mdm2
MEF	mouse embryonic fibroblasts
MMR	mismatch repair
mRNA	messenger RNA
mTOR	serine/threonine-protein kinase mTOR
NBS1	DNA repair and telomere maintenance protein nbs1
NER	nucleotide excision repair
NHEJ	non-homologous end joining
NLS	nuclear localisation sequence
NLS	nuclear localisation signal
OD	optical density
POI	protein of interest
p21	cyclin-dependent kinase inhibitor
p300	acetlyetransferase p300
pAb	polyclonal antibody
PARP	Poly [ADP-ribose] polymerase 1
PBS	phosphate buffered saline
PCAF	histone acetyltransferase KAT2B
PCNA	Proliferating cell nuclear antigen
PCR	polymerase chain reaction
PI	propidium iodide
PIN1	peptidyl-prolyl cis-trans isomerase NIMA-interacting 1
Pirh-2	RING finger and CHY zinc finger domain-containing protein 1
PKC	protein kinase C
PMA	phorbol-12-myristat-13-acetat
PP1	protein phosphatase 1
PP1 & 2A	protein phosphatase 1 & 2A
PRMT5	protein arginine N-methyltransferase 5
PRR	proline-rich region

PTM	posttranslational modification
Pu	purine
PUMA	p53 upregulated modulator of apoptosis
Py	pyrimidine
qRT	quantitative real-time
RAD51	DNA repair protein RAD51 homolog 2
RAI	Rel-A associated inhibitor
RB	retinoblastoma protein
RelA	transcription factor p65
RNA	ribonucleic acid
RNAi	RNA interference
ROS	reactive oxygen species
RPL26	60S ribosomal protein L26
S phase	synthesis phase
SDS	sodium sodecyl sulfate
SDS-PAGE	SDS polyacrylamide gel electrophoresis
sg	single guide
SH3	SRC Homology 3
siRNA	small interfering RNA
SIRT1	NAD-dependent protein deacetylase sirtuin-1
Smyd2	N-lysine methyltransferase SMYD2
SSB	single-strand breaks
TAD	transactivation domain
TAF1	transcription initiation factor TFIID subunit 1
TBP	TATA-binding protein
TD	tetramerisation domain
Tip60	histone acetyltransferase KAT5
TNF	tumor necrosis factor
TP53INP1	tumor protein p53-inducible nuclear protein1
TRiC	T-complex protein ring complex
TSS	transcriptional start site
USP10	ubiquitin carboxyl-terminal hydrolase 10
USP2a	ubiquitin carboxyl-terminal hydrolase 2
USP42	ubiquitin carboxyl-terminal hydrolase 42
USP7 or HAUSP	ubiquitin carboxyl-terminal hydrolase 7
UV	ultraviolet

WT	wild type
XBP	X-box-binding protein 1
XPC	DNA repair protein complementing XP-C cells

1 INTRODUCTION

The gene *TP53* that encodes the p53 protein belongs to a gene family that also includes *TP63* and *TP73* [1–3]. These three proteins show structural as well as functional similarities [4]. However, *TP53* from higher mammals evolutionary diverged from the other two family members. In this process, the p53 protein gained many of its tumor suppressor functions which both other proteins do not possess [5]. Studies with loss of function (LOF) variants in mice have revealed the functional differences of the protein family members. For example, p73 knockout mice show developmental problems of the nervous system and die within the first weeks. This is caused by increased neural cell death that results in distortion of the hippocampal formation [6]. Furthermore, the p73 knockout mice show malfunctions in fluid dynamics, which often lead to defects, such as hydrocephalus or hyperinflammation of the epithelial. Both defects are caused by hypersecretion by epithelial cells [6]. Additionally, the mice show defects in reproductive and social behaviour, resulting from a loss of pheromone guided signal transduction [3]. Similarly, p63 knockout mice die immediately after birth and show developmental issues concerning the epithelial structures. Due to fewer basal cells and less cell differentiation, the mice develop a very thin detached epithelial layer. Additionally, the mice show truncated limbs and craniofacial malformations. All phenotypes are caused by the loss of asymmetric cell division and the loss of reproductive potential of stem cells [1,2]. In contrast, p53 knockout mice develop an early onset of various cancers but show no developmental defects, underlining the predominant role of p53 in the prevention of cancer development [7]. Meanwhile, the pleiotropic functions of p53 such as cell cycle arrest, DNA repair, senescence and apoptosis upon genotoxic stress are broadly explored and led to the definition of p53 as the “guardian of the genome” [8]. Due to the important role of p53 in many pathological conditions, it became the most studied protein with more than 100.000 publications in PubMed.

1.1 The history of p53 research

In the late 20th century, researchers worldwide tried to characterise the molecular cause of cancer. During that time, the term oncoprotein was defined and described a protein with cancer-promoting functions. The large and small T-antigen of the Simian Virus 40 (SV40) were identified as oncoproteins with the ability to transform non-cancerous cells into cancer cells. In 1979, David Lane and Lionel Crawford identified a non-viral protein with a molecular mass of 53 kilo dalton (kDa) associated with the large T-antigen [9]. Daniel Linzer and Arnold Levine made similar observations and moreover were able to also detect the uncharacterised protein in SV40 lacking teratocarcinoma cells [10]. High levels of this protein were also found in cells transformed with a murine leukemia virus in the lab of David Baltimore [11]. Therefore, the protein was soon described as highly abundant in tumor tissues and less abundant in healthy non-transformed cells [12]. This raised interest in this protein and led to the first workshop of all involved research groups where the name “p53” was settled. Today, it is known that p53 actually has a molecular weight of 43.7 kDa and migrates slower in a sodium sodecyl sulfate (SDS) gel because of the proline rich regions [8].

Since full-length, active SV40 antigens lead to a higher expression of p53 than truncated or mutated and therefore inactive forms of the SV40 antigen, p53 was considered to play a role in the SV40-mediated transformation to a cancer cell. Therefore, it was considered an oncoprotein with cell transforming ability [13]. In order to investigate this potential oncogenic property, several workgroups isolated and cloned the cDNA of p53 in the early 1980s [14–20]. These early overexpression studies supported the oncoprotein theory, as p53 showed a similar behaviour compared to that of the already known oncogene *MYC.* The overexpression of p53 facilitated the immortalisation of cells [21–24]. First doubts about p53’s function as an oncogene were raised by Levine and Oren when some of their cloned p53 variants would not reproduce the transforming effect. A comparison of the sequences revealed that all p53 clones differed in their genomic sequence. After the p53 wildtype (WT) sequence derived from normal tissue was established, it was proven that most of the tumor-isolated p53 clones contained mutations [8]. Solely the mutated p53 variants were able to promote the transformation of cells, whereas WT p53 showed no such effect [25,26]. Notably, numerous follow up studies revealed that *TP53* contains mutations in approx. half of all cancer specimens. Therefore, it is the most mutated gene in all cancer types.

Later studies demonstrated that overexpression of the p53 WT protein repressed the transformation of cultured cells [27,28]. Germline mutations of p53 were identified as responsible for the Li-Fraumeni syndrome that is characterised by an early onset of diverse cancer types [29]. Both observations led to the theory that p53 WT has tumor-suppressing functions [8]. The progress in genetic engineering permitted further studies of the p53 WT function as it allowed the generation of p53 knockout mice [3]. Since these mice early developed cancer with very high penetrance, the p53 WT protein was finally characterised as a tumor suppressor [7]. The association with the large T-antigen was found to be a mechanism of the SV40 virus to counteract the p53 functionality [30].

1.2 Structure of the p53 protein

The p53 protein is a 393 amino acid (aa) long molecule that forms a native structure on its own and undergoes reversible conformational changes by forming tetramers [31–33]. The N-terminal region contains two transactivation domains (TAD1 and TAD2) (aa 1-62), followed by a proline-rich region (PRR) (aa 63-94) [34]. The PRR domain contains a SH3-domain binding motif (PXXP) that plays a regulatory role [35,36]. Through the interaction with proteins containing SH3 domains like Rel-A associated inhibitor (RAI), Histone acetlyetransferase p300 (p300) or Peptidyl-prolyl cis-trans isomerase NIMA-interacting 1 (PIN1), the PRR contributes to the modulation of the p53 response. There is evidence that the PRR contributes to the p53 activation but can also mediate an inhibitory function, depending on the profile of the interacting proteins [37]. The DNA binding domain (DBD) (aa 94-292) binds decameric motifs of double-stranded (ds) DNA that contains two half-sites with the sequence 5'-Pu-Pu-Pu-C-(A/T)-(A/T)-G-Py-Py-Py-3' [38]. For most p53 target genes the whole p53 binding site consists of two motifs separated by a spacer with a variable length between 0 to 13 base pairs (bp), and with four half-sites to allow the binding of four DBDs [39]. The C-terminal region contains the tetramerisation domain (TD) (aa 325-356) and a negative auto regulatory domain (aa 360-393) [40,41,42]. The N-terminal part is relatively unstructured apart from a small region with weakly formed turns or helices, which creates a full amphipathic α-helix by binding to the hydrophobic surface of E3 ubiquitin-protein ligase Mdm2 (MDM2) [43]. The C-terminal part is also unstructured in native conditions [32,44]. Intrinsic disorders are often characteristic for proteins with a high ability to form protein-protein interactions [45].

The core, or DNA-binding domain (DBD), has a well-defined conformation and its crystal structure has been revealed in several conditions: bound to cognate DNA [38,46], bound to other proteins [47–49], bound to viral oncoproteins and in a DNA free form [50,51]. The DNA-binding domain consists of two antiparallel β-sheets and two α-helices (H1, H2) connected by three loops (L1, L2, L3). The β-sheets provide two basic scaffolds for DNA binding, with four (S1, S3, S5, S8) and five (S4, S6, S7, S9, S10) β-strands. The interaction surface consists of loop L2 (aa 164-194) and loop L3 (aa 237-250). Both loops are stabilised by a zinc ion and a loop-sheet-helix motif. The zinc ion is bound by the residues C176, H179, C238 and C242. Notably, the loss of the zinc ion results in inability of sequence-specific DNA binding [52,53]. For the correct interaction with DNA, the loop-sheet-helix motif binds to the major grove and the L3 loop binds to the minor groove of the dsDNA with the residue R248. Every half-site DNA motif is bound by one p53 monomer. Thus, p53 forms a symmetrical homodimer of two p53 proteins to fully bind one p53 binding motif. This interaction is mediated by residues of the L3 loop, the H1 helix and the L2 loop [54,55]. The detailed conformation is further affected by the DNA sequence. The residue R273 contacts the DNA half-site in the center and mediates an invariant binding to a conserved guanine base. The other binding sites to the major groove vary depending on the half-site sequence [46].

The ability of p53 to form high molecular weight oligomers was observed in the first years after its discovery [56–58]. Interestingly, it was demonstrated that binding to DNA is not required to form the tetrameric shape of p53 [59,60]. A closer investigation of the mechanism revealed that the C-terminal region is responsible for the tetramerisation [61–64]. This association of individual p53 proteins to its oligomeric state was shown to be induced by post-translational modifications such as the S392 phosphorylation [65]. The structure of the TD has been examined by X-ray crystallography and nuclear magnetic resonance (NMR) [39,66,67,40]. These experiments showed that the TD consists of a β-sheet (aa 326-333) and an α-helix (aa 335-355) connected by a hairpin formed by a glycine [40,66]. A p53 monomer forms a v-shape with the β-sheet and the α-helix, mediated by the hydrophobic cluster of the residues I332, F328 and F341. During the dimerisation, the β-sheets of two monomers form an antiparallel double β-sheet while the α-helices form a double-helical bundle. Altogether, this leads to the creation of a hydrophobic core by the residues F328, L330, I332 from the β-sheet and F338, F341 and N345 from the α-helices. Since the dimerisation of two p53 proteins is the first step for forming the tetramer, they are called primary dimers [68]. Two dimers interact via their helices and form a tetramer with a flexible angle. The β-sheets are directed to the outside of the tetramer and are therefore not important for the association of two primary dimers. The importance of every residue involved in the tetramerisation has been investigated by alanine mutation scans and F328, L330, I332, R337, F338, M340, F341, L344 and L348 were identified as the most critical residues [69–71]. Mutations that prevent the tetramerisation have been shown to decrease p53 activity [69,71,72]. The TD is well conserved and also exists in p63 and p73. The TD of p53 is smaller than the TDs of p63 and p73 and contains, besides conserved regions also specific amino acid exchanges. Especially the hydrophobic amino acids are conserved among species. Moreover, the residues on the surface of the TD (E326, T329, R333, R335, E336, R337, E339, R342, E346, E349 and D352) also show a high conservation among vertebrates. While the conservation of the residues R337, D352 and E349 can be explained by their ability to stabilise the tetramer, the reason for the high conservation of other residues like T329 are unknown, since these residues do not seem to impact the tetramerisation [69,70,72]. The p53 protein exists in an active conformation with DNA binding activity and a latent conformation [73]. This conformational status is regulated by redox changes in the cell and is influenced by interactions with other proteins [74,75].

However, since p53 is able to bind to DNA even without the TD, the TD was estimated to have minor impact on the function of p53 [62,64,76–85]. Further experiments showed that the affinity of p53 lacking the TD to DNA is 10 to 100 times less than the affinity of the full-length protein [86]. The TD further affects the bending and twisting of the bound DNA [76,79]. Another essential function of the TD is the nuclear import of p53, since it contains the nuclear localisation signal (NLS) (aa 340-351). The NLS is more exposed in the monomeric form, whereas it is hidden in the tetrameric shape [87].

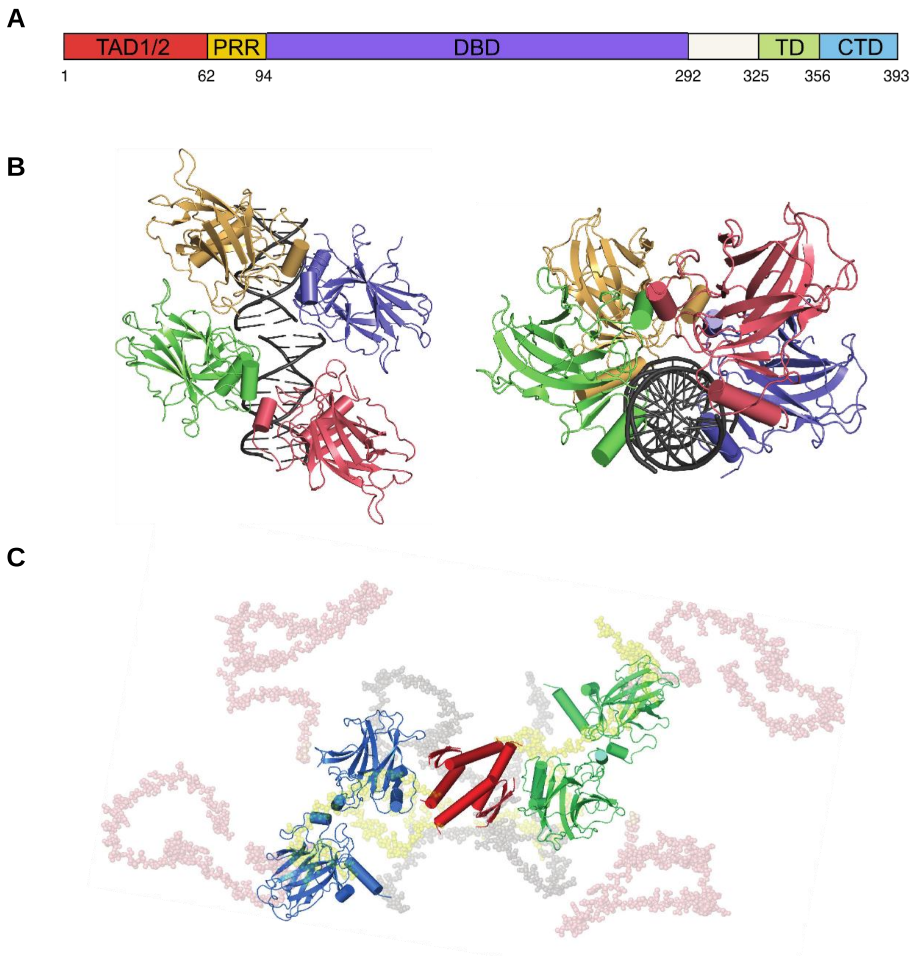

Fig. 1 Schematic visualisation of the p53 structure. A: Schematic picture of the p53 domains. p53 contains two TADs at the C-terminus, followed by a PRR. The structured DBD and TD are connected through a linker region (grey). At the C-terminal part, p53 contains the CTD. **B:** Schematic picture of the DNA-binding by the core domains of the p53 tetramer, as observed in the crystal structure of human p53 core domain in complex with palindromic half-site DNA (PDB code 2AHI) [46]. Two different views are shown of the four p53 proteins visualised in four different colours. **C:** Schematic picture of the full-length p53 tetramer abstracted from the SAXS model. The N-terminal region is highlighted in pink, the core domains in blue and green, the linker region in grey, the TDs in red and the C-terminal region in yellow. Figure adapted from Joerger and Fersht 2010 [88,89].

1.2.1 The thermodynamic instability of p53

The structural stability of p53 is highly temperature-dependent. The core domain already loses its structural integrity slightly above body temperature [52,90]. The equilibrium of folded to unfolded p53 can be described by the thermodynamic instability of p53. The warmer it gets, the more unfolded p53 can be detected. This equilibrium of folded to unfolded p53 can be influenced by p53 mutations. The reason for the kinetically unstable p53 structure are flexible regions such as the hydrogen bound between Y236 and T253, which is unsaturated and therefore highly unstable [51]. The paralogs p63 and p73 have a replacement with phenylalanine at this position and therefore show less thermodynamic instability [51]. A thermodynamic unstable p53 protein with structural plasticity allows the protein to fulfill its various functions and hence gained an evolutionary advantage. Due to this thermodynamic instability, many p53 mutations are characterised by dysfunction as a consequence of destabilisation. In contrast, other mutations (M133L, V203A, N239Y and N268D) have been shown to increase the stability of p53 [91].

In order to analyse the amount of folded and unfolded p53 proteins, conformation-specific antibodies were generated. PmAb1620, for example, solely detects the folded wild-type conformation of p53 [92]. Precisely, it detects a motif in the core domain of p53 distant from the DNA binding site, including the residues R156, L206, R209, and N210 [93]. To distinguish between folded and unfolded p53, the antibody PmAb240 can be used, which detects a motif in the β-strand S7 (aa 212-217) that only becomes accessible upon unfolding of this region [94].

1.3 Biological function of p53

1.3.1 The p53 core transcriptome

As p53 was identified to be a transcription factor, many studies revealed the function of p53 to induce gene transcription upon DNA damage, oncogene activation, ribosomal stress and hypoxia [95]. In order to investigate the link between p53 and cancer, it has been of great interest in the research community to examine the p53 responsive genes upon DNA damage [96].

The induction of p53-dependent transcription can be activated by its two TADs [34,97,98], which leads to tightly binding of the DBD to specific DNA sequences [39,99–102]. In contrast to the specificity of the DBD, the C-terminal region binds non-specifically to DNA [44,103,104]. The affinity of p53 to DNA sequences differs between the target genes. The affinity to genes regulating the cell cycle arrest was shown to be higher compared to genes involved in apoptosis [105,106]. The first identified p53 target genes were *CDKN1A* [107], *GADD45A* [108] and *MDM2* [109,110]. Numerous studies in the last century identified between hundreds and thousands of potential p53 target genes [111,112]. Comparing these studies, 346 common genes can be identified that show p53-dependent expression and harbor a p53 binding site close to the transcriptional start site (TSS) [113]. The transcription of 71 % of these direct target genes is upregulated upon p53 activation, while 26 % are repressed, and 3 % can be either activated or repressed by p53 [113]. To mediate this transcription control, p53 primarily binds to the promotor region or the first introns of the gene [113]. Notably, the repressed genes identified in different transcriptome studies show little overlap. Therefore, p53 is predominantly described as an activator of gene transcription and not as a repressor [114]. Functional characterisation revealed that most of the downregulated genes are involved in cell cycle regulation [115]. Furthermore, even if p53 binding sites are identified in the proximity of these promotors, the transcription is often shown to be affected by p21 and the dimerisation partner, RB-like, E2F and multi-vulval class B (DREAM) complex. Since both proteins are influenced by p53, it is likely, that the repressed genes are indirectly regulated by p53 [113].

1.3.2 The role of p53 in the DNA damage response (DDR)

The genome is continuously exposed to DNA damage. This damage can be caused by exogenous processes such as radiation as well as endogenous processes like reactive oxygen species (ROS) or replication defects [116]. These agents cause different forms of DNA damage such as single-strand breaks (SSB), double-strand breaks (DSB) or bulky lesions. In order to repair this damage, the cell has developed different mechanisms to induce the repair of DNA damage throughout the cell cycle [116]. The activation of specific kinases controls the DNA damage repair pathway and the cell cycle. Whereas kinases like Phosphoinositide 3-kinase related kinases Serine-protein kinase ATM (ATM), Serine/threonine-protein kinase ATR (ATR) and DNA-dependent protein kinase catalytic subunit (DNA-PK) are activated upon DNA damage and induce the DNA-damage repair, cyclin-dependent kinases (CDKs) mediate the transition to the next cell cycle phase in the absence of DNA damage. The CDKs are transiently activated during the cell cycle to phosphorylate target proteins, resulting in induced degradation of cell cycle inhibitory proteins and promotion of cell cycle progression [117]. The DNA damage response (DDR) is controlled by checkpoints, consisting of signaling pathways that coordinate DNA repair and cell cycle transition [118,119]. The transduction and amplification of the checkpoint signal to downstream targets is often mediated by phosphorylation [116]. The p53 protein plays a role in many DNA damage repair pathways, but it is explicitly linked to Nucleotide excision repair (NER) and Homologous repair (HR). Even though indirect contributions of p53 to Base excision repair BER, Mismatch repair (MMR) and Non-homologous end joining (NHEJ) are described, it only slightly effects their efficiency [120].

1.3.2.1 The role of p53 in the repair of bulky DNA lesions

UV radiation induces bulky lesions like cyclobutane pyrimidine dimers (CPDs) and pyrimidine photoproducts (6-4PP’s). Both lead to distortions of the DNA and need to be repaired by BER or NER. BER primarily removes oxidized bases during the G1 phase. However, the NER pathway is not limited to the G1 phase and can be divided into global repair and transcription-coupled repair [121].

The contribution of p53 to the **NER** became apparent in 1997, when Ford and Hanawalt demonstrated that p53 is required to remove CPD's and 6-4PP's [122]. Wang *et al*. later showed that p53 binds to several components of the NER complex like DNA repair protein complementing XP-C cells (XPC), X-box-binding protein 1 (XBP) and DNA excision repair protein ERCC-6 (CSB) [123]. In addition, p53 activation triggers the expression of DNA damage-binding protein 2 (DDB2) and XPC that are important to detect sites of DNA damage [124,125].

1.3.2.2 The role of p53 in the repair of DSB

DSB can be repaired by HR and NHEJ [126,127]. Both pathways get orchestrated by the kinase ATM, ATR and DNA-PK. ATM and DNA-PK are directly activated by DSBs, whereas ATR is activated by ssDNA and stalled replication forks [128]. These kinases are directly recruited to the site of DNA damage by their specific interactors. DNA repair and telomere maintenance protein nbs1 (NBS1) recruits ATM, ATR-interacting protein (ATRIP) interacts with ATR and ATP-dependent DNA helicase 2 subunit KU80 (Ku80) interacts with DNA-PK [129,130]. The transmission of DDR signaling to downstream targets is primarily mediated by Serine/threonine-protein kinase Chk2 (Chk2), activated by ATM and Serine/threonine-protein kinase Chk1 (Chk1), activated by ATR [129,130].

For **NHEJ**, the heterodimers Ku80 and X-ray repair cross-complementing protein 6 (Ku70) bind to the ends of DSB. They recruit DNA-PK, which in turn recruits a ligase complex to ligate the DSB. NHEJ is used when chromosomes are compact and no sister chromatids are available to use their genetic information for HR [126].

During the S phase and G2 phase, the DSBs are primarily repaired by **HR**, which is induced upon ATM activation and leads to an activation of CDK1 by protein recruitment [127]. CDK1 mediates the 5' to 3' restriction of the DSB ends, so that 3' overhangs become exposed and the ssDNA can be recognised [131]. This leads to ATR activation and the recruitment of RAD proteins that initiate the HR by invading the homologous region of the sister chromatid [132]. Additionally, the activated ATM comes in close proximity to histones and phosphorylates the histone variant H2AX (named γH2AX). This phosphorylation leads to the recruitment of several proteins, including TP53-binding protein 1 (53BP1). The interaction of 53BP1 and p53 mediates the localisation of p53 to sites of DNA damage [133]. P53 directly interacts with DNA repair protein RAD51 homolog 2 (RAD51) and thereby modulates the HR activity [134]. Apart from this direct contribution, p53 regulates several DNA repair genes that are involved in HR, including RAD51 [135].

1.3.3 The role of p53 in cell cycle arrest

The cell cycle consists of the G1 phase, the S phase, the G2 phase and the mitotic phase (M), in which the actual cell division occurs [136]. The progress through the cell cycle phases is mediated by transiently active CDKs [137]. These kinases are transiently activated during the cell cycle and phosphorylate their targets. This induces the degradation of cell cycle inhibitory proteins and promotes cell cycle progression [117]. The decision of the cell to re-enter another cell division needs to be tightly controlled to prevent the development of cancer by uncontrolled cell proliferation. During the G1 phase, the cell passes the restriction (R) point to re-enter another S phase. In this phase, the binding of cyclin D to CDK4 and CDK6 and the subsequent activation of these kinases is important to promote another cell cycle [138,139]. Cyclin D induces the kinase activity of the CDKs which results in the phosphorylation of the retinoblastoma protein (pRB). Afterwards, pRB dissociates from the transcription factor E2F and induces the E2F-dependent expression of proteins like cyclin E and cyclin A [140]. The progression from the G1 to the S-phase is primarily mediated by the active complex of CDK2 and cyclin E, what leads to further activation of E2F-mediated gene transcription. The transition from the G2 phase to mitosis is mainly dependent on increasing amounts of cyclin A and the interaction of CDK1 with cyclin B1 [141].

The p53 protein can impose growth arrest in the G1 and G2/M phase and is specifically essential for DNA damage-induced cell cycle arrest during the G1 phase [142–145,146]. This is primarily mediated by the induction of transcription of the cyclin-dependent kinase inhibitor *(CDKN1A)* gene. The corresponding protein p21 inhibits CDK1 and CDK2 thus mediating the cell cycle arrest [147,148,149]. Additionally, p21 directly binds to Proliferating cell nuclear antigen (PCNA), which is important for replication [150]. This interaction prevents the binding of PCNA to DNA and thereby cause stalled replication forks [149]. These stalled replication forks during the S phase lead to the activation of Killin by p53. This protein inhibits the DNA replication and causes a S-phase arrest [151]. Even though the G2/M arrest is not entirely dependent on p53, it can still contribute to the cell cycle arrest at this stage [152]. The CDKs gets mainly inhibited by two pathways. Firstly, p21 inhibits the CDK/Cyclin complexes and secondly, the activation of ATM leads to the degradation of Dual specificity phosphatase Cdc25 (Cdc25) that is usually activating CDKs by dephosphorylation. This leads to the reduction of phosphorylation of pRB by CDKs and results in the stabilisation of the pRB/E2F complex [152]. For the progression in the cell cycle, the pRB/E2F complex needs to be separated caused by phosphorylation of pRB to activate its function as a transcription factor and induce the expression of cell cycle promoting genes [152]. Therefore, the stabilisation of the pRB/E2F complex reduces the expression of cell cycle promoting genes like *CDK1*, *CCNB1* (cyclin B1) and *CDC25* [153,154]. Since p53 mainly regulates the abundance of p21 it indirectly reduces the expression of CDK1, cyclin B1 and Cdc25 and thereby interferes with the formation and activation of the CDK1-cyclin B1 complex [152,155]. In addition, the p53 target 14-3-3σ mediates the cytoplasmic localisation of CDK1 and

Cdc25 in the G2 phase, which prevents the mitosis [156,157]. Finally, the p53 target gene *GADD45A* inhibits the CDK1/cyclin B1 complex and mediates a cytoplasmic localisation of cyclin B1 in the G2 phase [158,159].

1.3.4 The role of p53 in apoptosis

There are two major pathways to induce apoptosis. One is the extrinsic or death receptor pathway, and the other is the intrinsic or mitochondrial pathway. Both pathways have a common end process that starts with the cleavage of Procaspase 3 and finally leads to DNA-fragmentation, degradation of the cytoskeleton and nuclear proteins, formation of apoptotic vesicles, expression of ligands for phagocytic cells and eventually, the phagocytic uptake of the apoptotic cell [160].

The extrinsic pathway is mediated by the transmembrane TNF receptor family [161]. The stimulation of the receptor leads to clustering of the intracellular death domain, which in turn leads to the recruitment of ligands like Tumor necrosis factor receptor superfamily member 6 (FAS). The recruitment of additional adaptor proteins finally leads to the recruitment and cleavage of Procaspase 8 [162].

The intrinsic pathway gets activated by intracellular signals upon stimuli like starvation, radiation and hypoxia [160]. These stimuli result in the permeabilisation of the mitochondrial membrane and the release of pro-apoptotic proteins such as Cytochrome c to the cytosol, what subsequently allows the formation of the apoptosome and then leads to the cleavage of Procaspase 9 [163]. The permeabilisation of the mitochondrial membrane is mainly regulated by the Bcl-2 protein family, whose expression is regulated by p53 [164].

The final cleavage of the corresponding Procaspases and the following activation of the proteolytic Caspase cascade cause the programmed death of the cell. This further leads to the externalisation of phosphatidylserine to the outer layer of the plasma membrane [165]. The exposure of phosphatidylserine can be used to identify apoptotic cells by the phosphatidylserine-binding protein Annexin V [166].

The induction of apoptosis was one of the first described functions of p53 [167,168]. The p53 target genes *FAS*, *TRAF4* and *TNFRSF10A-D* belong to the Tumor necrosis factor (TNF) receptor proteins and contribute to the extrinsic induction of apoptosis[,161,169,170]. Several Bcl proteins are associated with the intrinsic induction of apoptosis, including Apoptosis regulator BAX (BAX) and Bcl-2-binding component 3 (BBC3 or PUMA), and are activated by p53 [171,172]. Besides the activation of target genes, p53 can also possess transcription-independent activities. For instance, p53 has been shown to interact with members of the Bcl2 protein family in the cytoplasm and further participates in the permeabilisation of the outer mitochondrial membrane, thereby directly contributing to the induction of apoptosis by facilitating the release of Cytochrome c [173].

1.3.5 The role of p53 in senescence

Apart from the reversible cell cycle arrest, also the induction of senescence by p53 is also an essential tool to reduce neoplastic processes [174,175]. Senescence is an irreversible form of cell cycle arrest that is entered by cells upon aging and stimuli like ROS, DNA damage and starvation. Indications for senescence are morphological changes, chromatin remodeling, metabolic reprogramming and the secretion of pro-inflammatory factors [176]. The process is induced by p53 upon a mild but continuous stimulus, which is not strong enough to induce apoptosis and also prevents the repair of DNA damage due to its duration. Similar to the reversible cell cycle arrest, senescence is induced by p21 [176]. Further, the permanent cell cycle arrest results in the activation of p16, a factor that facilitates senescence [176]. One characteristic of the late phase of senescence is a high expression of β-galactosidase, which can be used to distinguish between senescent and non-senescent cells [177].

1.3.6 Other p53 functions

Autophagy is a pathway that is primarily induced by starvation. The cell recycles already existing metabolites to gain nutrients for cell growth and survival. Therefore, parts of the cytosol get engulfed in the autophagosome, which fuses with the lysosome to enable the degradation of its cargo [178]. The selective uptake of cargo into the autophagosome is mediated by the Microtubule-associated protein light chain 3 (LC3), located in the autophagosome membrane [178]. Interestingly, the general turnover by autophagy is increased upon p53 activation [179]. One explanation is the expression of the p53 target gene *DRAM1*, which encodes for a lysosomal protein, contributing to increased autophagy [180].

Moreover, p53 plays a role in the cellular metabolism. It increases the glutamine catabolism, supports the anti-oxidant activity, downregulates lipid synthesis, increases fatty acid oxidation and stimulates gluconeogenesis [181].

Furthermore, the activation of p53 leads to the repression of **protein synthesis** by the downregulation of rRNA genes and genes required for the transport of ribosomal proteins [182,183]. Additionally, the direct targets *SESN1* and *SESN2* block the Serine/threonine-protein kinase mTOR (mTOR) pathway and represses the mRNA translation [184].

The crosstalk between different p53 output functions further complicates the network of p53 functions. For instance, the changes in metabolism mediated by p53 contribute to the induction of apoptosis, autophagy and ferroptosis [185]. Stimulus-dependent post-translational modifications and the association with interactors are mechanisms that have been suggested to drive the p53 response in specific directions [186,187].

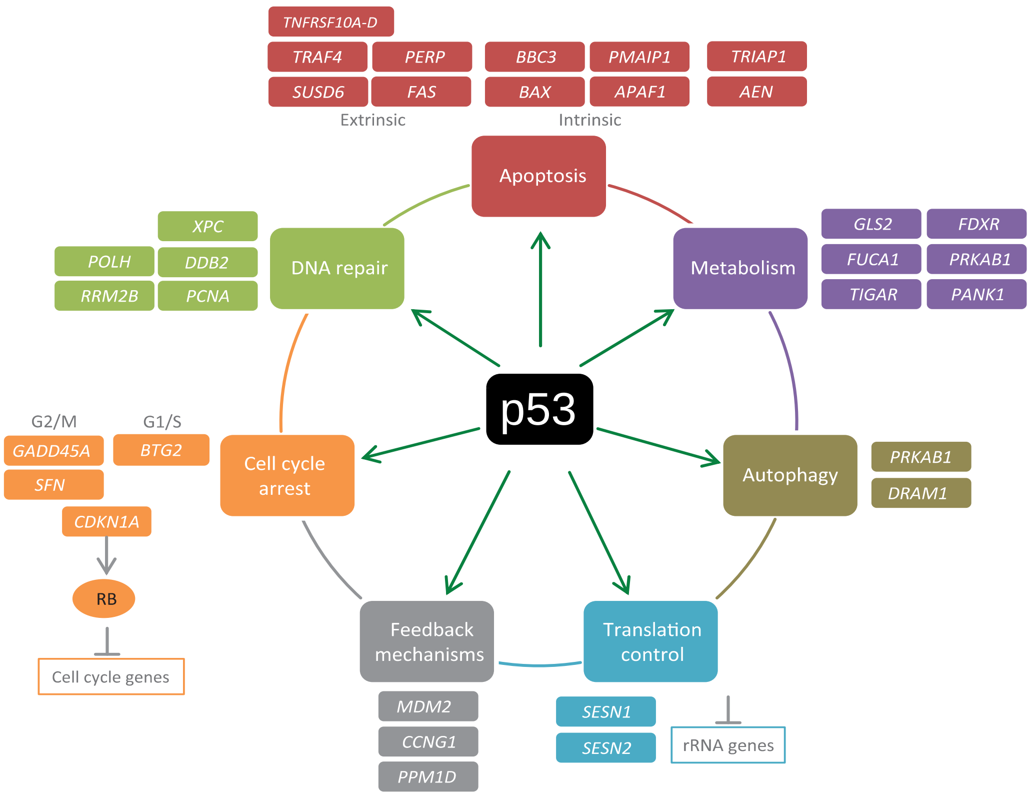

Fig. 2 The functions of p53. Displayed are the main pathways influenced by p53. The most prominent genes, activated by p53, are listed for each pathway. Figure adapted from Fischer et al. 2017 [113].

1.4 Regulation of the p53 response

The p53-mediated decision towards or against cell death is controlled by a very complex network of stimulus-specific post-translational modifications and interaction with other proteins [50,188]. Furthermore, p53 kinetics play an essential role in the target gene selection. For instance, the promotor of *CDKN1A* is already activated through a very transient p53 stimulation, whereas the promotor of *FAS* is only activated upon a continuous p53 activation [187]. Hence, short and mild stimuli mostly trigger the transcription of genes associated with cell cycle arrest, while more prolonged stimuli activate apoptosis-related gene transcription [189–191]. In general, the potential of p53 to activate cell cycle arrest genes is higher compared to activating apoptotic related genes [106].

1.4.1 Regulation of p53 levels by protein degradation

In unstressed cells, MDM2 binds tightly to the transactivation domain of p53 in order to inhibit its function [192,193]. Additionally, MDM2 acts as an E3 ubiquitin ligase and facilitates the K48-linked polyubiquitination and degradation of p53 by the proteasome [194–196]. Since this blockage of the TAD is a very efficient mechanism to inhibit the p53 function, also other proteins like MDMX are known to also bind the N-terminal region of p53 and inhibit its function [197,198,199]. The loss of MDM2 or MDMX in mice is embryonically lethal due to the increased p53 activation [200–202]. Mutations in the *MDM2* gene that lead to an increase in the *MDM2* expression are linked to an early onset of cancer [203]. Even though MDM2 is considered the primary E3 ligase responsible for p53 turnover, many other E3 ligases like Caspase recruitment domain-containing protein 16 (Cop-1), RING finger and CHY zinc finger domain-containing protein 1 (Pirh-2), E3 ubiquitin-protein ligase HUWE1 (ARF-BP1), the Trim proteins and the Cullin protein family have been identified to play a role in p53 degradation [204]. For the interaction with MDM2 and the proper ubiquitination, p53 needs to be oligomerised [205]. Hence, the degradation of p53 is impaired when the tetramerisation is inhibited [206]. To counteract the degradation upon ubiquitination, the deubiquitinases Ubiquitin carboxyl-terminal hydrolase 10 (USP10), Ubiquitin carboxyl-terminal hydrolase 7 (USP7 or HAUSP) Ubiquitin carboxyl-terminal hydrolase 2 (USP2a) and Ubiquitin carboxyl-terminal hydrolase 42 (USP42) have been shown to stabilise p53 by removing the ubiquitin modifications [207]. Since *MDM2* is a direct target of p53-dependent gene transcription, this leads to a negative feedback loop and consequently a reduction in the p53 protein level [109,208].

1.4.2 Regulation of p53 levels by transcriptional and translational control

Although the primary regulation of the p53 response is based on protein stabilisation, some factors are described to influence the *TP53* transcription and the translational rate of the p53 mRNA. The transcription of *TP53* can be activated by cAMP-responsive element-binding protein (CREB), Myc and p53 itself [209,210,211]. The 5’ UTR and 3’ UTR of the p53 mRNA play a crucial role in regulating mRNA translation [212,213]. For instance, 60S ribosomal protein L26 (RPL26) binds to the 5’ UTR and thereby increases the translational rate [214]. In order to counteract this effect, RPL26 also binds to MDM2, which leads to the polyubiquitination of RPL26 and subsequently the reduction of p53 translation [215]. Furthermore, Nucleolin binds to the 5’ UTR and inhibits the p53 translation under unstressed conditions [216].

1.4.3 Regulation by post-translational modifications

Post-translational modifications (PTM) play a very prominent and essential role in shaping p53 activation [186]. **Phosphorylation** was the first identified PTM with an impact on the p53 response [217]. Since then, 39 (according to phosphosite.org) residues were reported as phosphorylation targets, contributing to the modulation of the p53 response. Upon DNA damage, many kinases have been shown to phosphorylate residues at the N-terminal part of p53. Those phosphorylations prevent the binding of MDM2, what leads to increased p53 protein levels [218]. ATM, ATR and their downstream kinases Chk2 and Chk1 phosphorylate p53 at the residues S6, S9, S15 and S20 [219]. The phosphorylations at S15 and S20 play a crucial role in preventing the interaction with MDM2 and lead to the stabilisation of p53 [220]. The phosphorylations at S6 and S9 are mediated by the CK1 kinases and play important roles in development and cancer prevention [221]. The phosphorylation at S46 is mainly mediated by the kinases Homeodomain-interacting protein kinase 2 (HIPK2), Dual specificity tyrosine-phosphorylation-regulated kinase 2 (DYRK2) and Protein kinase C delta type (PKCδ) upon DNA damage, and increases the affinity of p53 to pro-apoptotic genes [222-223]. Furthermore, the phosphorylation at S392 by Casein kinase 2 (CK2) increases the stability of the p53 tetramer and enhances the transcriptional activity of p53 [224]. Other phosphorylations have been described as inhibitory modifications like the phosphorylation at S376 and the Transcription initiation factor TFIID subunit 1 (TAF1) meditated phosphorylation at T55 [225,226]. Notably, many PTM depend on the TD. The phosphorylation at S366 and T387 by Chk1, for example, is abolished when the TD is deleted [227]. Similarly, the phosphorylation at S392 is reduced when L330 in the TD like is mutated [228].

Phosphatases add another layer of control to p53 functionality, since the dephosphorylation of the described phospho-sites can reduce or inhibit the function of the p53 protein. Dual specificity protein phosphatase 26 (DUSP26) has been described to dephosphorylate S20 and S37, thereby inhibiting the apoptotic function of p53 [229]. Protein phosphatase 1 (PP1) dephosphorylates S15 and S37, thus leading to a reduction in the transcriptional activity of p53 [230]. Moreover, S46 is dephosphorylated by PP2, thus mediating the attenuation of apoptosis [231]. This reduction of p53 phosphorylation is important to re-enter the cell cycle after a completed DNA damage response [231,232]. The phosphatase Wip1 acts as an oncogene that often shows elevated amounts in cancer. It acts upstream of p53 and prevents ATM activation. This leads in turn to the inhibition of the phosphorylation of serine residues in the p53 protein and thereby reduces its activation [233–235]. Additionally, Wip1 dephosphorylates MDM2 and increases its stability, thereby mediating enhanced p53 degradation [236].

The **acetylation** of lysine residues in the p53 protein is an essential influencing factor on the p53 response. It influences the transcriptional activity and the recruitment of modulating interactors of p53 [37]. For instance, the acetyl transferases p300/CBP (CREB-binding protein) acetylate lysine residues at the C-terminal part (K372, K373, K381, K382), which are involved in MDM2 binding, and thereby contributes to the activation of p53 by MDM2 dissociation [237]. The acetylations at K373 and K382 depend on the prior phosphorylation at S46 and have been shown to increase the DNA-binding affinity, resulting in the enhanced expression of apoptosis-related genes [238–240]. Furthermore, the acetylation at K320 mediated by Histone acetyltransferase KAT2B (PCAF) primarily leads to the induction of cell cycle arrest and reduces the apoptotic response [241]. The induction of apoptosis, in contrast, is facilitated by the acetylation at K120 that is mediated by Histone acetyltransferase KAT5 (Tip60) and Histone acetyltransferase KAT8 (hMOF) [242,243].

Deacetylases maintain acetylation homeostasis. For instance, NAD-dependent protein deacetylase sirtuin-1 (SIRT1) deacetylates K382 and thereby reduces the induction of apoptosis [244]. Moreover, Histone deacetylase 5 (HDAC5) mediates the deacetylation of K120, facilitating the induction of cell cycle arrest and clearance of ROS but reducing the induction of apoptosis [245].

The lysines in p53 can be **mono- or dimethylated** by methyl transferases such as the family of SET proteins, N-lysine methyltransferase SMYD2 (Smyd2), Histone-lysine N-methyltransferase EHMT2 (EHMT2). Some methylations have been shown to reduce the p53 response, whereas others contribute to the acetylation of p53, what results in p53 activation [246,247]. Additionally, arginine methylations in the TD (R333, R335, R337) mediated by Protein arginine N-methyltransferase 5 (PRMT5) promote apoptosis by influencing the target gene specificity of the p53 protein [248].

1.4.4 Regulation by interacting proteins

The interaction of p53 with other proteins constitutes an important regulatory level to adjust the p53 response [187]. According to the MINT and BioGRID databases, 619 (MINT) and 1129 (BioGRID) unique physical interactors of p53 have been identified to date.

Many direct interaction partners have been shown to interact with p53 via the TAD [249,250]. These include, among others, MDM2 and also proteins of the transcription initiation complex and acetyltransferases [251,252]. The interaction with acetyltransferases such as p300 and CBP leads to the activation of p53 via the acetylation at the C terminus as described in 1.4.3 [253,254].

In contrast, the interactors belonging to the Ankyrin-repeat-SH-domain-and proline-rich-region-containing-protein (ASPP) family bind to the DBD of p53. ASPP1 and ASPP2 facilitate the binding of p53 to pro-apoptotic target genes, whereas inhibitory ASPP (iASPP) inhibits the induction of apoptosis and promotes cell cycle arrest [255,256]. Moreover, the interaction with Zinc finger protein 385A (Hzf) via the DBD enhances the selectivity of p53 for cell cycle arrest-related target genes [257].

The TD in the C-terminal part is further known to mediate numerous protein interactions. It binds, for instance, two kinases that are known to play a role in p53 activation. CK2 binds to the region between residues 325-344, whereas the Ca^{2+}-dependent PKC binds to the residues 320-346 [258,259]. Moreover, the residues 300-393 mediate interaction with Transcription factor p65 (RelA) [260]. Besides human proteins, many viral proteins are known to bind the C-terminal region of p53. For instance, the adenovirus protein E4orf6 binds to the residues 318-360, and the hepatitis B virus protein HBx binds to the residues 300-393 [261,262]. Interestingly, many proteins do not interact with the TD itself but can only interact with the tetrameric form of p53. It is likely that the TD affects many protein interactions indirectly. Therefore, the TD affects for example the following interactions between p53 and proteins: the interaction with MDM2 which binds site at the N-terminus of p53, the interaction with human papillomavirus type 16 E2 protein (HPV-16 E2) and Tyrosinekinase ABL1 (C-abl) which binds site at the C-terminus, as well as the interaction with TATA-binding protein (TBP) which binds site at the N-terminus are dependent on the tetrameric form of p53 [263–268].

Many of the described interactions depend on post-translational modifications of the p53 protein. For instance, the phosphorylation at S46 allows the interaction with PIN1, displacing iASPP from the DBD and facilitates apoptosis [269]. The K382 acetylation and S392 phosphorylation promote the interaction with Mediator of DNA damage checkpoint protein 1 (MDC1), a mediator of the DNA damage response [270]. Further, the interactions are not only influenced by PTMs, but also themselves influence the PTM pattern. For instance, the interaction with ATM and p53-associated KZNF protein (APAK) affects the p53 response by recruiting HDAC1 under physiological conditions. This reduces the activation of p53 due to its deacetylation [271].

Therefore, the interaction of p53 with kinases is of particular interest, as for example CK2 and PKC as direct p53 interactors also influence the PTM pattern of p53 [258,259].

Since many mutations influence the p53 conformation, it seems plausible that p53 mutations alter the interactome. For instance, the interaction of p53 with CBP/ASPP2 is inhibited in the R181E or G245S mutants [90,272].

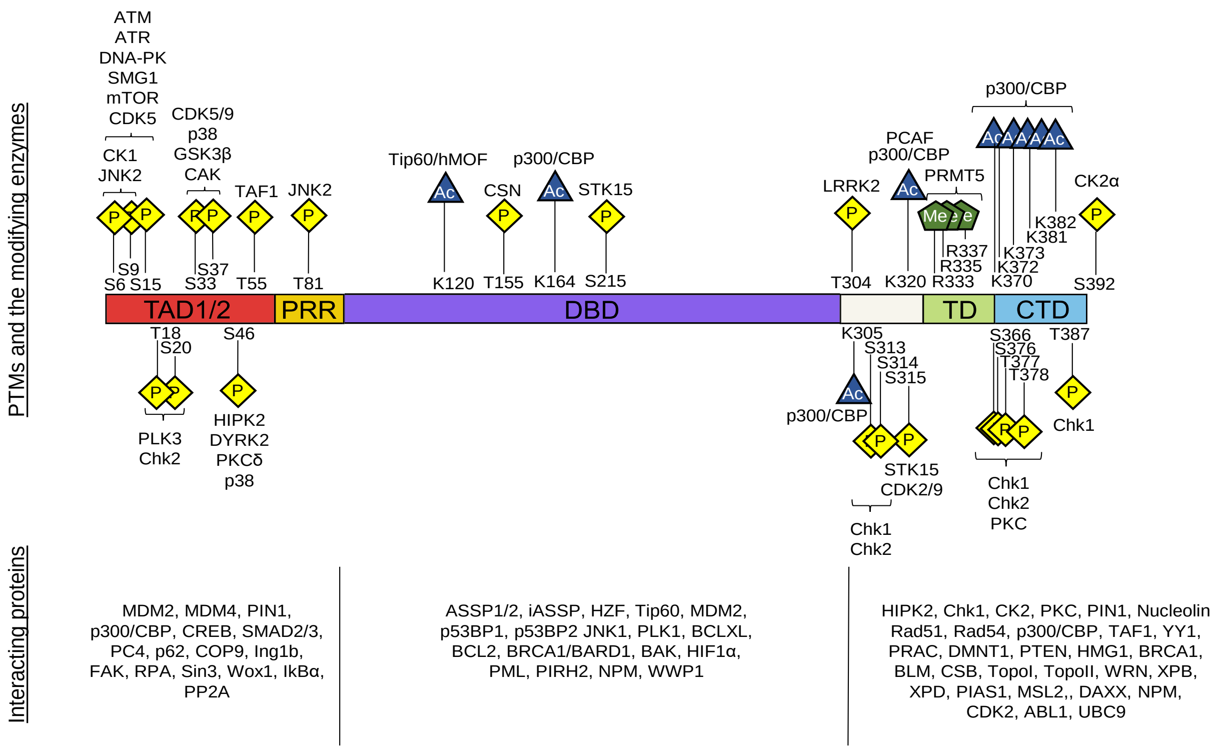

Fig. 3 Regulation of p53 by post-translational modifications and interacting proteins. In the upper part common phosphorylations (P), acetylations (Ac) and methylations (Me) are displayed with the corresponding modifying enzymes. In the lower part a selection of interacting proteins are displayed that bind to the N-terminal part, the DBD and the C-terminal part.

1.5 Mutations of p53

TP53 is the most common mutated gene in cancer cells with the highest prevalence in colorectal cancer. Most mutations of *TP53* are missense mutations, located in the DNA binding domain [273,274] (Fig. 4). The functional consequences are complex and while some mutations cause loss-of-function (LOF), others cause a gain-of-function (GOF) phenotype or do not have any impact on p53's function at all [275–278]. The frequency of p53 mutations leading to LOF of p53 highlights that loss of anti-proliferative functions is an important selection factor in tumorgenesis. This observation is supported by the fact that many hot-spot mutations exert a dominant-negative effect on p53 WT, resulting in LOF even in the heterozygous genotype [277]. Nevertheless, it became clear that many of the hotspot mutations cause a cellular phenotype that is distinctly different from that of p53 LOF. Over the years, a GOF has been demonstrated for many p53 mutations. This often results from the high expression level and lack of degradation of the mutant p53. Also, the dominant-negative effect due to the interaction of mutant p53 with other transcription factors can promote genomic instability and thus tumor growth. In summary, it can be assumed that the selection for the hotspot mutations of p53 is based on a combination of loss of function and gain of function [279]. Since mutations affect prognosis and response to cancer

treatment, *TP53* sequencing became important in cancer diagnostics [280]. The most common cancer mutations are R175H, Y220C, G245S, R248W, R249S, R273H and R282W [68]. All of them are located in the DBD (distribution along the p53 structure is shown in Fig. 4). They can be classified as mutations that directly interfere with DNA binding and mutations that alter the p53 structure and reduce the p53 functionality.
R175H is located in the L2 loop and diminishes the binding of the zinc ion. This results in complete loss of p53 DNA binding and thus functionality [52,275,277]. Another DNA binding defective mutant is R273H. This mutant has the same thermodynamic stability as p53 WT and also shows residual DNA-binding activity, which is insufficient to activate p53 target sites *in vivo* [90,281]. The structural mutations G245S and R249S are located in the L3 loop. Since this loop structure is important for DNA binding, both mutants expectedly reduce p53 functionality [46]. The mutation of the DNA contact residue R248 results in a loss of DNA-binding to the minor groove of the target DNA [46]. Some mutations affect only specific p53 functions. For instance, the tumor-derived mutants p53 R175P and p53 E180R fail to induce apoptosis, but can still mediate cell cycle arrest [282]. Other p53 mutations alter the interactome. For example, the mutations R181E or G245S show no interaction with CBP/ASPP2, in contrast to the p53 WT protein [90,272].

Besides the conformation changes in the critical DBD, the structural mutations also reduce the thermodynamic stability of p53 and increase the amount of unfolded p53 in the cell. Most temperature-sensitive mutants, such as V142A, are hydrophobic large to small amino acid substitutions located in the β-sheet region of p53 [283,52].
The TD generally shows less mutations, compared to the N-terminal part or the DNA binding domain [284–287]. Mutations in the TD are more often germline than somatic mutations. The mutation R377H can be found in 20% of Li-Fraumeni patients [288]. As R377 forms an intermolecular salt bridge and is involved in hydrophobic packaging during tetramerisation, the mutation of this residue reduces the p53 affinity to DNA [70]. Furthermore, L344P breaks the helix structure of the TD, and F341L weakens the hydrophobic core of the primary dimers. Both mutations destabilise the secondary structure of the TD [289–292]. Moreover, G334V leads to structural distortions and has been linked to lung cancer. The mutant is still able to form tetramers but mediates the formation of amyloid fibrils [293]. The low frequency of mutations in the TD has been attributed to the fact that impaired tetramerisation often interferes less with the p53 function than mutations in the DBD [291]. Furthermore, the tetramerisation may be necessary for the dominant-negative effect or gain of function of other mutations [69,294–296].
In order to adapt to deleterious mutations, the cell often develops second site mutations [297]. For instance, N239Y and N268D are tumor suppressor mutations that increase the stability of p53 and counteract the oncogenic mutations [298,299]. DNA contact mutations like

R273H and R273C often lead to the suppressor mutations S240R and T284R [299,300]. The induction of a new arginine may lead to the development of a novel DNA interaction surface. No rescue mutations are known for mutations in the zinc ion binding site R175H, C176F and H179R [297].

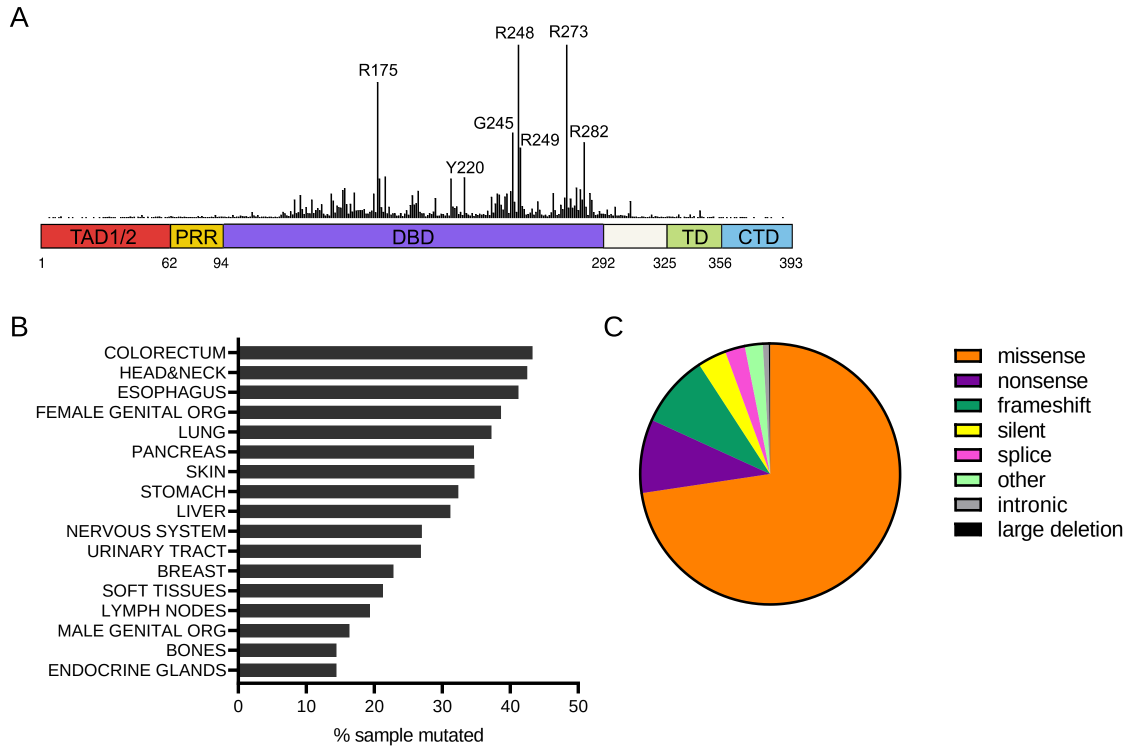

Fig. 4 Prevalence of the most common p53 mutations in cancer. **A:** The distribution of mutations in the amino acid sequence of p53 is displayed. Most mutations occur in the DBD. In the TAD, the PRR, the TD and the CTD mutations are less common. **B:** The prevalence of somatic p53 mutations in cancer according to the IARC TP53 database is displayed. **C:** The distribution of mutation types among all p53 mutations according to the IRAC TP53 database is displayed. The source data for this figure was abstracted from: https://p53.iarc.fr/

1.6 p53 in cancer therapy

1.6.1 Gene therapy

The transfer of the *TP53* gene inside an adenoviral vector was the first approved p53-related gene therapy treatment in China in 2004 [301]. Furthermore, the drug Advexin was developed as an anti-cancer drug consisting of an adenovirus carrying *TP53*. However, the benefit for patients was not sufficient for drug approval [302].

1.6.2 Treatment of p53 mutant cancer cells

Many compounds were developed to restore the p53 WT function in cells with mutations in *TP53*. The idea was that the compound would restore the WT conformation and thereby the p53 WT function of mutated p53 [303,304]. One of these compounds is PRIMA-1 that binds and modifies thiol groups in the central domain of mutated p53 [305]. First trials in mice showed no significant decrease in tumor size [306]. Nevertheless, PRIMA-1, under the name APR-246, is still in clinical trial phase two [307]. Another approach to restore the WT p53 function is the use of metallochaperons, which may facilitate the reincorporation of the zinc ion into mutated p53 and restore the DNA binding activity [308].

Moreover, mutated p53 can also serve as a novel anti-tumor antigen. Several immunotherapy approaches were developed and are still in clinical trials, for example peptide vaccination with p53 mutant peptides [309]. Another approach to target p53 mutant cancer cells is synthetic lethality. The p53 mutated cells are known to evade the apoptosis induced by DNA damaging agents. It could be shown that further inhibition of DDR components like ATM, ATR, Chk1 or Chk2 leads to hypersensitivity to genotoxic stress in p53 mutant tumors [310,311].

Finally, yet another approach to restore the p53 functionality is the peptide CDB3. It is derived from the p53 binding site of ASPP2, which binds the p53 core domain and raises the melting temperature of destabilised mutants [312,284–287].

Overall the p53 mutation status impacts the effect of DNA damaging drugs and patients' prognosis. Therefore, the sequencing of the *TP53* locus and the adjustment of cancer therapy to the p53 status is important to improve cancer therapy [313–315].

1.6.3 Treatment of p53 WT cancer cells

The aim of p53-dependent cancer therapy in p53 WT cells is to interrupt the interaction with MDM2 to enable elevated p53 function. The best working compounds, the Nutlins, were developed by Roche. Nutlins bind to the p53 binding pocket of MDM2, leading to extensive p53 response and tumor shrinkage in animal models [316,317].

Another small molecule with a comparable mode of action is RITA, which binds the MDM2 binding site of p53 [318]. Many of these compounds entered into clinical trials in the early 2000s [319]. Some MDM2 antagonists completed clinical trial phase one for the usage in leukaemia. Unfortunately, dose-dependent toxicities caused adverse effects such as neutropenia and thrombocytopenia [320]. However, MDM2 inhibitors may also be helpful in cyclotherapy. This is a strategy to increase the specificity of chemotherapeutic agents towards tumor cells with mutated p53 by arresting the cell cycle of p53 WT non-tumorous cells [321]. Therefore, a compound is used to transiently activate p53 WT in non-cancerous cells. As a result, the p53 mutant cancerous cells are not affected and progress in their cell cycle. Since the healthy cells are arrested, they are not as sensitive to the applied chemotherapeutic agents as the tumor cells. This strategy allows for higher dosages of chemotherapeutics by increasing their selective effect on the tumor cells [322].

1.7 Aim of this Study

The phosphorylation of residues in p53 plays a critical role in activating and modulating the p53 response. Therefore, investigating and understanding which phosphorylation and kinases play a role in the p53 response can improve individual cancer therapy.

To identify phosphorylations, endogenous p53 will be isolated from HCT116 cells and phosphorylations will be detected by mass spectrometry. To assign the phosphorylations to specific scenarios, p53 will be isolated from unstimulated cells and cells under DNA damage. The aim is to identify phosphorylation patterns and conditions and thus to gain new aspects in the modulation of the p53 response. Within this study the impact of these phosphorylations on the p53 functionality will be characterised with the help of phospho-mutant and phospho-mimic cell lines. In particular, the following will be investigated:

- Occurrence of the phosphorylations during the p53 response
- Relationship to other known p53 phosphorylations and mutations
- Influence of the phosphorylation on the p53 functionality as a transcription factor
- Influence of the phosphorylation on the p53 interactome
- Identification of possible kinases involved in the phosphorylation

2 MATERIAL AND METHODS

2.1 Material

2.1.1 Cells

2.1.1.1 Eukaryotic cell lines

Name	Cell type/ feature	p53 status	Source
HCT116 p53 WT	Human epithelial colorectal carcinoma cells	WT	Schmitz Lab (ATCC: CCL-247)
HCT116 p53$^{-/-}$	HCT116 cells with deletion in the 2. intron of *TP53*	-/-	Schmitz Lab
HCT116 p53$^{-/-}$ rec. p53 WT	HCT116 p53$^{-/-}$ cells reconstituted with p53 WT cDNA in the AAVS1 locus	WT	M. Treusch (this study)
HCT116 p53$^{-/-}$ rec. p53 T329A^{-}	HCT116 p53$^{-/-}$ cells reconstituted with p53 T329A cDNA in the AAVS1 locus	T329A	M. Treusch (this study)
HCT116 p53$^{-/-}$ rec. p53 T329E	HCT116 p53$^{-/-}$ cells reconstituted with p53 T329E cDNA in the AAVS1 locus	T329E	M. Treusch (this study)
HEK 293T	Human embryonic kidney cells expressing the large T antigen of SV40 virus	loss of function	Schmitz Lab (ATCC: CRL-3216)
HeLa	Human cervical carcinoma cells	loss of function	Schmitz Lab (ATCC: CRM-CCL-2)
A549	Human lung epithelial carcinoma cells	WT	Schmitz Lab (ATCC: CRM-CCL-185)
IGROV	Human ovarian endometrioid adenocarcinoma cell line	V126C	Schmitz Lab (ATCC: HTB-161)
MEF	Mouse embryonic fibroblast cells	WT	Schmitz Lab (ATCC: SCRC-1008)

2.1.1.2 E.coli strains

Strain	**Genotype**	**Source**
TOP10	F– *mcr*A Δ(*mrr-hsd*RMS-*mcr*BC) Φ80*lac*ZΔM15 Δ*lac*X74 *rec*A1 *ara*D139 Δ(*ara leu*) 7697 *gal*U *gal*K *rps*L (StrR) *end*A1 *nup*G	Invitrogen
BL21	fhuA2 [lon] ompT gal (λ DE3) [dcm] ∆hsdS λ DE3 = λ sBamHIo ∆EcoRI-B int::(lacI::PlacUV5::T7 gene1) i21 ∆nin5	Lab of Prof. Dr. Kracht (Giessen)

2.1.2 Antibodies

2.1.2.1 Primary antibodies

Name (clone)	**Species**	**Source**
anti-Flag (M2)	mouse mAb	Sigma
anti-H2A.X Ser139-P (JBW301)	mouse mAb	Millipore
anti-H3	rabbit pAb	Abcam
anti-HA (3F10)	rat mAb	Roche
anti-HIPK2 (5C6)	rat mAb	PMID: 27122605
anti-MDM2 (2A10)	mouse mAb	Merck Millipore
anti-p21^{WAF1} (EA10)	mouse mAb	Calbiochem
anti-p53 (DO-1)	mouse mAb	Santa Cruz
anti-p53 (FL-393)	rabbit aAn	Santa Cruz
anti-p53 Ser15-P	rabbit pAb	CST
anti-p53 Ser46-P	rabbit pAb	CST
anti-p53 Ser392-P	rabbit pAb	CST
anti-p53 Thr329-P	rabbit pAb	PSL
Anti-acetyl-p53 (Lys373, Lys382)	rabbit pAb	Upstate
anti-PARP (C-2-10)	mouse mAb	Sigma
IgG control	mouse pAb	Santa Cruz
IgG control	rabbit pAb	Santa Cruz
IgG control	rat pAb	Santa Cruz
anti-α-Tubulin (12G10)	mouse mAb	DSHB
anti-Vinculin (V9131)	mouse mAb	Sigma

anti-Chk1 Ser345-P (133D3)	rabbit mAb	CST
anti-Chk2 Thr68-P (C13C1)	rabbit mAb	CST
PmAb240	mouse mAb	Sigma
PmAb1620	mouse mAb	Sigma

2.1.2.2 Secondary antibodies

Name	Conjugated to	Source
goat-anti-mouse IgG	HRP	Dianova
goat-anti-rabbit IgG	HRP	Dianova
goat-anti-rat IgG	HRP	Dianova
Mouse TrueBlot® ULTRA: Anti-Mouse Ig HRP	HRP	ROCKLAND

2.1.3 Plasmids and vectors

Construct	Vector	Source
AAVS1 CRISPR-Cas9 clone	SH100	GeneCopoeia
AAVS1 MCS cloning vector puro	SH200	GeneCopoeia
AAVS1 p53 WT donor cloning vector puro	SH200	Maja Treusch (this study)
AAVS1 p53 T329A donor cloning vector puro	SH200	Maja Treusch (this study)
AAVS1 p53 T329E donor cloning vector puro	SH200	Maja Treusch (this study)
pCMV6–p53WT-IRES-GFP-Puro	pCMV6	Maja Treusch (this study)
pCMV6–p53T329A-IRES-GFP-Puro	pCMV6	Maja Treusch (this study)
pCMV6–p53T329E-IRES-GFP-Puro	pCMV6	Maja Treusch (this study)
HA-HIPK2	pEF-HA	S. Ritterhoff
pMSCV-neo-p53_V143A_72R	pMSCV	O. Timoveev AG Stieve (Marburg)

pMSCV-neo-p53_R175H_72R	pMSCV	O. Timoveev AG Stieve (Marburg)
pMSCV-neo-p53_R248W_72R	pMSCV	O. Timoveev AG Stieve (Marburg)
pMSCV-neo-p53_R273H_72R	pMSCV	O. Timoveev AG Stieve (Marburg)
pZW6-HA-CK2α	pZW6	Addgene (27086)

2.1.4 Oligonucleotides

2.1.4.1 qRT-PCR primer

Name	**Sequence (5’-3')**	**Target**
BAX_qPCR_fw	CGGGTTGTCGCCCTTTTCTA	*BAX*
BAX_qPCR_rv	GAAGTCCAATGTCCAGCCCA	*BAX*
MDM2_qPCR_fw	TAGGAGATTTGTTTGGCGTGC	*MDM2*
MDM2_qPCR_rv	CTGAGTCCGATGATTCCTGCT	*MDM2*
p53_qPCR2_fw	CAGTCACAGCACATGACGGA	*TP53*
p53_qPCR2_rv	GTACAGTCAGAGCCAACCTCA	*TP53*
TPI-cDNA-1-F	GGACTCGGAGTAATCGCCTG	*TPI*
TPI-cDNA-1-R	TGTTGGGGTGTTGCAGTCTT	*TPI*
BBC3_qPCR_fw	CGACCTCAACGCACAGTACG	*BBC3*
BBC3_qPCR_rv	GGGTGCAGGCACCTAATTGG	*BBC3*
CDKN1A_qPCR_fw	TACCCTTGTGCCTCGCTCAG	*CDKN1A*
CDKN1A_qPCR_rv	ATCAGCCGGCGTTTGGAGTG	*CDKN1A*
XPC_qPCR_fw	TGCGCTGATCGTTTCTTCCA	*XPC*
XPC_qPCR_rv	CTCAGGGGAAGGTAAGTGGC	*XPC*
CHEK1_qPCR_fw	GTGTCAGAGTCTCCCAGTGGAT	*CHK1*
CHEK1_qPCR_fw	GGTCACAGGAGAGAAGGAAT	*CHK1*
CSNK2A1_qPCR_fw	CTTCTCAGGGGAGGCAGGA	*CSNK2A1*
CSNK2A1_qPCR_rv	AAATGTTGAGTGAGTTGTGC	*CSNK2A1*
CDKN1A_ChIP_-2283_fw	AGCAGGCTGTGGCTCTGATT	*CDKN1A*
CDKN1A_ChIP_-2283_rv	CAAAATAGCCACCAGCCTCTTCT	*CDKN1A*
CDKN1A_ChIP_+11443_fw	TCTGTCTCGGCAGCTGACAT	*CDKN1A*

CDKN1A_ChIP_+11443_rv	ACCACAAAAGATCAAGGTGAGTGA	*CDKN1A*
MDM2_ChIP_fw	GGTTGACTCAGCTTTTCCTCTTG	*MDM2*
MDM2_ChIP_rv	GGAAAATGCATGGTTTAAATAGCC	*MDM2*
GADD45a_ChIP_fw	GCCTTTGTCCGACTAGAGTGT	*GADD45a*
GADD45a_ChIP_rv	GGATCTCTTCCGCTGCTG	*GADD45a*

2.1.4.2 Oligonucleotides for genome engineering and cloning

Name	Sequence (5'-3')	Target	Purpose
p53-seq-fw	CCCTGCCCTCAACAAGATGT	*TP53*	gDNA PCR, cloning
p53-seq-rv	GCACCACCACACTATGTCGA	*TP53*	gDNA PCR, cloning
p53-T329E-fw	ACTGGATGGAGAATATTTCGAACTT CAGATCCGTGGGC	*TP53*	mutagenesis
p53-T329E-rv	GCTCACGCCCACGGATCTGAAGTT CGAAATATTCTCCATC	*TP53*	mutagenesis
p53-T329A-fw	ACTGGATGGAGAATATTTCGCGCTT CAGATCCGTGGGC	*TP53*	mutagenesis
p53-T329A-rv	GCTCACGCCCACGGATCTGAAGCG CGAAATATTCTCCATC	*TP53*	mutagenesis
SH400 5' fw	CCGGAACTCTGCCCTCTAAC	*AAVS1*	gDNA PCR
SH400 5' rv	CCCGTGAGTCAAACCGCTAT	*AAVS1*	gDNA PCR
SH401 3' fw	AAGCTCATCTGGTCTCCCTTCC	*AAVS1*	gDNA PCR
SH401 3' rv	TCCTGGGATACCCCGAAGAG	*AAVS1*	gDNA PCR

2.1.4.3 siRNAs

Name	Sequence (5'-3')
MDM2_A SR302849A (ORIGENE)	CCCUAGGAAUUUAGACAACCUGAAA
MDM2_B SR302849B (ORIGENE)	GUACUAGACAACAUGUAAUUAAUGA
CHK1_1 s502 (Ambion)	GACACGAUUCUUUACCAAAtt (sense) UUUGGUAAAGAAUCGUGUCat (antisense)

CHK1_2 s503 (Ambion)	GCAUGGUAUUGGAAUAACUtt (sense) AGUUAUUCCAAUACCAUGCag (antisense)
CHK1_2 s503 (Ambion)	GCAACAGUAUUUCGGUAUAtt (sense) UAUACCGAAAUACUGUUGCca (antisense)
CSNK2A1_A SR319817A (ORIGENE)	GGUGGAAUAUUUCAUGGACAAAUTT
CSNK2A1_B SR319817B (ORIGENE)	AGUUUAAAAUGUUGAUACCUUCCCT
CSNK2A1_C SR319817C (ORIGENE)	CUGUACAGGUUUCAUGCUAGAGCTA
SR30004 siScramble negative control	

2.1.5 Enzymes

Name	**Source**
FastAP, alkaline Phosphatase	Thermo
Phusion HF DNA polymerase	Thermo
Restriction enzymes	Thermo, NEB
T4 DNA Ligase	Thermo
Taq DNA Polymerase	Thermo
Trypsin/0.05 % (v/v) EDTA	Life Technologies
Lambda protein phosphatase	NEB
RNase A	Thermo
Thermolysin from Geobacillus stearothermophilus	Sigma

2.1.6 Antibiotics

Name	**Working concentration**	**Source**
Ampicillin	100 μg/ml	Thermo
Kanamycin	50 μg/ml	Thermo
Puromycin	1 μg/ml	Thermo
Penicillin/streptomycin	1000 U/ml	Thermo

2.1.7 Inhibitors

Name	Working concentration	Target	Source
Anisomycin	5 µg/ml	protein synthesis	Sigma
Camptothecin	20 µM	type I topoisomerases	Sigma
MG132	10 µM	proteasome	Sigma
Nocodazole	100 ng/ml	microtubules	Sigma
Etoposide	20-100 µM	type II topoisomerases	Biotrend
4NQO	40 µM	type I topoisomerases	Sigma
Doxorubicin	200 ng/ml	type II topoisomerases	Santa Cruz
Nutlin-3a	10 µM	HMD2	Sigma
ATM Kinase Inhibitor (KN55933)	10 µM	ATM	Merck
ATM/ATR Kinase Inhibitor	10 µM	ATM, ATR	Merck
Chk2 Inhibitor II hydrate	10 µM	Chk2	Sigma
Gö 6983	10 µM	PKCα, β, γ, δ, ζ	Tocris
NU 7026	10 µM	DNA-PK	Biomol
NU 7441	10 µM	DNA-PK	Tocris
Roscovitrine	10 µM	CDK	Sigma
SB203580	10 µM	p38	Invitrogen
SB218078	10 µM	Chk1	Merck
Sp600125	10 µM	JNK	Enzo
Trichostatin A (TSA)	1 µM	HDAC	Adipogen
Casein kinase I inhibitor	10 µM	CK1	Merck
Aprotenin	10 µg/ml	Proteases	Sigma
Leupeptin	5 µg/ml	Proteases	Sigma
Sodium fluoride (NaF)	10 mM	Phosphatases	Roth
Phenylmethylsulfonyl fluoride (PMSF)	1 mM	Proteases	Sigma
Sodium orthovanadate (Na_3VO_4)	1 mM	ATPases, Phosphatases	Merck
CX-4945	10 µM	CK2α	Adooq

Gö 6976	10 µM	PKCα, β	Tocris
PKCα (C2-4) inihibitor peptide	10 µM	PKCα	Cayman Chemical
Ro-32-0432	10 µM	PKCα, β, ε	Millipore
Rotlerin	10 µM	PKCδ	Millipore
BJE6- 106 (B106)	10 µM	PKCδ	MedChem Express
LY333531 hydrochloride	10 µM	PKCβ, γ, δ, η	Sigma
Bafilomycin A1	500 nM	Autophagy	Invivogen
Chloroquine Di-Phosphate-salt ($C_{18}H_{26}ClN_3$ x $2H_3PO_4$)	100 nM	Autophagy	Sigma
NH_4Cl	50 mM	Autophagy	Merck

2.1.8 Chemicals

Name	Source
2-propanol (isopropanol)	Roth
4-(2-hydroxyethyl)-1-piperazineethanesulfonic acid (HEPES)	Sigma
Acetic acid	Roth
Acrylamide/bisacrylamide mix (37.5:1)	Roth
Adenosine triphosphate (ATP)	Thermo
Ammonium persulfate (APS)	Sigma
Bromophenol blue	Merck
Calcium chloride ($CaCl_2$)	Merck
Citric acid	Merck
PhosDimethyl sulfoxide (DMSO)	Sigma
Dithiothreitol (DTT)	Invitrogen
Ethanol	Sigma
Ethidium bromide	Roth
Ethylene glycol-bis(β-aminoethyl ether)-N,N,N',N'-tetraacetic acid (EGTA)	Sigma
Ethylenediaminetetraacetic acid (EDTA)	Sigma
Formaldehyde	Roth

Glutaraldehyde	Roth
Glycerol	Roth
Glycine	Roth
Hydrochloric acid (HCl)	Sigma
Hydrogen peroxide (H_2O_2)	Merck
Igepal CA-630	Sigma
Magnesium chloride ($MgCl_2$)	Sigma
Magnesium sulfate ($MgSO_4$)	Sigma
Methanol	Sigma
N,N,N',N'-tetramethylethylendiamin (TEMED)	Roth
PhosSTOP	Roche
Potassium chloride (KCl)	Sigma
Potassium ferricyanide ($K_3Fe(CN)_6$)	Sigma
Potassium ferrocyanide trihydrate ($K_4Fe(CN)_63H_2O$)	ICN Biomedicals
Potassium hydroxide (KOH)	Merck
Potassium phosphate (KH_2PO_4)	Sigma
Sodium azide (NaN_3)	Sigma
Sodium chloride (NaCl)	Sigma
Sodium deoxycholate	Sigma
Sodium dodecyl sulfate (SDS)	Bio-Rad
Sodium hydrogen phosphate (Na_2HPO_4)	Roth
Sodium hydroxide (NaOH)	Roth
Sodium meta-arsenite ($NaAsO_2$)	Sigma
Tris(hydroxymethyl)aminomethane (Tris)	Roth
Triton X-100	Sigma
Tween 20	Gerbu
β-mercaptoethanol	Roth

2.1.9 Other reagents and consumables

Name	**Source**
ABsolute qPCR SYBR green ROX Mix	Thermo

Agar	AppliChem
Agarose	PeqLab
Bovine serum albumin (BSA)	Sigma
Cell culture plastics	Sarstedt
Deoxynucleoside triphosphates (dNTPs)	Thermo
DMEM (Dulbecco's Modified Eagle Medium) high glucose, GultaMAX	Life Technologies (Gibco)
RPMI (Roswell Park Memorial Institute) 1640 Medium 1(x) GlutaMAX	Life Technologies (Gibco)
OptiMEM I (1x)	Life Technologies (Gibco)
FACSFlow	BD Bioscience
FACSRinse	BD Bioscience
FACSClean	BD Bioscience
Fetal calf serum	Life Technologies
GeneRuler 100bp & 1kb DNA ladders	Thermo
Melinex polyester film	Agar Scientific
PageRuler Plus prestained protein ladder	Thermo
Polyethylenimine, linear (PEI)	PolyScience
Protein G Plus/Protein A-Agarose beads	Millipore
Skimmed milk powder	Merck
Western Lightning ECL solutions	Perkin Elmer
Tryptone	Roth
Yeast Extract	AppliChem
TrypLE Express Enzyme (1x)	Gibco
Annexin V APC Ready Flow Reagent	Invitrogen
10x Annexin V Binding Buffer	Thermo Fisher Scientific
Lipofectamine 3000 Transfaction Kit	Invitrogen

2.1.10 Software

The Western blotting results were analysed with Image Lab by Bio-Rad. All FACS experiments were analysed with CellQuest Pro by DB. Graphs and the corresponding statistics were created with Graph Pad Prism 9. To arrange the figures, Microsoft Office

Powerpoint 2016 or Inkscape was used. The interactome network for the mass spectrometry analysis was created with Cytoscape.

2.2 Methods in molecular biology

2.2.1 Transformation of competent *E. coli*

To transform chemically competent *E.coli,* 0.5 -1 µg of plasmid DNA was added to the thawed cells on ice. After 30 min of incubation, the cells were treated with a 90 sec heat shock at 42 °C followed by a cool down on ice for 2 min. 800 µl of 1 x LB medium was added and the cells were incubated for 1 h at 37 °C. 50 µl were plated on an LB agar plate supplemented with the respective antibiotic. The plates were incubated for 16 h at 37 °C.

Lysogeny broth (LB) medium:	1 % (w/v) Tryptone; 0.5 % (w/v) Yeast extract; 1 % (w/v) NaCl
Lysogeny broth (LB) agar:	1.5 % (w/v) Agar in LB medium + antibiotics

2.2.2 Isolation of plasmid DNA from transformed *E. coli*

To amplify and isolate plasmid DNA, an overnight bacterial culture was prepared. One colony from an agar plate was selected and incubated in 1 x LB medium with the appropriate antibiotic for selection for 16 h at 37 °C with 180 rpm shaking. According to the required amount, either 2 ml for a Miniprep or 250 ml for a Maxiprep were prepared The plasmid DNA was isolated using the GeneJet Plasmid Maxiprep Kit (Thermo) or the GeneJet Plasmid Miniprep Kit (Thermo) following the manufacturer's instructions.

The concentration of the isolated plasmid DNA was measured in a microliter cuvette using an Eppendorf photometer. The measurement is based on the optical density (OD) at 260 nm (OD 1 at 260 nm = 50 ng/µl). The relation to OD at 280 nm was used to determine the purity of the isolated plasmid DNA (OD_{260}/OD_{280} for pure DNA approx. 1.8).

2.2.3 Isolation of genomic DNA

The genomic DNA from cultured cells was isolated with the NucleoSpin Tissue Kit (Macherey-Nagel). After following the user manual for cultured cells, a RNase treatment was performed for 1 h at 37 °C. The quantity and quality were determined by the OD_{260} measurement and the relation to OD_{280}.

2.2.4 Polymerase chain reaction (PCR)

PCR was used for different approaches, either with genomic DNA or plasmid DNA. All reactions were performed in a T100 Thermal Cycler (Bio-Rad) in 0.2 ml PCR stripes.

PCR with purified plasmid DNA or transformed bacteria:

Reaction mix:	Cycling conditions:		
2.5 U Tag DNA polymerase	Initial denaturation:	5 min at 94°C	
1 x PCR buffer –Mg	Denaturation:	45 sec at 94°C	x 30 - 35
1.5 mM $MgCl_2$	Annealing:	30 sec at 55-65°C	
0.2 mM dNTPs	Elongation:	30-120 sec at 72°C	
0.5 µM primer fw	Final elongation:	10 min at 72°C	
0.5 µM primer rv			
100 ng plasmid or 1 bacterial colony			
MilliQ water (add to a total volume of 50 µl)			

PCR with human genomic DNA:

Reaction mix:	Cycling conditions:		
1.2 U Phusion HF DNA polymerase	Initial denaturation:	30 sec at 98°C	
1 x Phusion HF buffer	Denaturation:	10 sec at 98°C	x 30
0.2 mM dNTPs	Annealing:	10 sec at 55-65°C	
0.5 µM primer 1	Elongation:	30 sec at 72°C	
0.5 µM primer 2	Final elongation:	1 min at 72°C	
100 ng genomic DNA			
MilliQ water (add to a total volume of 50 µl)			

The PCR products were visualised by agarose gel electrophoresis.

2.2.5 Restriction digestion of DNA with endonucleases

For cleavage of specific sequences by restriction enzymes, 3 µg plasmid was used. 5 U of restriction enzyme and the appropriate buffer were added to a total volume of 30 µl. All digestions were performed at 37 °C for 2 - 16 h. To inhibit the re-ligation, 4 U of FastAP was added to the digestion mix, to dephosphorylate the 5' phosphate groups. The reaction took place at 37 °C for 2 h and was followed by the deactivation of the enzymes for 15 min at 65 °C. The resulting fragments were analysed on a 1 - 2 % agarose gel stained with ethidium bromide.

2.2.6 Agarose gel electrophoresis

To visualise DNA fragments, an agarose gel electrophoresis was performed with a 1 - 2 % (w/v) agarose gel dissolved in 1 x TAE buffer and mixed with 0.2 µg/ml ethidium bromide. The DNA sample was mixed with loading dye and loaded to the horizontal gel covered with 1 x TAE buffer. The samples and a molecular weight marker were separated at 80 V for 30 - 120 min. The DNA was visualised with a UV lamp. For further use, the required DNA fragments were removed with a scalpel and extracted with the SmartPure Gel Kit (Eurogentec) following the manufacturer's instructions.

Tris-acetate-EDTA (TAE) buffer: 4 mM Tris (pH 8.3); 50 mM acetic acid; 1 mM EDTA

2.2.7 Ligation of DNA fragments

200 ng of vector DNA was ligated with an insert in the molecular ratio of 1 : 3. 1 U of T4 DNA ligase and the appropriate buffer were added to the DNA. Water was added to a total volume of 10 µl. The ligation was incubated at RT for 30 min. Ligations of blunt-end fragments took place at a temperature gradient from RT to 4 °C overnight.

2.2.8 Isolation of RNA

For the total RNA isolation, the eukaryotic cells were harvested by scraping and washed twice with cold PBS. The RNA was extracted with the NucleoSpin RNA Kit (Macherey-Nagel) by following the manufacturer's protocol. The eluted RNA quantity was checked by optical density measurement at 260 nm (OD_{260}) with an Eppendorf photometer using a microliter cuvette. To determine the quality of the isolated RNA, the ratio of OD_{260}/OD_{280} was determined.

Phosphate buffer saline (PBS): 137 mM NaCl; 8.1 mM Na_2HPO_4; 2.7mM KCl; 1.5 mM KH_2PO_4 (pH 7.4)

2.2.9 Synthesis of complementary DNA (cDNA)

A reverse transcription reaction was performed with the TaKaRa PrimeScriptTMRT Master Mix Kit following the manufacturer's protocol to synthesise cDNA from RNA. A total amount of 0.5 µg RNA was used and diluted to a final volume of 50 µl after cDNA synthesis.

2.2.10 Quantitative real-time PCR (qRT-PCR)

To determine the relative expression of mRNA, a quantitative real-time PCR (qRT-PCR) was performed. The PCR reaction was performed in a volume of 10 µl in duplicates in 96 well PCR plates (Sarstedt).

<u>Reaction Mix:</u>

1 x SYBR Green ROX Master Mix

10 ng cDNA

0.2 µM Primer Mix (fw and rv)

The plate was sealed with an optical adhesive plate. The PCR was performed with a StepOnePlus Real-Time PCR system (Applied Biosystems) with the following program:

Initial denaturation	95°C	10 min	
Denaturation	95°C	15 sec	
Annealing	60°C	30 sec	x 35
Elongation	72°C	30 sec	
Final elongation	72°C	30 sec	

A melting curve was generated to visualise the amplified products and to review the specificity of the used primer.

The amount of dsDNA in the reactions was measured via fluorescence. The OneStepPlus software determines a C_T value compared to the measured background. By subtracting the C_T value from a housekeeping gene, the relative ΔC_T was determined. In order to relate the samples to each other, the ΔC_T value of a control sample was subtracted from the ΔC_T value of the unknown samples. The given $\Delta\Delta C_T$ values were transformed into absolute values using the formula: $R = 2^{-\Delta\Delta CT}$. This value can be used to compare the expression of genes in different samples.

2.2.11 Mutagenesis

To mutate a specific residue, the QuickChange II Site-Directed Mutagenesis Kit (Agilent Technologies) was used. The mutagenesis was carried out according to the manufacturer's protocol with some adjustments. The length of the primer was extended to approx. 40 bp.

<u>Reaction mix:</u>

2.5 U PfuUltra High Fidelity DNA polymerase
1 x reaction buffer
1 µl dNTP Mix
125 ng primer 1
125 ng primer 2
3 µl QuickSolution
100 ng plasmid DNA
MilliQ water (add to a final volume of 50 µl)

<u>Cycling conditions:</u>

Initial denaturation:	1 min at 95°C	
Denaturation:	50 sec at 95°C	
Annealing:	50 sec at 55°C	x18
Elongation:	2.5 min per/kb. at 68°C	
Final elongation:	1 min at 68°C	

The *Dpn I* digested samples were transformed into TOP10 E.coli cells using 1 x LB medium.

2.2.12 RNA-Seq

The total RNA was sequenced to analyse the transcriptome. The cells were seeded in a 10 cm cell culture dish. After 24 h, half of the plates were stimulated with 20 µM etoposide for 16 h. The total RNA was isolated with the NucleoSpin RNA Kit (Macherey-Nagel) by following the manufacturer's protocol. The RNA sequencing was performed in collaboration with PD Dr. Torsten Hain (Medical institute of microbiology; JLU Giessen). The quality and quantity were determined with Qubit RNA HS Assay Kit and Bioanalyzer RNA 6000 Nano assay Kit. The rRNA was depleted with NEBNext rRNA Depletion Kit (Human/Mouse/Rat). The sequencing library was created with the NEBNext Ultra II Directional RNA Library Prep Kit for Illumina following the manufacture's protocol. The RNA was sequenced in 75 cycles with a single-read method by Illumina NextSeq500 High Output. Per sample $2x10^7$ – $2,6x10^7$ reads were detected. The Adaptor trimming was carried out with Cutadapt, followed by the mapping to the human genome with Tophat. The reads were counted with featureCounts. The differential expression analysis was performed by DESeq2.

2.3 Methods in cell biology

2.3.1 Maintenance of eukaryotic cell lines

The used eukaryotic cell lines were cultured at 37 °C with 5 % of CO_2 in cell culture flasks (Sarstedt). They were grown in the appropriate medium:

HCT116, HeLa, HEK3934, A459, MEF:	DMEM complete
IGROV:	RPMI complete
HCT116 $p53^{-/-}$ rec. p53:	DMEM complete + 1 µg/ml Puromycin

In order to split the cells, the medium was removed. The adhered cells were carefully washed with warm PBS. To detach the cells, trypsin was added and incubated for 3 - 5 min at RT. To stop the proteolytic reaction, medium was added in a 1 : 1 ratio. The cell suspension was resuspended and centrifuged (300 x g 3 min). After removing the supernatant, the cells were resuspended in fresh medium and distributed in new cell culture flasks or counted and seeded for experiments.

For storage at -150 °C, approx. $1x10^7$ cells were pelleted and resuspended in 1 ml of freezing medium. The aliquots were frozen in a styrofoam box at -80 °C and transferred to -150 °C after 3 days. After thawing, the cells were washed once in medium and seeded in cell culture flasks.

DMEM complete:	Dulbecco’s Modified Eagle Medium (DMEM) high glucose (1x) GultaMAX (gibco) + 10 % (v/v) FCS + 1 % (v/v) Penicillin/Streptomycin
RPMI	Roswell Park Memorial Institute (RPMI) 1640 Medium 1(x) GlutaMAX (gibco) + 10 % (v/v) FCS + 1 % (v/v) Penicillin/Streptomycin
Freezing medium:	10 % (v/v) DMSO in FCS

Phosphate buffer saline (PBS): 137 mM NaCl; 8.1 mM Na2HPO4; 2.7mM KCl; 1.5 mM KH2PO4 (pH 7.4)

2.3.2 Counting of cells

To count the eukaryotic cells, a 10 µl aliquot of a well resuspended cell suspension was used. The cells were mixed 1 : 1 with trypan blue to allow differentiation between alive and dead cells. The cell membrane of dead cells cannot prevent the penetration of trypan blue into the cell, which results in blue staining. 10 µl of the cells were added into a Luna cell counting slide (logos), and the cell number was counted used the LUNA II Automated Cell Counter (logos).

2.3.3 Transfection of eukaryotic cells

One day before transfection, the cells were seeded in cell culture dishes. The transfection reagent was chosen separately for each cell line to achieve the best transfection efficiency.

HEK393T: linear PEI

HCT116: Lipofectamine 3000

For transfection with PEI, 1 µg plasmid was used to transfect $1x10^6$ cells. The plasmid and 3 µl PEI per 1 µg plasmid were added to 500 µl of Opti-MEM. The transfection mix was incubated at RT for 15 min. For the transfection with Lipofectamine 3000, 3 µg Plasmid was used to transfect $1x10^6$ cells. The DNA and 2 µl P3000 reagent per 1 µg DNA were added to 250 µl OptiMEM. To another 250 µl OptiMEM, the Lipofectamine 3000 was added (6 cm dish: 3.75 µl; 10 cm dish: 7.5 µl). Both solutions were mixed and incubated at RT for 15 min.

The cells were washed once with PBS and covered with DMEM Medium + 10 % FCS. The transfection mixture was added dropwise to the cells. In order to absorb the plasmid into the cell, the cells were incubated at 37 °C for 4 h. After the transfection, the medium was removed and the cells were covered with DMEM complete. For the expression of proteins, the cells were grown for 24 - 48 h.

2.3.4 Transfection of eukaryotic cells with siRNA oligos

One day before transfection, the cells were seeded in cell culture 6 well plates. The siRNA (final concentration of 10 nM) was premixed with 3.75 µl Lipofectamine 3000 in 250 µl Opti-MEM. The transfection mixture was incubated at RT for 15 min. The medium on the cells was exchanged to DMEM Medium + 10 % FCS. The transfection mixture was added dropwise to the cells. The cells were incubated for 24 h before the medium was removed, and the cells were covered with DMEN complete. After further incubation for 24 – 48 h, the cells were harvested and analysed by Western blotting or qPCR.

2.3.5 Reconstitution of HCT116 $p53^{-/-}$ cells with p53 variants in the safe harbor locus

To reconstitute HCT116 $p53^{-/-}$ cells with p53 variants, the Genome-CRISPR™ Human AAVS1 Safe Harbor Gene Knock-in Kit was used. It allows the integration of the gene of interest (GOI) into the AAVS1 locus, which results in adequate expression levels and does not affect adjacent genes. $1x10^4$ – $1x10^5$ cells were seeded in a 10 cm cell culture dish to allow colony formation. The cells were transfected with two plasmids:

1. AAVS1 CRISPR Cas9 vector to cut the AAVS1 locus,
2. AAVS1 donor Vector containing the p53 variant with a puromycin resistance- and a GFP selection gene embedded in two homology arms for the AAVS1 locus.

One day after transfection, the cell medium was supplemented with 1 µg/ml puromycin to select cells containing the donor plasmid. The homolog sequences can lead to the integration of the plasmid into the AAVS1 locus by homology-directed repair (HDR). To trigger HDR, the Cas9 enzyme cuts the AAVS1 locus in the homolog region. The cell clones that have integrated p53 into the AAVS1 locus were selected by Western blotting and confirmed with genomic PCR and sequencing.

2.3.6 Preparation of whole-cell extracts

To analyse proteins, the cells were lysed with the appropriate lysis buffer depending on the localisation and solubility of the protein of interest (POI). The cells were harvested by scraping and pelleting (300 x g; 3 min; 4 °C), followed by washing with cold PBS. The pellet was then resuspended in lysis buffer and incubated for 30 min on ice. Afterwards, the samples were centrifugated (16000 x g; 10 min) and the supernatant was removed and used for later experiments. To determine the protein concentration, a BCA was performed with the BCA Protein Assay Kit (Thermo) following the manufacturer's instructions. The lysates were stored at -20 °C. For Western blotting, the samples were mixed with 5 x SDS sample buffer and incubated at 95°C for 10 min.

To analyse insoluble or chromatin bound proteins, the cell pellet was resuspended in 1 x SDS sample buffer and sonicated twice for 20 sec. The samples were also incubated at 95 °C for 10 min.

RIPA lysis buffer:	50 mM Tris/HCl (pH 7.4); 150 mM NaCl; 0.5 % (w/v) Na-deoxycholate, 0.1 % (w/v) SDS; 1 % (v/v) Igepal CA-630; 1 mM EDTA; <u>freshly added</u>: 10 mM NaF; 1 mM Na_3VO_4; 10 µg/ml Aprotinin; 5 µg/ml Leupeptin; 1 mM PMSF
NP40 lysis buffer:	20 mM Tris/HCl (pH 7.5); 150 mM NaCl; 10 % (v/v) Glycerol; 1 % (v/v) Igepal CA-630; <u>freshly added</u>: 10 mM NaF; 1 mM Na_3VO_4; 10 µg/ml Aprotinin; 5 µg/ml Leupeptin; 1 mM PMSF

5x SDS sample buffer: 250 mM Tris/HCl (pH 6.8); 10 % (w/v) SDS; 40 % (v/v) Glycerol; 15 % (v/v) β-Mercaptoethanol; 0.1 % (w/v) Bromphenol blue

2.3.7 Subcellular fractionation of cells

To analyse the protein localisation, the cells were partly lysed to achieve subcellular fractionation. After harvesting and washing the cells with PBS, they were resuspended in a mild lysis buffer A to extract the cytoplasmic proteins. The samples were incubated on ice for 5 min. 5 µl of a 10% (v/v) Igepal CA-630 solution was added to the samples, followed by vortexing and centrifugation (16000 x g; 4 °C; 30 sec). The supernatant (C fraction) was removed and stored. The pellet was washed with buffer A, and the supernatant was discarded. The remaining pellet was lysed in 100 µl of buffer C for 20 min on ice. The samples were again centrifuged (16000 x g; 4 °C; 10 min), and the supernatant removed and stored (N1 fraction). The pellet was washed with buffer C. The supernatant was discarded, and the pellet was lysed with 1 x SDS buffer. Therefore, the sample was sonicated twice for 20 sec with 150 µl 1 x SDS sample buffer (N2 fraction). The fractions C and N1 were mixed with 5 x SDS sample buffer, and all samples were incubated at 95°C for 10 min.

Buffer A: 10 mM HEPES (pH 7.9); 10 mM KCl; 0.1 mM EDTA; 0.1 mM EGTA; 1 mM β-Mercaptoethanol freshly added: 10 mM NaF; 1 mM Na_3VO_4; 10 µg/ml Aprotinin; 5 µg/ml Leupeptin; 1 mM PMSF

Buffer C: 20 mM HEPES (pH 7.9); 400 mM NaCl; 1 mM EDTA; 1 mM EGTA; 1 mM β-Mercaptoethanol; freshly added: 10 mM NaF; 1 mM Na_3VO_4; 10 µg/ml Aprotinin; 5 µg/ml Leupeptin; 1 mM PMSF

2.3.8 UVC radiation

To induce DNA strand breaks, the cells were treated with UVC radiation. The cells were cultured in 10 cm or 6 cm cell culture dishes. The medium was removed, and the cells were carefully washed once with warm PBS. The PBS was removed, and the dish was placed in the UV Stratalinker 1800 (STRATAGENE) without the lid. The cells were exposed to 20 - 50 J/m^2. After UVC radiation, the cells were washed once with warm PBS and fresh medium was added.

2.3.9 Fluorescence-activated cell scanning (FACS) analysis

2.3.9.1 Measurement of apoptosis

The staining of phosphatidylserine (PS) on the cells' surface with Annexin V was used to determine the amount of apoptotic cells. PS exists in healthy cells only in the cytoplasmatic layer of the cell membrane. In the case of apoptosis, it flips to the outer layer and gets exposed to the cell's surroundings. It can then be stained with the PS binding protein Annexin V, which is linked to allophycocyanin (APC), and can thereby be detected with a FACS approach. The cells were harvested by detaching them with a mild trypsin digest (TrypLE). The cells were washed once with PBS and a second time with binding buffer (Annexin Binding Buffer 5x by Thermo Fisher SCIENTIFIC). The pellet was resuspended in 300 µl binding buffer, and one drop of Annexin V APC Ready Flow Konjugate (Thermo Fisher SCIENTIFIC) was added. The samples were vortexed and incubated at RT for 15 min. The APC signal was analysed with a FACSCalibur (BD Biosciences) flow cytometer with the BD CellQuest Pro software.

2.3.9.2 Cell cycle distribution analysis

The amount of DNA in the cells was measured in order to determine the cell cycle state. The DNA was stained with propidium iodide (PI) and measured by a FACSCalibur (BD Biosciences) flow cytometer. The cells were harvested by detaching with TrypLE Express. The cells were washed twice with PBS (300 x g; 2 min) and resuspended in 500 µl PBS. The cells were fixed with 1 ml of chilled 70 % (v/v) ethanol, which was added dropwise during continuous vortexing. The samples were incubated at 4 °C for 1 h. The samples were washed twice with PBS (300 x g; 2 min), followed by resuspension with 500 µl of PI staining solution. The staining took place in dark at 37 °C for 15 min. The samples were transferred to ice, and the PI staining was analysed by FACS. Since the amount of DNA doubles during the S phase, the intensity of the PI signal can be translated into cell cycle phases. The data were recorded with the BD CellQuest Pro software.

PI staining solution: 20 µg/ ml Propidium Iodide; 200 µg RNase A; 0.1 % (v/v) Triton-X-100 in PBS

2.3.10 Measurement of cell senescence

To detect senescent cells, the amount of active β-galactosidase was stained. The expression of the β-galactosidase is highly increased in senescent cells, and therefore, the staining in these cells is more intense than in non-senescent cells. The cells were seeded in a cell culture 12 well plate. The senescence was induced by doxorubicin or bleomycin. Before staining, the cells were washed twice with PBS and fixed with fixation solution for 5 min. After two additional washing steps with PBS, the cells were incubated for 16 h at 37 °C with X-gal staining solution. The β-galactosidase hydrolyses the x-gal to galactose and a blue dye. After the incubation, the cells were washed once with methanol. The plate was air-dried at RT. The developed blue staining was visualised with a light microscope and a Motic Moticam 1000.

Fixation solution: 2 % (v/v) Formaldehyde; 0.2 % (v/v) Glutaraldehyde in PBS

X-gal staining solution: 20 mM Citric Acid; 40 mM Na_2HPO_4; 150 mM NaCl; 5 mM $K_4Fe(CN)_6 3H_2O$; 5 mM $K_3Fe(CN)_6$; 2 mM $MgCl_2$; 1 mg/ml X-gal

2.4 Biochemical methods

2.4.1 SDS polyacrylamide gel electrophoresis (SDS-PAGE)

To analyse the protein lysates, they were separated via molecular weight in a SDS-PAGE. The samples were mixed with SDS sample buffer, incubated at 95 °C for 10 min, and loaded on a denaturing polyacrylamide gel. The percentage of acrylamide was adjusted to the molecular weight of the POI. The electrophoresis was performed at 80 V for 2.5 h in a Bio-Rad mini gel system. A pre-stained molecular marker was used to determine the molecular weight of the analysed proteins. Depending on their primary structure, the reduced denatured proteins migrate through the gel matrix faster or slower and they separate depending on their molecular weight.

Stacking gels: 4 % (v/v) Acrylamide; 125 mM Tris/HCl (pH 6.8); 0.1 % (w/v) SDS; 0.1 % (v/v) APS; 0.1 % (v/v) TEMED

Separating gels: 6 - 15 % (v/v) Acrylamide; 375 mM Tris/HCl (pH 8.8); 0.1 % (w/v) SDS; 0.05 % (v/v) APS; 0.05 % (v/v) TEMED

SDS running buffer: 25 mM Tris; 200 mM Glycine; 1 % (w/v) SDS

2.4.2 Western blot and immune detection

The separated proteins were transferred from the polyacrylamide gel to a PVDF membrane to enable the detection via antibodies. The membrane was activated in 100 % methanol, and the Whatman filter papers were soaked in transfer buffer. The Western blotting was assembled on a Bio-Rad blotting chamber using a semidry approach (Two Whatman papers – membrane – gel – Whatman paper). The transfer took place at 24 V for 1 - 1.5 h per membrane. The membranes were blocked for 1 h in the blocking solution to minimise the primary antibody's unspecific binding. The incubation with the primary antibody was carried out for 16 h at 4 °C. Afterwards, the membranes were washed four times with TBS-T for 5 min. The secondary antibody was added to the membranes and incubated for 1 h at RT. The membranes were washed four times for 5 min, and the signal was analysed via a ChemiDoc Touch imaging system (Bio-Rad) by detection of enhanced chemiluminescence (ECL).

Transfer buffer:	50 mM Tris; 40 mM Glycine; 20 % (v/v) Methanol; 0.04 % (w/v) SDS
TBS-T:	25 mM Tris (pH 7.4); 137 mM NaCl; 5 mM KCl; 0.7 mM $CaCl_2$; 0.1 mM $MgCl_2$; 0.1 % (v/v) Tween 20
Blocking buffer:	5 % (w/v) Skimmed milk powder or BSA in TBS-T
1st antibody solution:	1 - 5 % (w/v) Skimmed milk powder or BSA in TBS-T; 0.05 % (v/v) NaN_3
2nd antibody solution:	1 % (w/v) Skimmed milk powder or BSA in TBS-T

2.4.2.1 Stripping for re-probing of membranes

The membranes were incubated with stripping buffer with a low pH to remove the primary and secondary antibodies from the membrane and enable re-staining. The membranes were incubated in stripping buffer two times for 10 min at RT. The membranes were then washed two times for 5 min in PBS and two times for 5 min in TBS-T. The membrane was blocked again and incubated with the next primary antibody.

Stripping buffer:	0.2 M Glycine; 0.1 % (w/v) SDS; 1 % (v/v) Tween-20 pH: 2.0

2.4.3 λ protein phosphatase (λ PP) assay

To determine the specificity of phospho-specific antibodies, the protein lysates were dephosphorylated by λ phosphatase (λ-PP). The lysate was carried out without inhibitors for phosphatases and proteases. 1 x NEBuffer for Protein Metallo-Phosphatases (PMP) containing 1 mM $MnCl_2$ and 400 U of λ-PP were added to the lysate. The samples were incubated for 30 min at 30 °C. The samples were mixed with 5 x SDS sample buffer and incubated at 95 °C for 10 min to stop the reaction. The samples were stored at -20 °C and analysed via SDS-PAGE and Western blotting.

2.4.4 Protein crosslinking

To visualise protein aggregates or oligomers, the native proteins in the lysate were crosslinked before denaturation. The cells were lysed with the crosslinking lysis buffer for 30 min on ice followed by centrifugation (16000 x g; 10 min; 4 °C). 0.025-0.05 % of glutaraldehyde was added to the lysate for 5 min at RT. The glutaraldehyde creates a covalent binding between the existing protein aggregates. The reaction was terminated by the addition of 5 x SDS buffer and incubation at 95°C for 10 min. The samples were analysed by SDS-PAGE and Western blotting.

Crosslinking lysis buffer: 50 mM HEPES (pH 7.5); 350 mM NaCl; 10 % (v/v) glycerol; 1 % (v/v) Igepal CA-630; freshly added: 10 mM NaF; 1 mM Na_3VO_4; 10 µg/ml aprotinin; 5 µg/ml leupeptin; 1 mM PMSF

2.4.5 Limited protein digest

Digestion of native proteins with proteases leads to a conformation-specific cleavage pattern which can be visualised by Western blotting. To investigate the conformation of isolated proteins the cells were lysed according to 2.3.6 without protease inhibitors. Parts of the lysate were treated with trypsin (diluted in the lysate to a final ratio of trypsin:lysate of 1:6 or 1:12) or thermolysin (final concentration 5 ng/µl) for 20 min at 37 °C. To stop the proteolytic digest, the samples were mixed with 5 x SDS sample buffer and incubated at 95°C for 10 min.

Trypsin cuts proteins after arginine or lysine, and thermolysin after hydrophobic amino acids like leucine, isoleucine and phenylalanine. This cleavage pattern was visualised with DO-1 antibody which detects the N-terminal part of p53 and the FL-393 antibody which detects the C-terminal part of p53. A mixture of both were used to visualise all fragments containing the C- and/or the N-terminal part.

2.4.6 Co-Immunoprecipitation (Co-IP)

For co-immunoprecipitation of native proteins to confirm their interaction, the cells were lysed in RIPA buffer as described in 2.3.6. The lysate was diluted in a 1 : 2 ratio with dilution buffer and incubated with constant rotation for 1 h at 4 °C with AG-Sepharose beads for pre-clearing. After centrifugation (800 x g; 1 min), 10 % of the cleared lysate was removed as an input. Fresh AG-Sepharose beads were washed 2 x with wash buffer and mixed with the residual pre-cleared lysate and the antibody against the POI (25 µl AG-Sepharose beads per 1 µg of antibody). The precipitation took place at constant rotation for 3 h at 4 °C. The samples were washed four times for 5 min at 4 °C (centrifugation: 800 x g; 4 °C; 1 min). After the last washing step, the supernatant was removed thoroughly, and the beads were resuspended in 50 µl 2 x SDS sample buffer. During a 10 min incubation at 95 °C, the proteins were eluted from the beads. The eluate was separated from the beads by centrifugation (16000 x g; 3 min; RT) and was analysed by SDS-PAGE and Western blotting.

RIPA lysis buffer: 50 mM Tris/HCl (pH 7.4); 150 mM NaCl; 0.5 % (w/v) Na-deoxycholate, 0.1 % (w/v) SDS; 1 % (v/v) Igepal CA-630; 1 mM EDTA; freshly added: 10 mM NaF; 1 mM Na_3VO_4; 10 µg/ml Aprotinin; 5 µg/ml Leupeptin; 1 mM PMSF

Dilution/Wash buffer: 20 mM Tris/HCl (pH 7.5); 150 mM NaCl; 10 % (v/v) Glycerol; 0.5 % (v/v) Igepal CA-630; freshly added: 10 mM NaF; 1 mM Na_3VO_4

2.4.7 ChIP

The cells were fixed by incubation in cell culture medium with 1 % formaldehyde for 10 min at RT. To stop the reaction, glycine was added to a final concentration of 0.1 M and incubated for 5 min at RT. The cells were harvested by scraping and centrifugation (300 x g; 5 min; 4 °C). The cell pellet was washed with PBS containing 1 mM PMSF to remove residual formaldehyde. After resuspension of the cell pellet in lysis buffer, the samples were incubated on ice for 10 min. The chromatin was sheared with a Covaris S220-Sonicator with the following settings: Power: high; 30 sec on – 30 sec off; 13 cycles. The samples were centrifuged (16000 x g; 15 min; 4 °C), and a 20 µl aliquot was taken to determine the chromatin concentration. The remaining samples were frozen at -80 °C. The aliquot was mixed with 100 µl TE buffer and 1 µl RNase A (10 mg/ml) and incubated at 37°C for 30 min. Subsequently, 7.5 µl 10 % SDS and 3.8 µl Proteinase K (20 mg/ml) were added to re-crosslink the samples and to digest the bound proteins. The reactions were carried out for 2 h at 37 °C followed by 65 °C for 16 h. The DNA was purified with the PCR Clean-Up Kit (Macherey & Nagel) with the NTB binding buffer, suitable for cleaning up SDS-containing samples. The DNA was eluted in 50 µl elution buffer. The concentration of the isolated genomic DNA was measured in a microliter cuvette using an Eppendorf photometer. To control the chromatin shearing efficiency, 20 µl DNA was analysed on a 1 % agarose gel (100 V; 30 - 45 min). The chromatin fragments' size should be between 100 - 500 bp to enable an efficient qPCR later on. The frozen chromatin samples were thawed on ice. 25 µl of AG-Sepharose beads were equilibrated in dilution buffer. 24 µg chromatin was used for one antibody, and 2.4 µg chromatin was removed as a 10 % input control. The chromatin was diluted with 900 µl dilution buffer and incubated with the beads for 2 h at 4 °C for pre-clearing. The diluted pre-cleared chromatin was removed from the beads and mixed with the appropriate amount of antibody. The incubation of the lysate with the antibody was carried out with continuous rotation for 16 h at 4 °C. Afterwards, the equilibrated beads (25 µl per 1 µg antibody) were added to the chromatin and incubated for 2 h at 4 °C under continuous rotation. The samples were washed four times for 5 min at 4 °C by centrifugation (800 g; 1 min; 4 °C) and resuspension in the appropriate buffer (1 x high salt buffer; 1 x LiCl buffer; 2 x TE buffer). The input was thawed and treated the same way as the beads with removed supernatant. The beads/input were resuspended in 100 µl TE buffer, supplemented with 1 µl RNase A (10 mg/ml) and incubated at 37°C for 30 min. Subsequently, 7.5 µl 10 % SDS and 3.8 µl Proteinase K (20 mg/ml) were added.

The reactions were carried out for 2 h at 37 °C followed by 65 °C for 16 h. The DNA was purified with the PCR Clean-Up Kit (Macherey & Nagel) with the NTB binding buffer suitable to clean up SDS-containing samples. The DNA was eluted in 50 µl elution buffer. For following qRT-PCR experiments, the input was diluted in water to 1 %. The determined C_T values were evaluated relative to the C_T value of the 1 % input.

Lysis buffer:	50 mM Tris/HCl (pH 8.1); 1 % (w/v) SDS; 10 mM EDTA; freshly added: 1 x PhosStop phosphatase inhibitor cocktail; 1 mM PMSF
Dilution buffer:	16.7 mM Tris/HCl (pH 8.1); 167 mM NaCl; 1.1 % (v/v) Triton X-100; 0.01 % (w/v) SDS; 1.2 mM EDTA
High salt buffer:	20 mM Tris/HCl (pH 8.1); 500 mM NaCl; 1 % (v/v) Triton X-100, 0.1 % (w/v) SDS; 2 mM EDTA
Low salt buffer:	20 mM Tris/HCl (pH 8.1); 150 mM NaCl; 1 % (v/v) Triton X-100; 0.1 % (w/v) SDS; 2 mM EDTA
TE buffer:	10 mM Tris/HCl (pH 8.0); 1 mM EDTA
LiCl buffer:	10 mM Tris/HCl (pH 8.1); 250 mM LiCl; 1 % (w/v) Deoxycholate; 1 % (v/v) Igepal CA-630; 1 mM EDTA

2.4.8 Mass spectrometry

A mass spectrometry analysis of immunoprecipitated p53 was performed to identify the p53 interacting proteins. The cells were seeded in 15 cm cell culture dishes and stimulated with 30 µM etoposide for 16 h. The cells were lysed with RIPA lysis buffer as described in 2.3.6. The lysate was diluted 1:3 with dilution buffer. The diluted lysate was pre-cleared with AG-Sepharose beads for 1 h at 4 °C. The pre-cleared lysate was removed from the beads and added to 40 µl of fresh equilibrated beads. 2 µg of the α p53 antibody DO-1 was added to each reaction to precipitate p53. The precipitation was carried out for 4 h at 4 °C. The beads were washed 5 x (1 min; 2 min; 3 min; 5 min; 10 min) with washing buffer. The proteins were eluted with 2 x LDS sample buffer for 10 min at 70 °C. The samples were reduced with DTT to a final concentration of 10 mM and heated to 70 °C for 10 min. Alkylation with 55 mM iodoacetamide (IAA) took place for 20 min in the dark before the samples were loaded onto a polyacrylamide gel. The following sample preparation and analysis were made in collaboration with Prof. Dr. Markus Krüger (CECAD; Cologne). The gel run for approximately 5 min at 200 V until the whole sample was incorporated in the gel. Subsequently, the gel was stained in Instant Blue (Expedeon) for 10 minutes. The gel was washed twice in H_2O. One piece per lane was chopped into smaller pieces of approximately 1 mm^2. The gel pieces were transferred into a 96-deep-well plate and 500 µl H_2O was added. The pieces were washed twice with 100 µl 50 % acetonitrile (CAN) for

15 min at room temperature, discarding the solution in between. Dehydration was performed with 100 % ACN for 15 minutes at room temperature. If the gel pieces were still stained, the washing steps were repeated until the gel was fully destained. Finally, the gel pieces were dried in a centrifugal evaporator (hereafter referred to as Speed Vac) (Eppendorf) for 5 min. For protein digestion, 3 ng/µl trypsin/LysC solution (90 % trypsin/10 % LysC) was added. After 30 min incubation at 4 °C, 50 mM 50 mM ammonium bicarbonate (ABC) was added to the swollen gel pieces and incubated overnight at 37 °C. The following day, the supernatant was placed into a new 96-deep-well plate. The gel pieces were incubated in 100 µl 30 % CAN with 3 % TFA for 20 min. The liquid was removed and combined with the supernatant of the earlier step. The gel pieces were then incubated in 100 % ACN for 20 min and the liquid was again combined with the other supernatants. The collected supernatants were placed in a Speed Vac to remove organic solvents to a remaining volume of <100 µl. Finally, FA was added to a final concentration of 1%. Before continuing with sample purification, StageTips (containing two layers of styrene divinylbenzene-reverse phase sulfonate (SDB-RPS) in a 200 µl pipette tip) were equilibrated. These StageTips are optimized to extract polar and non-polar peptides by cation exchange and hydrophobic reversed-phase affinity purification. First, 20 µl methanol were loaded onto the StageTips followed by centrifugation at 500 x g for 2 min. This step was repeated once with 20 µl of buffer B (0.1 % FA, 80 % ACN) and twice with 20 µl of buffer A (0.1 % FA). After equilibration, the acidified samples could be loaded onto the StageTips and the samples were centrifuged at 500 x g for 5 minutes. After loading, the StageTips were washed once with 30 µl buffer A and twice with 30 µl buffer B centrifuging at 500 x g for 3 min in between. The StageTips were finally dried using a syringe and stored until further use at 4 °C. To elute the proteins for mass spectrometry analysis, 30 µl 1 % ammonia in 60 % ACN were added onto the StageTips and incubated for 15 minutes. Elution into a 96-well plate was performed either manually by using a syringe or by centrifugation at 500 x g for 5 min. The plate was then dried in a Speed Vac and 10 µl buffer R (0.1 % FA, 5 % ACN) was added before measurement. Immunoprecipitation samples were analysed using a liquid chromatography tandem mass spectrometry set up in a Q-Exactive™ Plus Hybrid Quadrupole-Orbitrap™ (Thermo Fisher). Chromatographic peptide separation was achieved on PoroShell 120 packed 50 cm analytical columns coupled to an EASY-nLC 1000 HPLC system and a binary buffer system consisting of buffer A and B. In-gel digested samples were analysed over a 60 min gradient, raising the content of buffer B from 4 - 29 % over 42 min, from 29 - 55 % over 8 min, and from 55 – 95 % over 2 min. Full MS spectra (300–1,750 m/z) were recorded at a resolution (R) of 60,000, maximum injection time (max. IT) of 20 ms and AGC target of 3e6. The ten most abundant ion peptides in each full MS scan were selected for HCD fragmentation at

nominal collisional energy (NCE) of 28. MS2 spectra were recorded at R = 15,000, maximum IT of 22 ms, and AGC target of 1e5.

2.4.8.1 MS data processing and analysis

The following analysis was made in collaboration with Prof. Dr. Markus Krüger (CECAD; Cologne). Raw MS data were analysed using MaxQuant analysis software and the implemented Andromeda software [323,324]. Peptides and proteins were identified using the mouse UniProt database with common contaminants. All MaxQuant parameters were set to default values. Trypsin was selected as the digestion enzyme; a maximum of two missed cleavages was allowed.

Methionine oxidation and N-terminal acetylation were set as variable modifications; carbamidomethylation of cysteines was chosen as a fixed modification. The label-free quantification (LFQ) algorithm was used to quantify the measured peptides and the "match between runs" option was enabled to quantify peptides with a missing MS2 spectrum.

Statistical analysis was performed using Perseus software. Potential contaminants and reverse peptides were excluded, and values were log2 transformed. Two-sided t-tests and ANOVA were used to identify differentially expressed proteins between conditions. Identified peptides were annotated with the following Gene Ontology terms: Biological Process, Molecular Function, Cellular Compartment, and the Reactome database terms. Graphical visualisations were created using Instant Clue software [325]

3 RESULTS

3.1 Identification of the T329 phosphorylation in the TD of p53

The phosphorylation of amino acid residues within the p53 protein plays a major role in its activation. To investigate the occurrence of phosphorylations in the p53 protein, a mass spectrometry analysis of immunoprecipitated p53 was performed. HCT116 WT cells were seeded and stimulated with 20 µM etoposide for 16 h. The cells were lysed and the endogenous p53 was precipitated with the DO-1 antibody. The precipitated proteins were digested into peptides, and phosphorylated peptides were enriched with TiO 2 beads. The peptides were analysed via mass spectrometry. The analysis identified seven already well-characterised phosphorylations in the isolated p53 protein: pS6, pS15; pT150, pS303, pT304, pS314 and pS315. In addition, the analysis detected the previously unknown phosphorylation at T329 in the etoposide treated cells. The mass of T329 in the MS/MS spectrum corresponds, upon etoposide treatment, to the mass of a phosphorylated threonine (Fig. 5). It occurred together with other previously described phosphorylations in the C-terminal part of p53, such as pS303, pT304 and pS315.

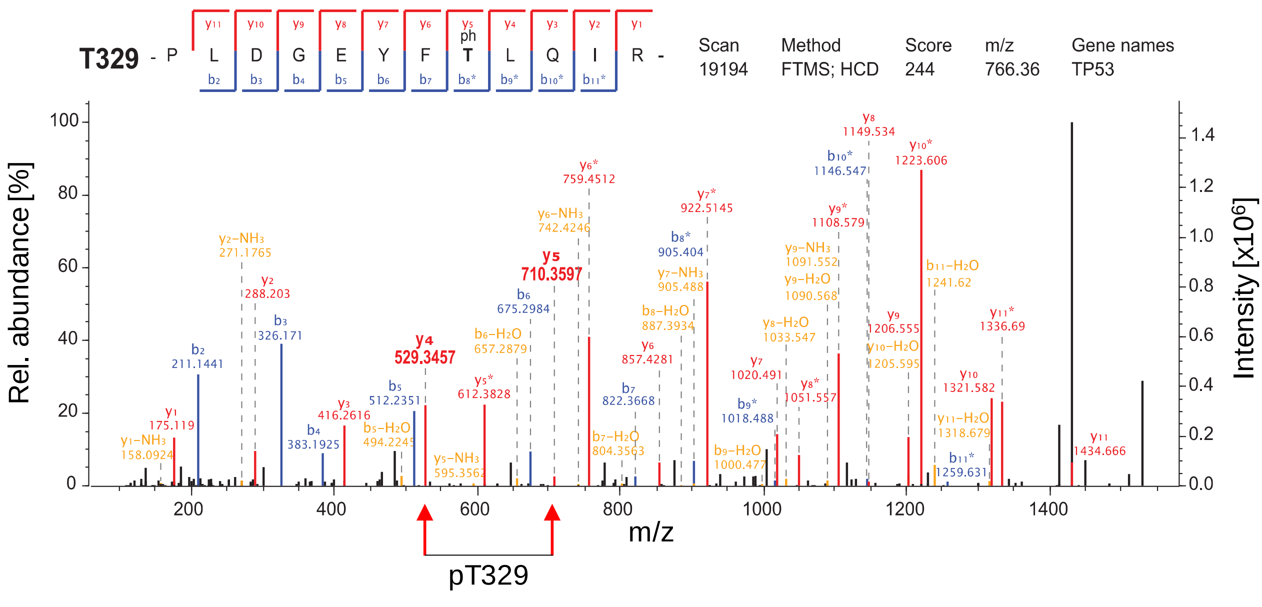

Fig. 5 Identification of the T329 phosphorylation in the TD of p53. HCT116 p53 WT cells were treated with 20 µM etoposide for 16 h. The cells were lysed and p53 was precipitated with the DO-1 antibody. The precipitated proteins were analysed by mass spectrometry. Shown is a MS/MS spectrum of the detected phospho-site at T329 of p53. The arrows indicate the measured mass for the phosphorylated T329.

3.2 The occurrence of T329 phosphorylation in eukaryotic cancer cell lines

3.2.1 Generation of a pT329 specific antibody

To further investigate the occurrence of the T329 phosphorylation (pT329), a phospho-specific antibody, recognising this phosphorylated residue, was generated by PSL on request for this study. HCT116 p53 WT cells were treated with 30 J/m^2 UVC radiation and were incubated for 8 h. The DNA damage leads to the phosphorylation and activation of p53. The cells were lysed with and without phosphatase inhibitor and one half of each sample was treated with λ phosphatase to dephosphorylate the proteins. The lysates were analysed by Western blotting. The signal of the generated pT329 antibody increases due to the UVC radiation and reduces by the lysate's dephosphorylation (Fig. 6A).

3.2.2 Occurrence of pT329 upon different stimulations

To determine the occurrence of pT329, HCT116 p53 WT cells were treated with several DNA-damaging agents. The cells were lysed and analysed by Western blotting. The induction of DNA damage was determined with the γH2AX antibody. T329 was phosphorylated along with other phospho-sites like S15, S392 and S46, which are known to contribute to the activation of p53 upon DNA damage (Fig. 6B). The mutagenic compound 4-nitrochinoline-1-oxide (4NQO) and the antineoplastic compound nocodazole did not induce pT329 or other phosphorylations, although DNA damage was observed by the signal of the α γH2AX antibody.

3.2.3 Occurrence of pT329 in dependence of MDM2

Since it is known that the p53 dependent gene transcription can be induced without induction of the DNA damage pathway, the occurrence of phosphorylations was investigated upon nutlin 3a treatment. HCT116 p53 WT cells were treated with 10 µM nutlin 3a for 16 or 24 h. The cells were lysed and analysed by Western blotting. Nutlin 3a leads to the dissociation of p53 and MDM2, which results in an accumulation and activation of p53 [196,317]. This dissociation was sufficient to trigger T329 phosphorylation (Fig. 6C). To confirm this result, the abundance of MDM2 was reduced by siRNA transfection. Indeed, the reduction of MDM2 leads to the phosphorylation of T329, which confirmed that pT329 occurred upon DNA damage and independent of DNA damage after MDM2 dissociation.

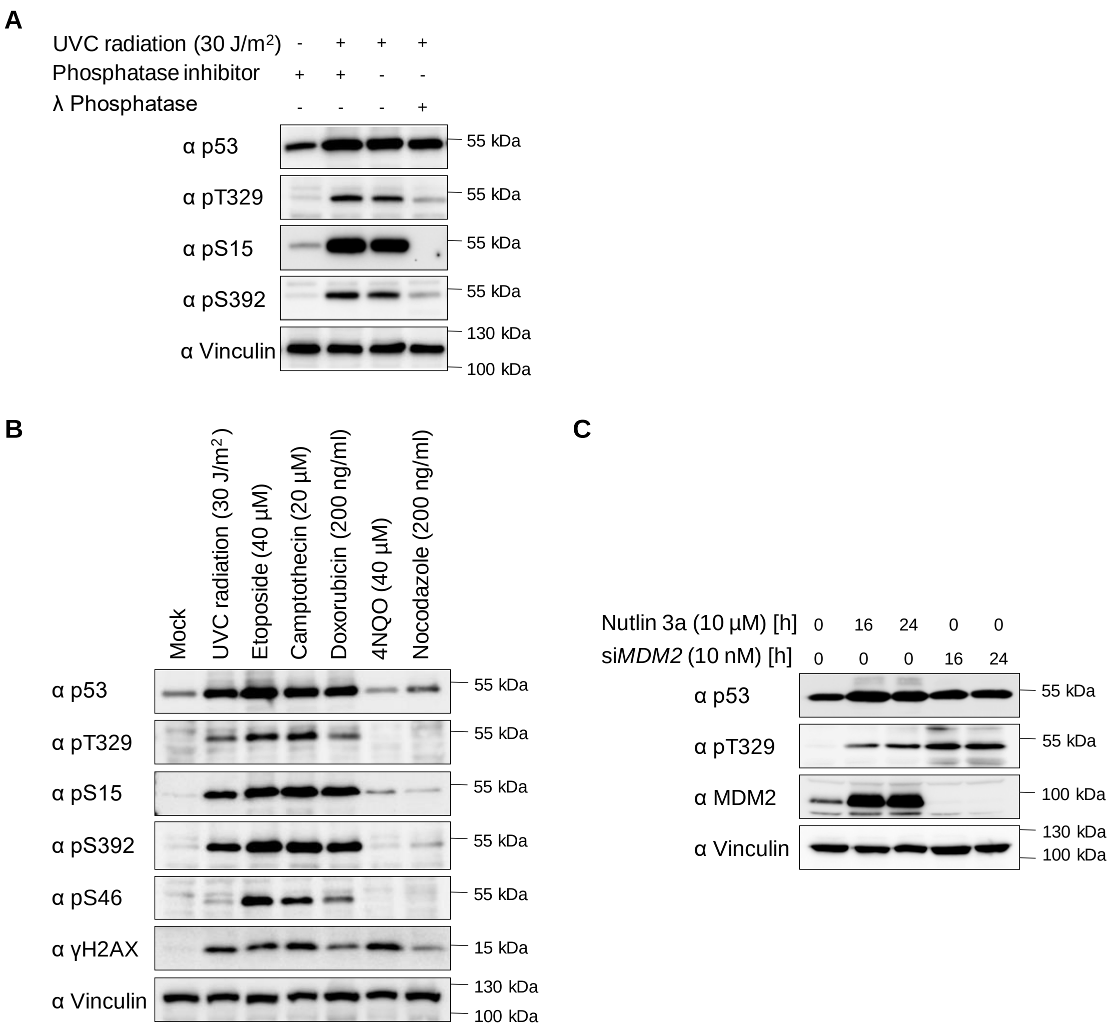

Fig. 6 The occurrence of the T329 phosphorylation in eukaryotic cancer cell lines. A: HCT116 p53 WT cells were treated with UVC radiation and were incubated for 8 h subsequently. The cells were lysed with and without phosphatase inhibitor and were treated with λ phosphatase as indicated. The lysates were analysed by Western blotting. **B:** HCT116 p53 WT cells were treated with the indicated DNA damaging agents for 16 h. The cells were lysed and analysed by Western blotting**. C:** HCT116 p53 WT cells were treated with nutlin 3a or transfected with siRNA, targeting the *MDM2* transcript for 16 h or 24 h respectively. The cells were lysed and analysed by Western blotting**.**

3.3 Influence of other p53 mutations on pT329

Many examples show that mutations in p53 influence the phosphorylation pattern and thereby the activity of p53 [326]. To investigate the role of p53 mutations in the occurrence of pT329, several cell lines with different p53 mutations were analysed. The indicated cell lines were treated with 40 µM etoposide for 16 h. The cells were lysed and analysed by Western blotting. Both human cancer cell lines that express wild-type (WT) p53 (HCT116 and A549) showed inducible T329 phosphorylation (Fig. 7A). In HeLa cells, the WT p53 protein undergoes continuous degradation due to the presence of the HPV18E6 protein [327]. Therefore, p53 loses its functionality and HeLa cells are presumed to contain a loss of function (lof) p53 phenotype. Neither the p53 in HeLa cells nor the mutated p53 (V126C) in IGROV cells showed inducible T329 phosphorylation. In HEK239T cells, the p53 protein is associated with the SV40 large T-antigen and therefore loses functionality [328]. In these cells, p53 shows hyper-phosphorylation already in unstimulated conditions. Although the T329 is conserved among all vertebrates, no pT329 signal was observed in mouse embryonic fibroblasts (MEF) with the used antibody.

Even though T329 is not described as a common mutation of p53 in cancer, it may still play a role in cancer development and treatment if common cancer mutations affect its occurrence. Therefore, the impact of well-characterised common cancer mutations of p53 on the occurrence of pT329 was investigated. Plasmids encoding the p53 protein with common mutations in cancer were expressed in HCT116 $p53^{-/-}$ cells. The transfected cells were treated with 40 µM etoposide for 16 h, lysed and analysed by Western blotting. The mutated p53 variants show less or no T329 phosphorylation (Fig. 7B). Besides T329, also the phosphorylation of S392 and S46 were absent. However, S15 was still phosphorylated in the p53 R248W and R273H mutants. This result suggests that common cancer mutations reduce the phosphorylation of T329 and other residues, which are essential for proper p53 activation.

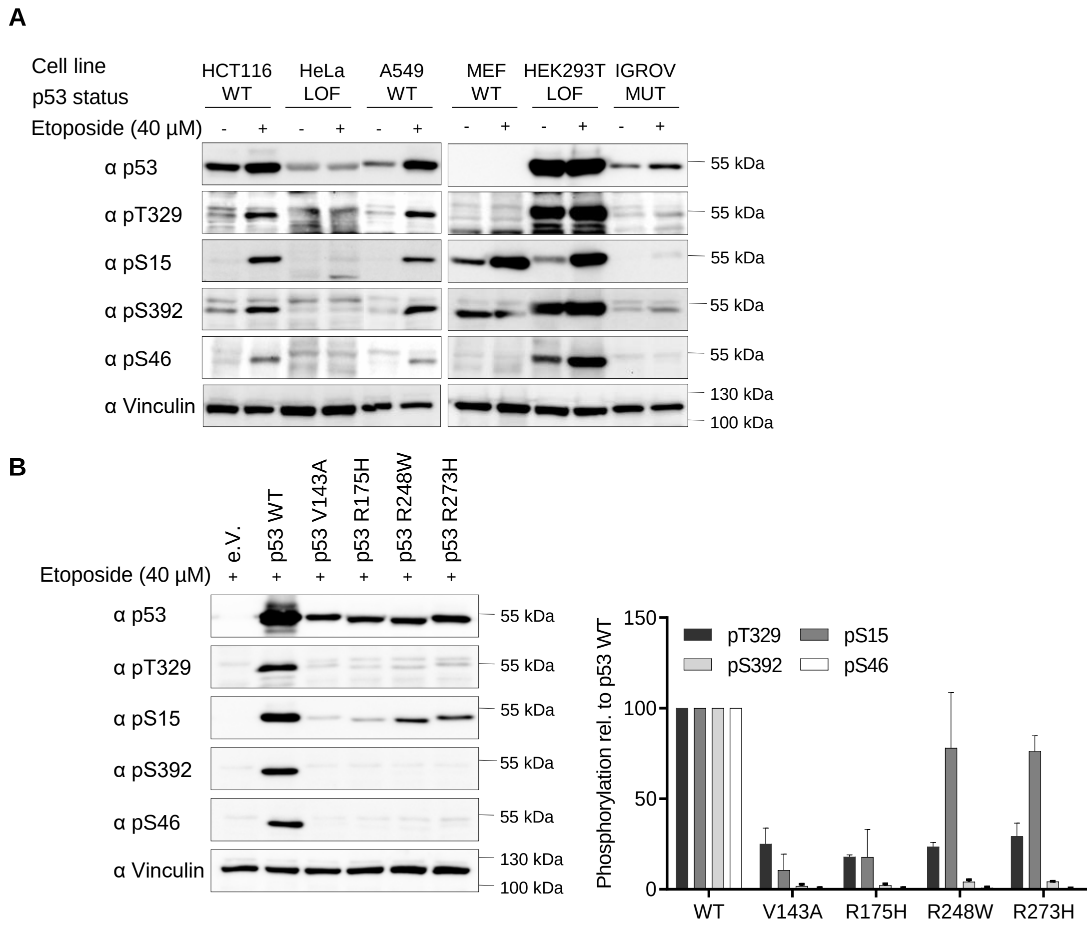

Fig. 7 The phosphorylation of T329 is affected by mutations of p53. A: The indicated cell lines were treated with etoposide for 16 h. The cells were lysed and analysed by Western blotting**. B:** HCT116 p53$^{-/-}$ cells were transfected with the indicated p53 mutants or an empty vector control (e.V.) for 24 h. The cells were treated with etoposide for 16 h. The cells were lysed and analysed by Western blotting. Densitometric analysis was performed normalising the phospho-specific antibodies' signal to the total p53 signal given by the DO-1 antibody (α p53). The phosphorylation is shown relative to that of p53 WT. The mean of two replicates with deviation is shown.

3.4 Kinetics of pT329 under UVC radiation

Besides the pattern of phosphorylated residues, time-dependent phosphorylation and dephosphorylation are essential to modulate the p53 response [190]. To investigate the time-dependent phosphorylation, HCT116 p53 WT cells were treated with UVC radiation to induce the DNA damage response. Upon radiation the cells were incubated up to 24 h, lysed and analysed by Western blotting. Due to the different time points of harvesting transient phosphorylations can be monitored. The phosphorylation of S15 occurred rapidly (after 2 h) and remained during the next 24 h (Fig. 8A). Also, T329 was rapidly phosphorylated after 2 – 4 h of treatment. The signal reached its maximum after 16 h and decreased afterwards. The transient phosphorylation of S392 followed the same pattern.

3.4.1 Localisation of pT329

Since p53 acts as a transcription factor mainly in the nucleus and temporarily binds to the DNA, the intracellular distribution of phosphorylated p53 was visualised by fractionation. Therefore, HCT116 p53 WT cells were treated with UVC radiation and were subsequently treated with stronger lysis buffers to separate the cytoplasmic, the soluble nuclear and the chromatin fraction. The fractions were analysed by Western blotting. The p53 protein was primarily localised in the cytoplasmic and nuclear fractions (Fig. 8B). Only a minor amount could be detected in the insoluble chromatin-bound fraction. Consistent with the early and robust phosphorylation of S15, it was detected in both the cytoplasmic and nuclear fractions. The phosphorylation of T329 and S392 mainly occurred in the nucleus and increased after 3 - 6 h of incubation. The late pro-apoptotic phosphorylation of S46 was exclusively detected in the nuclear fraction. The chromatin-bound p53 amount was too low to investigate phosphorylations in this fraction by Western blotting.

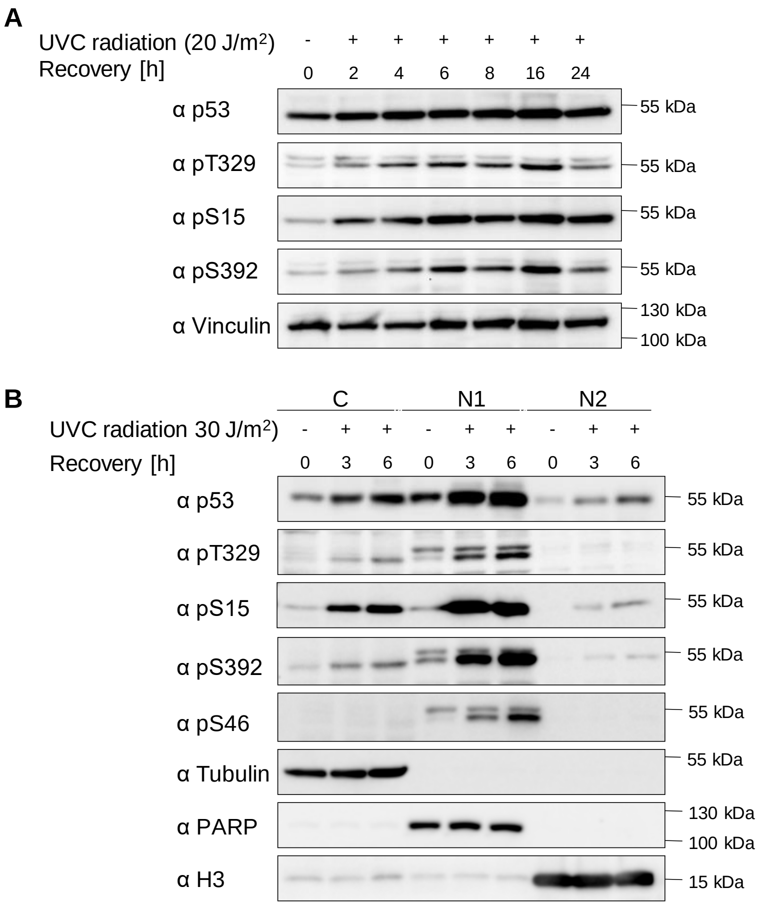

Fig. 8 The phosphorylation of T329 occurred transiently in the nucleus during the DNA damage response. A: HCT116 p53 WT cells were treated with UVC radiation and were incubated for the indicated periods. The cells were lysed and analysed by Western blotting. **B:** HCT116 p53 WT cells were treated with UVC radiation and fractionated into cytoplasmic (C), soluble nuclear (N1) and insoluble nuclear (N2) fraction. The fractions were analysed by Western blotting. Tubulin, PARP and H3 were stained to ensure the purity of the fractions.

3.5 Characterisation of phospho-mutant (T329A) and phospho-mimic (T329E) cell lines

To characterise the function of T329 phosphorylation, phospho-mutant (T329A) and phospho-mimic (T329E) cell lines were generated. For this purpose, HCT116 p53$^{-/-}$ cells were transfected with plasmids containing homologous regions to the AAVS1 safe harbour locus, and the cDNA of p53 WT, p53 T329A and p53 T329E. The cells were selected for the stable integration of the donor plasmid via the plasmid-encoded puromycin resistance. From the puromycin resistant cells, single-cell clones were picked. Two single-cell clones per construct were analysed by Western blotting (Fig. 9A). The reconstituted cells were compared to HCT116 p53 WT cells. The two individual clones of HCT116 p53$^{-/-}$ rec. p53 WT cells showed a similar expression of p53 to HCT116 p53 WT cells. The HCT116 p53$^{-/-}$ rec. p53 T329A clones expressed slightly less p53 compared to the HCT116 p53$^{-/-}$ rec. p53 WT clones. In contrast, the HCT116 p53$^{-/-}$ rec. p53 T329E clones showed a higher p53 expression than the HCT116 p53$^{-/-}$ rec. p53 WT clones.

3.5.1 p53 dependent gene transcription in phospho-mutant (T329A) and phospho-mimic (T329E) singe cell clones

As a transcription factor, p53 mediates most of its functions by activating gene transcription. Therefore, the p53-dependent gene transcription was induced by etoposide and investigated in the generated clones. The RNA of the cells was extracted and cDNA was generated. The expression of five p53 target genes was determined by qPCR. Under unstimulated conditions (mock), all target genes showed low expression levels (Fig. 9B), with only minor differences between the cell clones. Only the expression of *CDKN1A,* was significantly decreased in the HCT116 p53$^{-/-}$ rec. p53 T329A clones. Upon etoposide stimulation, the transcription of all target genes was induced in all cell lines containing the p53 WT protein. The p53 deficient cells showed no induction of p53-dependent gene transcription. The HCT116 p53$^{-/-}$ rec. T329E clones showed comparable p53-dependent gene transcription to the HCT116 p53$^{-/-}$ rec. p53 WT cell clones. The HCT116 p53$^{-/-}$ rec. p53 T329A cell clones showed impaired transcriptional activation of all p53-target genes. Especially the transcription of *CDKN1A* was decreased. Hereinafter the HCT116 p53 WT cells are referred to as WT. The two individual clones of each p53 construct were mixed and are referred to as rec. WT (HCT116 p53$^{-/-}$ rec. p53 WT), rec. T/A (HCT116 p53$^{-/-}$ rec. T329A) and rec. T/E (HCT116 p53$^{-/-}$ rec. T329E).

3.5.2 Comparison of p53 mRNA and protein amount in T329 mutant cell lines

As the amount of p53 protein is crucial for its activation, the p53 mRNA and protein level of the generated cell lines were examined. RNA was isolated from the indicated cell lines and the expression of p53 mRNA was analysed by qPCR. All three reconstituted cell lines showed a lower level of p53 mRNA transcription compared to the WT cells (Fig. 9C). The rec. WT cells showed a slightly higher mRNA expression than the mutant cell lines. To further investigate the previously mentioned differences in the p53 protein level, Western blotting was used to quantify the p53 protein levels in each cell line, by comparing total p53 levels to the expression of the housekeeping protein vinculin. The protein level showed a wide variety between the biological replicates. Overall, the protein amount in the rec. T/A cells was less compared to the rec. WT cells. In contrast, the protein level of the rec. T/E cells tended to be higher compared to the rec. WT cells.

3.5.3 Confirmation of T329A and T329E cell lines by pT329 detection

To confirm the transient phosphorylation of T329 in the reconstituted cell lines, the cells were treated with UVC radiation, and pT329 was detected by Western blotting. The rec. WT cells displayed the already shown transient phosphorylation upon DNA damage (Fig. 9D). The staining of p53 in the rec. T/A cells with the α pT329 antibody showed a slight background signal. The pT329 antibody showed in the T/E cells a consistent signal already without stimulation.

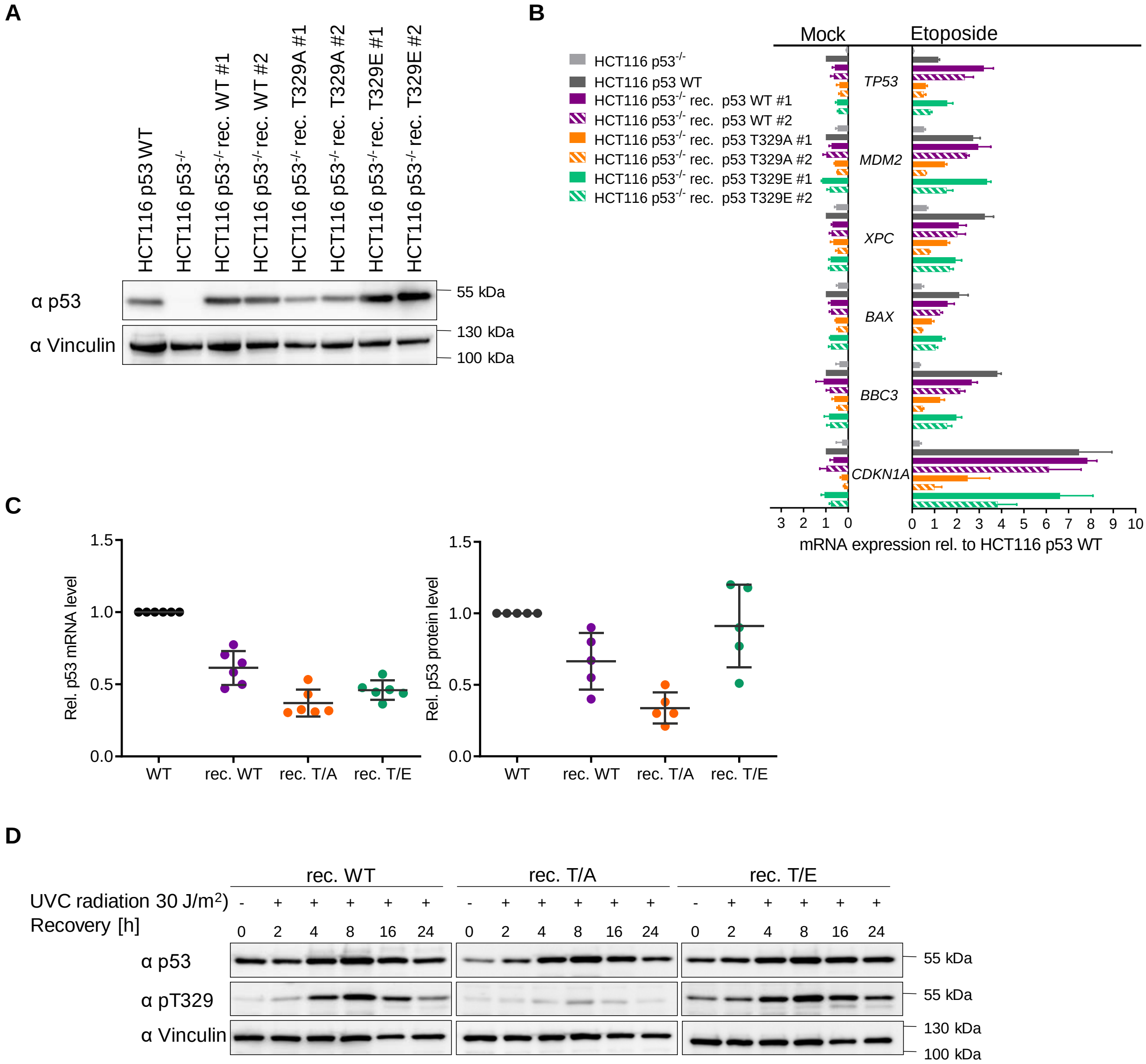

Fig. 9 Characterisation of T329 mutant cell lines: p53 WT, p53 T329A and p53 T329E constructs were created with the GeneCopoeia Genome-CRISPR Human AAVS1 Safe Harbour Gene Knock-in Kit. HCT116 p53$^{-/-}$ cells were transfected with donor and CRISPR Cas9 vectors targeting the AAVS1 locus. The cells were selected with puromycin and singe cell clones were analysed by Western blotting. **B:** The cells were treated with etoposide for 24 h. The total RNA was isolated and mRNA levels were analysed by qPCR. Triosephosphate isomerase (TPI) was used as a housekeeping gene to determine ΔCT values. The relative expression (ΔΔCT) of the mRNA expression for each gene is shown normalised to the MOCK sample of HCT116 WT. Mean values with standard deviation (SD) of three replicates are shown. **C:** Comparable amounts of cells of the indicated cell lines were seeded, and the total RNA was isolated and lysates for the protein analysis were made. The relative p53 mRNA expression was determined by qPCR. Shown are six replicates with SD. Protein lysates were analysed by Western blotting to determine the p53 protein level. Quantification of five replicates are shown with SD. The relative p53 protein level was normalised to vinculin and compared to the protein amount in HCT116 p53 WT cells. **D:** The indicated cell lines were treated with UVC radiation and incubated for the indicated time periods. The cells were lysed and analysed by Western blotting.

3.6 Functional characterisation of the T329 mutations

3.6.1 Influence of T329 mutations on the tetramerisation

The p53 protein acts as a tetrameric transcription factor. The correct assembly of the four monomers to a tetramer is crucial for its activation [291]. Since T329 is localised in the TD, the ability for tetramerisation of the T329 mutants was investigated. Therefore, p53 was activated with etoposide and the protein lysates were cross-linked with glutaraldehyde to maintain the protein complexes during separation by SDS-Page. Under unstimulated conditions, less p53 protein and consequently fewer p53 dimers and tetramers were observed (Fig. 10A). Upon DNA damage, the dimerised and tetramerised p53 protein was clearly visible in the cross-linked lysate, suggesting that the mutants showed no severe defects in the tetramerisation of p53. This observation is consistent with alanine mutation scans, which show that T329 is not crucial for tetramerisation of p53 [329].

3.6.2 Influence of T329 mutations on intracellular distribution of p53

As already described, p53 executes its main function in the nucleus. In order to address the localisation of the p53 mutants in the cell, their intracellular distribution was monitored. Therefore, the indicated cell lines were treated with UVC radiation and subsequently treated with stronger lysis buffers to separate the cytoplasmic, the soluble nuclear and the chromatin fraction. The fractions were analysed by Western blotting. The majority of p53 protein was localised in the cytoplasmic (C) and soluble nuclear (N) fraction (Fig. 10B). Only upon severe DNA damage (100 µM etoposide), a distinct p53 signal was detected in the insoluble chromatin-bound fraction. All cell lines showed an equal distribution of p53 between the cytoplasmic, nuclear and chromatin fractions.

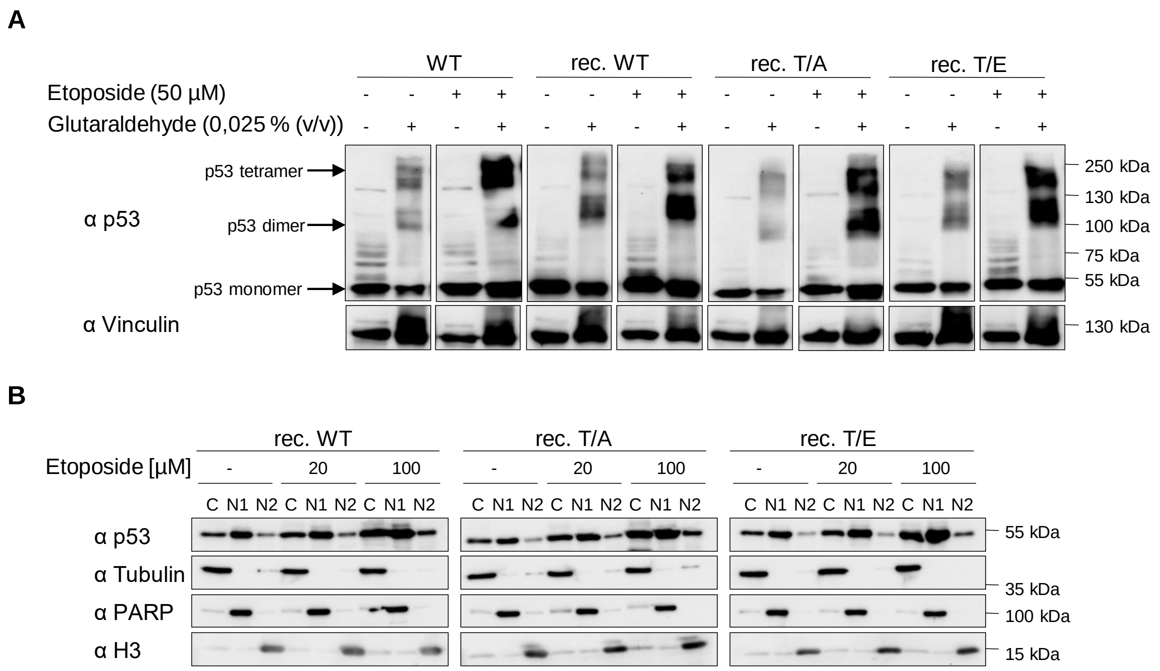

Fig. 10 The mutation of T329 does not influence the tetramerisation or localisation of p53. A: The indicated cells were treated with etoposide for 3 h to induce tetramerisation of p53. The cells were lysed and half of the lysate was cross-linked with glutaraldehyde at room temperature (RT) for 5 min. Samples were analysed by Western blotting. **B:** The indicated cells were treated with etoposide for 16 h to stimulate p53. The cells were lysed in fractions containing the cytoplasmic (C), soluble nuclear (N1) and nuclear insoluble (N2) proteins. The samples were analysed by Western blotting. Tubulin (C), PARP (N1) and H3 (N2) were used as marker proteins for each fraction.

3.6.3 Influence of T329 mutations on the degradation of p53

To further investigate the differences in the p53 protein level between the reconstituted cell lines, the degradation of p53 was investigated. Therefore, the reconstituted cell lines were treated with anisomycin to inhibit the protein synthesis. The stability of p53 was determined by Western blotting. In all cell lines degradation of the p53 protein was observed upon anisomycin treatment (Fig. 11A). The quantification indicated a 40 – 60% reduction of the protein level after 8 h. The rec. T/A p53 protein showed slightly less degradation.

In order to further characterise this effect, the cells were treated with inhibitors for proteasomal degradation (MG132) and autophagy (bafilomycin A, chloroquine, NH_4Cl). The residual amount of p53 was analysed by Western blotting. The inhibition of the proteasome did not affect the p53 protein levels (Fig. 11B). This result is not sufficient to evaluate the impact of the proteasome on the turnover of p53, since no positive control for verification of the MG132 function has been included. The inhibition of autophagy resulted in an increased p53 protein level in all cell lines. The p53 protein turnover was constantly more impaired by autophagy than by the proteasome. Notably, the p53 protein level in the rec. T/A cells show a tendency to be slightly more elevated compared to the other cell lines. Nevertheless, the differences between the cell lines are only minor and not significant..

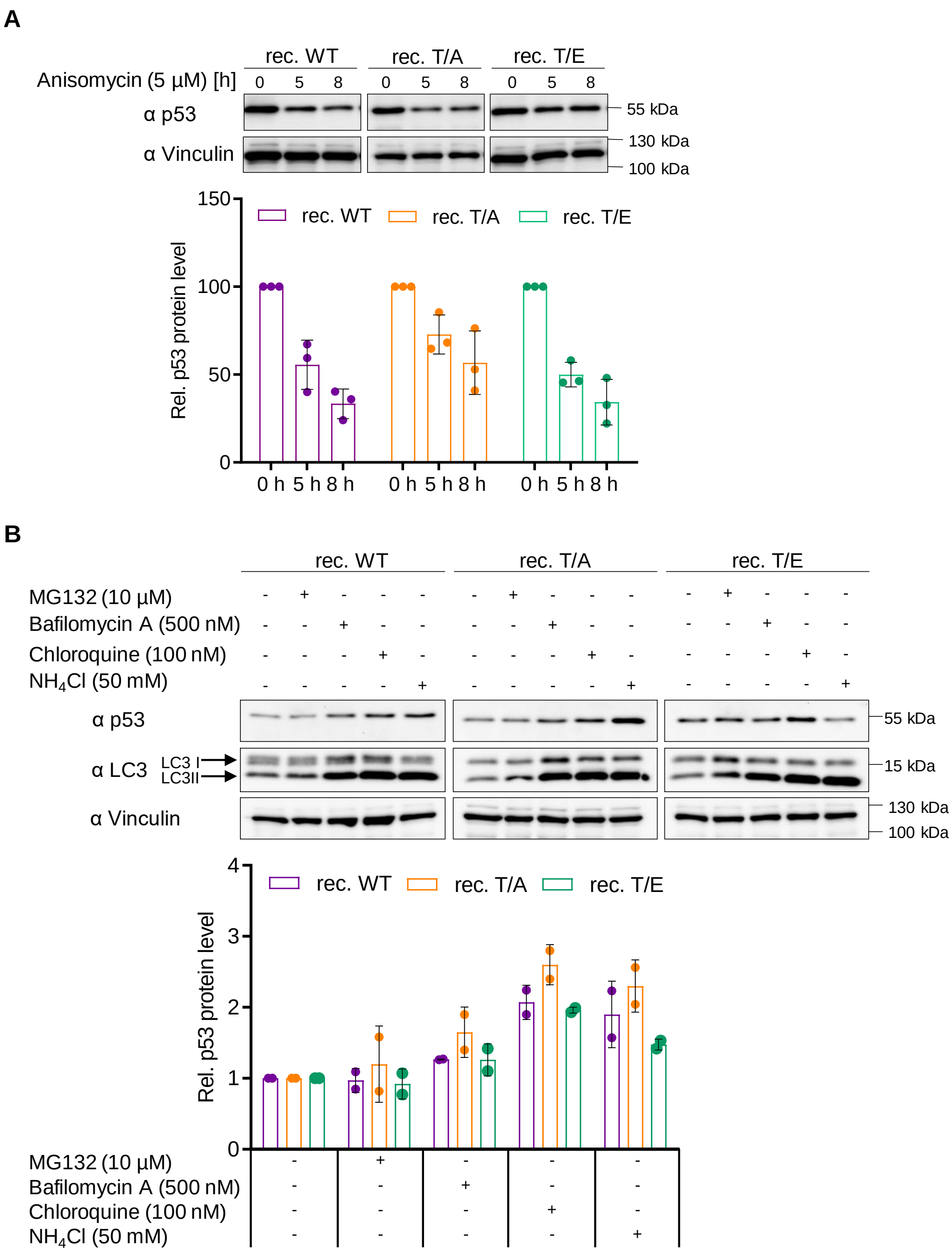

Fig. 11 Impact of T329 mutation on p53 degradation. A: The indicated cells were treated with anisomycin for 5 h or 8 h to inhibit the protein biosynthesis. The cells were lysed and analysed by Western blotting. The p53 protein level was normalised to vinculin and is shown relative to the untreated control. The mean of three replicates is shown, including the SD. **B:** The cells were treated with MG132, bafilomycin A, chloroquine or NH_4Cl for 4 h to inhibit proteosomal degradation and autophagy respectively. The cells were lysed and analysed by Western blotting. The p53 level were normalised to vinculin and are shown relative to the untreated control. The mean of two replicates is shown with deviation.

3.7 Functional consequences of T329 phosphorylation on the p53 activity

3.7.1 Influence of T329 phosphorylation on the p53-dependent gene transcription

To get an overview of pT329's influence on multiple p53 functions, an entire transcriptome was analysed in cooperation with the workgroup of PD Dr. Hain - JLU Giessen. Therefore, the reconstituted cell lines were treated with etoposide or remained untreated to distinguish between basal and induced gene transcription. To determine the p53 dependent effects, HCT116 $p53^{-/-}$ cells were used to normalise the gene expression levels. The analysis revealed that 158 (rec. WT mock) to 1709 (rec. WT etoposide) genes were significantly (p-value adjusted ≤ 0,05) altered in their expression level, compared to the $p53^{-/-}$ cells. The distribution of these genes upon their $\log_2$ fold change revealed that the expression of the differentially expressed genes in the rec. WT and rec. T/E cells was elevated compared to the $p53^{-/-}$ cells (Fig.12A). In contrast, most of the differentially expressed genes in the rec. T/A cells showed a reduced expression compared to the $p53^{-/-}$ cells.

The significantly (p-value adjusted ≤ 0,05) regulated genes ($\log_2$ fold change ≥ 1 or ≤ -1) in the rec. WT cells were defined as the p53 WT-responsive gene set. The expression of these genes was compared between all cell lines in the displayed heat map to determine how efficient the p53 mutants mimic the p53 WT-dependent gene expression. In the T/A cells, a minority of the p53 WT-responsive genes showed comparable expression levels (Fig 12B). 39 % of the genes in untreated conditions and 55 % in etoposide-treated conditions showed no comparable gene expression (indicated by the grey colour in the heat map). The rec. T/E cells showed no significantly altered gene expression for 22 % (mock) and 31 % (etoposide-treated) of the p53 WT-responsive genes. Overall, both cell lines were impaired in the p53-dependent gene expression. Nevertheless, the expression pattern of the rec. T/E cells showed higher similarity to the rec. WT cells compared to the rec. T/A cells.

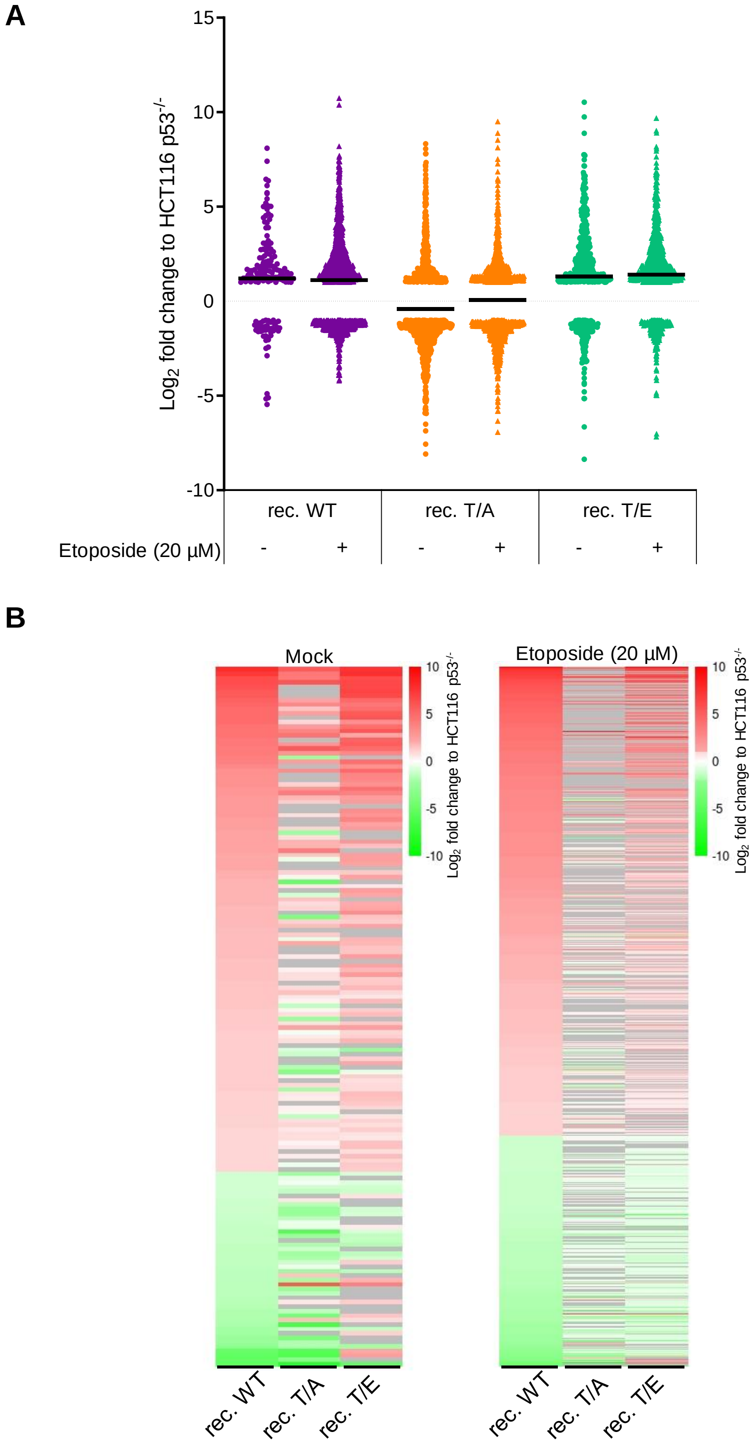

Fig. 12 Impact of pT329 on the p53-dependent gene transcription. A: The cells were treated with etoposide for 24 h. The total RNA was isolated and analysed by RNA-sequencing (RNA-seq). To determine the p53 dependent gene transcription, the mRNA abundance was normalised to HCT116 $p53^{-/-}$ cells. Displayed are the significantly (p-value adjusted ≤ 0,05) regulated genes (log_2 fold change ≥1 or ≤ -1) for each cell line compared to HCT116 $p53^{-/-}$. **B:** The significantly (p-value adjusted ≤ 0,05) regulated genes (log_2 fold change ≥1 or ≤ -1) of rec. WT cells compared to HCT116 $p53^{-/-}$ cells were defined as the p53 WT-responsive gene set. The transcriptional changes for the defined gene set of each cell line are shown in the heat map. Grey colour indicates a p-value > 0,05.

To take a closer look at the well-characterised p53 core transcriptome, the expression levels of selected p53 target genes are displayed in the heat map. The transcription of all selected genes is directly induced by p53 [113]. The genes are clustered accordingly to the p53 function they contribute to. In general, the rec. T/E cells showed a comparable expression pattern to the rec. WT cells (Fig. 13). The direct binding and induction of transcription of p53 target genes is not impaired due to the T/E mutation, while the expression levels in the rec. T/A cells showed an overall reduction. Especially the genes involved in cell cycle arrest and differentiation already showed a significantly reduced expression under unstimulated conditions. Therefore, the direct activation of gene transcription seemed to be affected by the T/A mutation of T329.

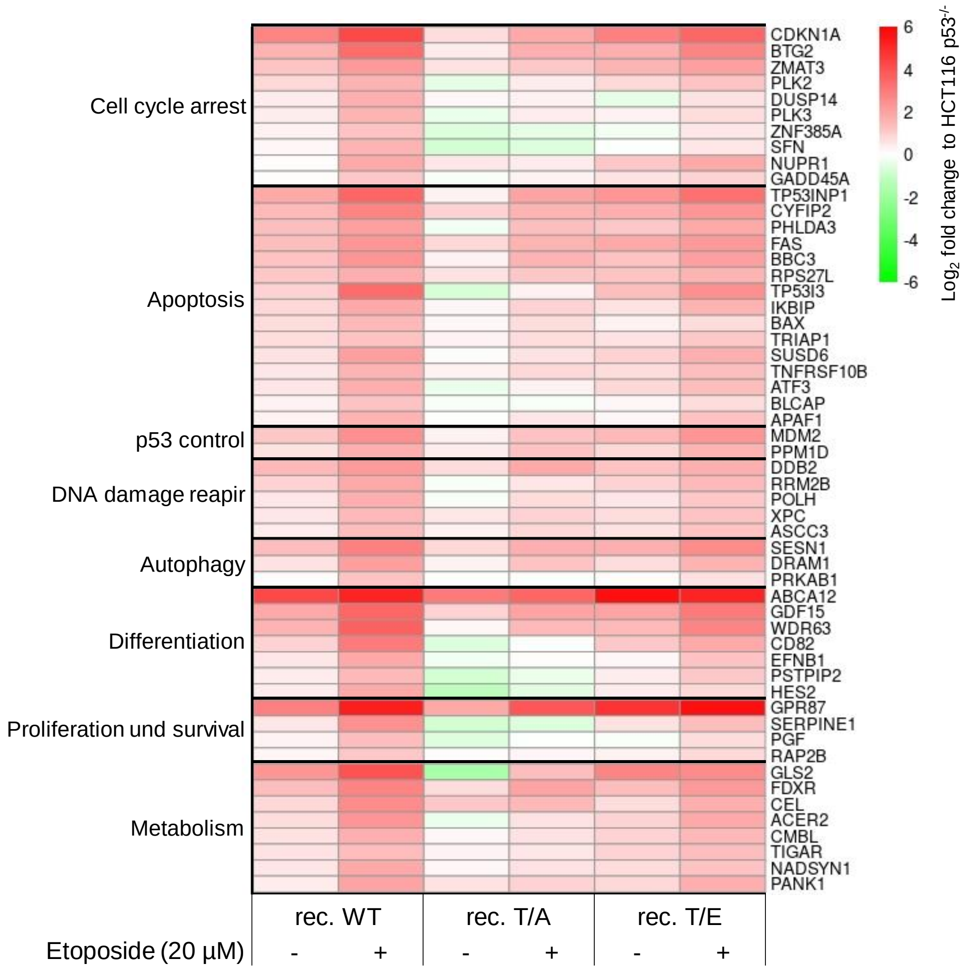

Fig. 13 Impact of pT329 on the p53 core transcriptome. The cells were treated with etoposide for 24 h. The total RNA was isolated and analysed by RNA-seq. To determine the p53 dependent gene transcription, the mRNA abundance was normalised to HCT116$^{-/-}$ cells. The relative expression of the p53 core transcriptome is displayed in the heat map.

To determine the difference in gene expression upon the mutation of T329, the mRNA expressions in the rec. T/A and the rec. T/E cells were normalised to the rec. WT cells. The significantly (p-value adjusted ≤ 0.05) differentially (log_2 fold change ≥ 2 or ≤ -2) expressed genes in the rec. T/A and the rec. T/E cells compared to the rec. WT cells were displayed with their log_2 fold change (Fig. 14A). The rec. T/A cells showed altered gene expression for 395 (mock) and 750 (etoposide-treated) genes. Most of these genes were less expressed compared to the rec. WT cells. In the rec. T/E cells 120 (mock) and 127 (etoposide-treated) genes were differentially expressed. Most of the affected genes were higher expressed than in rec. WT cells.

In order to assign the genes to biological functions, they were analysed with the Kyoto Encyclopedia of Genes and Genomes (KEGG) pathway analysis and gene ontology (GO) term enrichment. Pathways or terms were solely considered to be significantly (false discovery rate (FDR) ≤ 0.05)) enriched for the differentially expressed genes in the rec. T/A cells. As expected, the p53 signalling pathway itself showed significant enrichment (Fig. 14B). Additionally, the arachidonic acid metabolism and the PI3K-Akt signalling pathway were present in the KEGG analysis. Furthermore, several cellular adhesion and extracellular matrix related terms were enriched in the GO analysis.

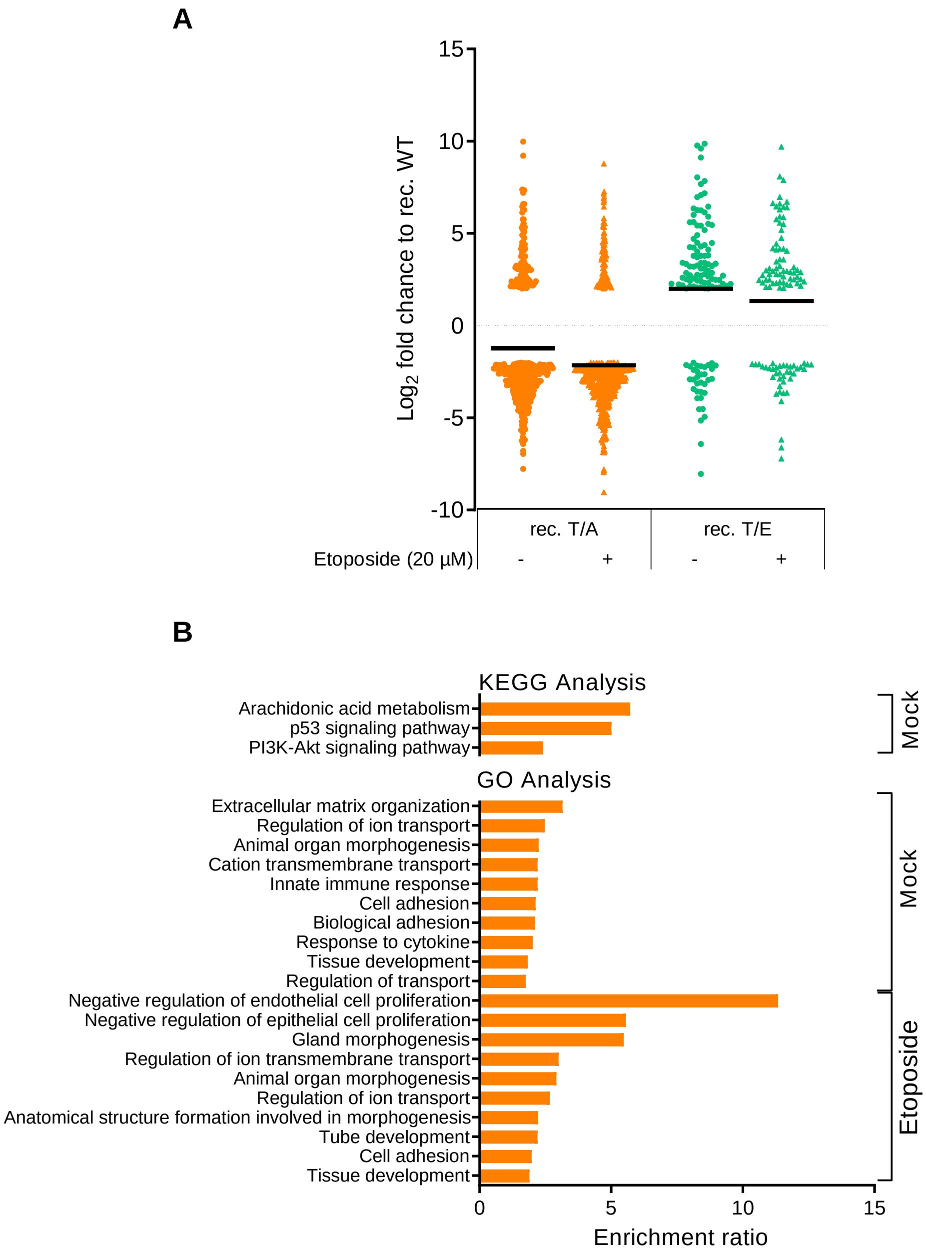

Fig. 14 Functional assignment of the deregulated genes upon T329 mutation A: The cells were treated with etoposide for 24 h. The total RNA was isolated and analysed by RNA-seq. To determine the T/A and T/E dependent deregulated genes, the mRNA abundance was normalised to rec. WT cells. Displayed are the significantly (p-value adjusted ≤ 0.05) regulated genes (log_2 fold change ≥2 or ≤ -2) for each cell line compared to rec. WT. **B:** The significantly (p-value adjusted ≤ 0.05) regulated genes (log_2 fold change ≥2 or ≤ -2) comparing the expression in p53 WT cells with p53 T/A cells, were analysed with WebGestalt for GO and KEGG enrichment. Displayed are the significantly (FDR ≤ 0.05) enriched KEGG pathways and GO terms.

3.7.2 Influence of T329 phosphorylation on cellular adhesion

Functional analysis of the deregulated genes in the rec. T/A cells was performed and revealed that many genes are related to cellular adhesion. Since the mutation of p53 has already been shown to impact cellular adhesion [330,331], the strength of adhesion to a cell culture plate was investigated. The cells were seeded and cultured for two days to fully develop adhesion molecules. The cells were treated with diluted and undiluted trypsin, respectively for 15 min at RT. The floating cells were counted and displayed relative to the total number of cells in each sample (Fig. 15). The rec. WT cells showed a higher adhesion with fewer floating cells than the p53$^{-/-}$ cells. In line with the reduced expression of genes involved in cell adhesion, the rec. T/A cells were less adherent than the rec. WT or rec. T/E cells. Thus, the mutation of T329 to the phospho-mutant T/A significantly decreased the adherence of the cells.

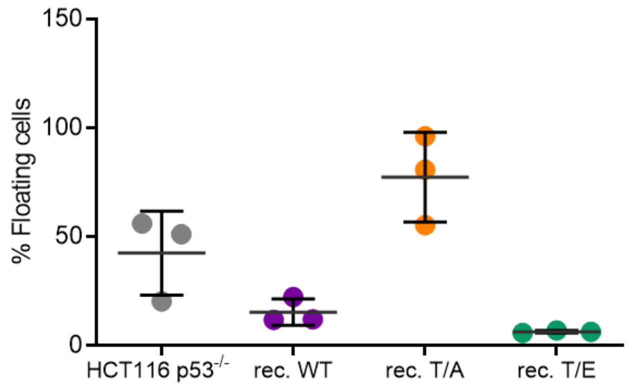

Fig. 15 Impact of the T329 mutation on cell adherence. The cells were treated with trypsin diluted 1:10 in PBS. After 15 min incubation, the floating cells were harvested and counted. To determine the percentage of floating cells, a control sample was treated with undiluted trypsin and the amount of floating cells was set to 100 %. Shown are means of three replicates with SD.

3.7.3 Influence of T329 phosphorylation on the DNA binding activity of p53

To further investigate the impaired p53 dependent gene expression, the binding to p53 target DNA was verified. Three direct p53 binding sites that show an inducible p53 occupancy upon DNA damage were analysed by chromatin-immunoprecipitation (ChIP), followed by qPCR. For this purpose, the cells were treated with etoposide and the chromatin was isolated, shared and immunoprecipitated with the α p53 antibody DO-1. The precipitated chromatin was analysed by qPCR with primers that amplified the DNA around the p53 binding motif for *CDKN1A*, *MDM2* and *GADD45.* The determined C_T values were normalised to the C_T values determined in the whole chromatin input. As a negative control, an α mouse IgG antibody was used for the IP. As expected, the rec. WT p53 protein showed inducible binding to all three target genes upon DNA damage (Fig. 16). The p53 protein in the rec. T/E cells showed a comparable occupancy of p53 to the three target sites. Due to the clear difference between the binding of rec. T/A p53 to its targets compared to the p53$^{-/-}$ cells, the detection and binding of p53 targets is still possible in the rec. T/A cells. However, the induction of DNA binding upon DNA damage is severely reduced compared to the rec. WT or rec. T/E cells.

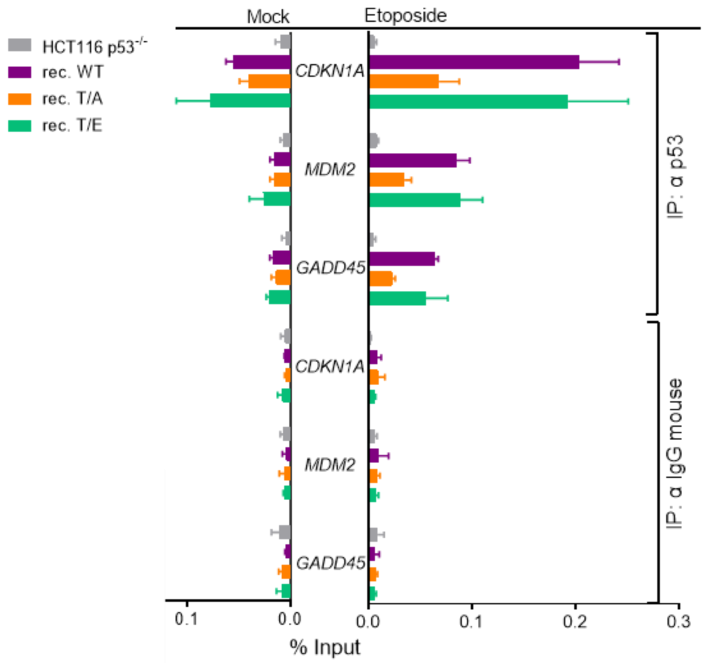

Fig. 16 Impact of T329 mutations on the DNA binding activity of p53. The cells were treated with etoposide for 24 h. The chromatin was isolated and precipitated with the p53 (DO-1) antibody or an IgG control antibody. The retrieved DNA was analysed by qPCR. The primers were chosen for regions representing known p53 binding motives. The C_T values are normalised to the whole chromatin input. Mean values with SD of three replicates are shown.

3.7.4 Influence of T329 phosphorylation on the induction of cell cycle arrest

The progression through the cell cycle can be inhibited at several checkpoints to prevent uncontrolled cell proliferation. In the case of DNA damage, the activated p53 protein induces the expression of cell cycle inhibiting factors like p21 (*CDKN1A)*. This leads to a cell cycle arrest at the next cell cycle checkpoint [147]. To investigate the role of T329 in the induction of cell cycle arrest, the cells were treated with etoposide or doxorubicin and were subsequently analysed regarding their distribution in the different cell cycle stages. Propidium iodide (PI) was used to stain the DNA and visualise the different cell cycle stages by the amount of DNA. In untreated conditions, the unsynchronised cells showed a distribution of 40 – 60 % of cells in G1 phase and 30 – 40 % of cells in G2/M phase, while the rest of the cells showed an intermediate DNA content during S phase (Fig. 17). Upon DNA damage, the cells showed a G2/M arrest. This G2/M arrest was not dependent on p53 since nearly 100 % of the p53$^{-/-}$ cells are arrested in G2/M phase. After DNA damage, the rec. WT cells still showed a clearly visible fraction (approx. 20 % after etoposide and approx. 35 % after doxorubicin) of cells in the G1 phase. It can be assumed that upon p53 activation, the G1 arrest was induced, before these cells undergo G2/M arrest. This fraction of G1 arrested cells was also detectable in the rec. T/E cells. The rec. T/A cells showed a significantly decreased fraction of G1 arrested cells. The cell cycle distribution upon DNA damage was comparable to the p53$^{-/-}$ cells. The induction of p53 dependent G1 cell cycle arrest was impaired in the phospho-mutant rec. T/A cell line.

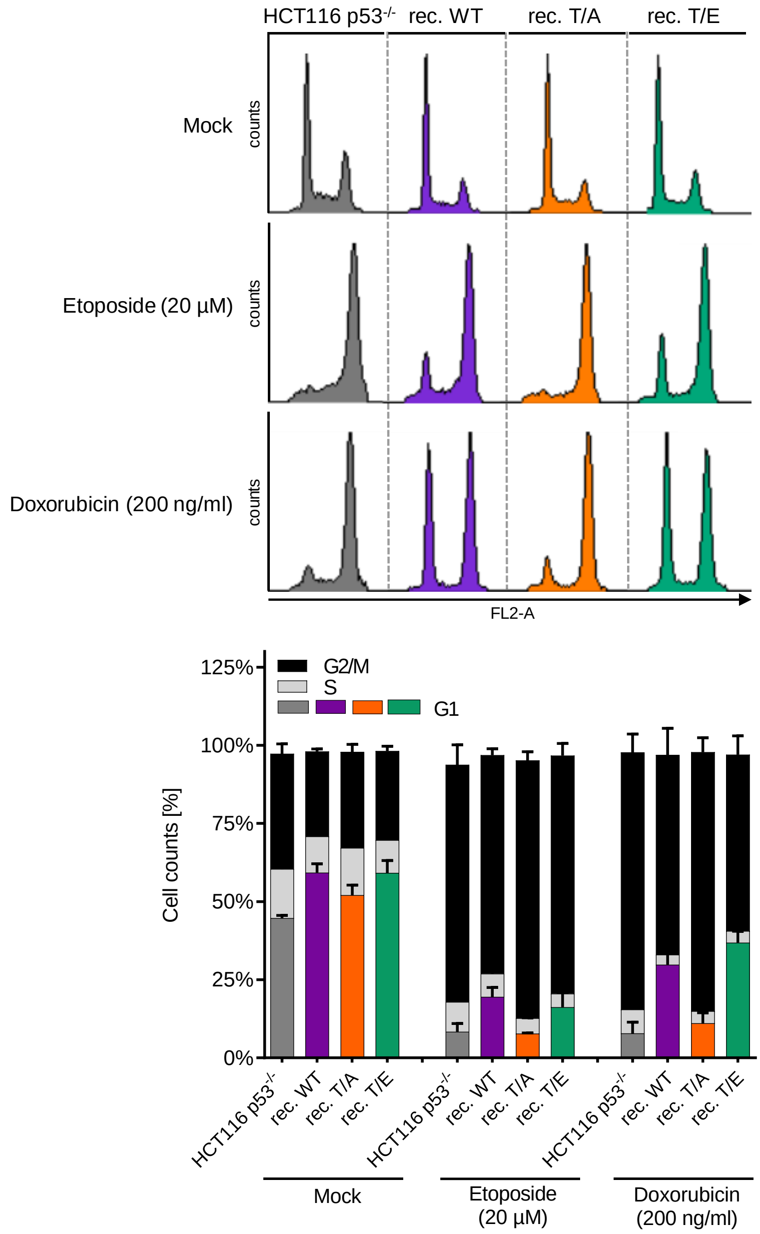

Fig. 17 Impact of T329 mutations on the p53-dependent G1 arrest upon DNA damage. The cells were treated with etoposide or doxorubicin for 24 h to induce a cell cycle arrest by p53 activation. The fixed cells were stained with propidium iodide (PI). The cells were analysed by FACS. The distribution between the cell cycle phases was analysed with the Cell Quest Pro software. Representative FACS profiles of the cell cycle distribution are shown. Quantitative analysis of three replicates are shown with mean and SD.

3.7.5 Influence of T329 phosphorylation on the induction of apoptosis

If the detected DNA damage cannot be repaired, the induction of apoptosis is one of the most important functions of p53 to prevent cancer development or to destroy cancerous cells during cancer therapy [168]. To determine the effect of pT329 on the induction of apoptosis, the cells were treated with etoposide, which will continuously damage the DNA and induce apoptosis. The cells were stained with Annexin V, which binds phosphatidylserine on the cell membrane and thereby marks cells that undergo apoptosis. The cells were analysed via FACS. The induction of apoptosis was significantly decreased in the p53$^{-/-}$ cells compared to the rec. WT cells (Fig. 18). After 24 h, approx. 40 % of the rec. WT cells underwent apoptosis, whereas the p53$^{-/-}$ cells showed nearly no apoptotic cells after 24 h and approx. 40 % apoptotic cells after 48 h. The induction of apoptosis was still possible but severely reduced in the p53$^{-/-}$ cells. The rec. T/E cells showed similar but slightly fewer apoptotic cells upon DNA damage. In contrast, the rec. T/A cells showed a significantly decreased number of apoptotic cells than the rec. WT cells. Thus, the induction of apoptosis was severely impaired in the phospho-mutant T/A cells.

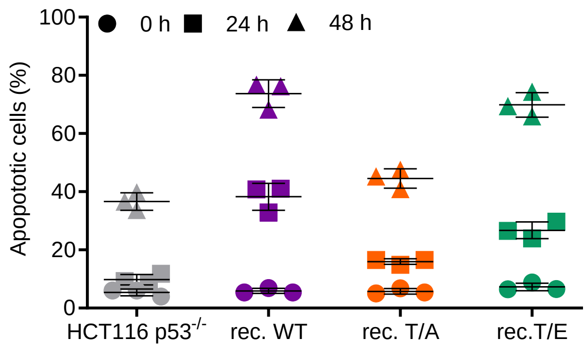

Fig. 18 Impact of pT329 on the p53 dependent apoptosis. Cells were treated with etoposide for 24 h or 48 h to induce apoptosis. The cells were stained with Annexin V conjugated with Allophycocyanin (APC). The cells were analysed by FACS. Displayed are the Annexin V positive cells after the indicated time points. Three replicates are shown with mean and SD.

3.7.6 Influence of T329 on the induction of senescence

To determine the influence of T329 phosphorylation on the induction of senescence, the cells were treated with bleomycin or doxorubicin to induce senescence. Bleomycin was used as a continuous stimulus for 4 d, whereas doxorubicin was added for 16 h to induce DNA damage, followed by a recovery of 4 d. During this recovery, the cells that did not manage to re-enter the cell cycle underwent apoptosis or senescence. During the senescence, the β-galactosidase expression is increased [332]. The cells were incubated with X-gal and the abundance of this enzyme was determined by the development of blue staining. The rec. WT cells contained many senescent cells in both stimulations (Fig. 19). The $p53^{-/-}$ cells showed overall less senescent cells with lighter staining than the rec. WT cells. The rec. T/A cells showed a comparable number of senescent cells to the $p53^{-/-}$ cells. The staining in some cells upon bleomycin treatment seemed stronger than the $p53^{-/-}$ cells. Thus, under continuous stimulation, the abundance of the p53 T/A protein may have a residual effect on the induction of senescence. The rec. T/E cells showed a staining intensity comparable to the rec. WT cells.

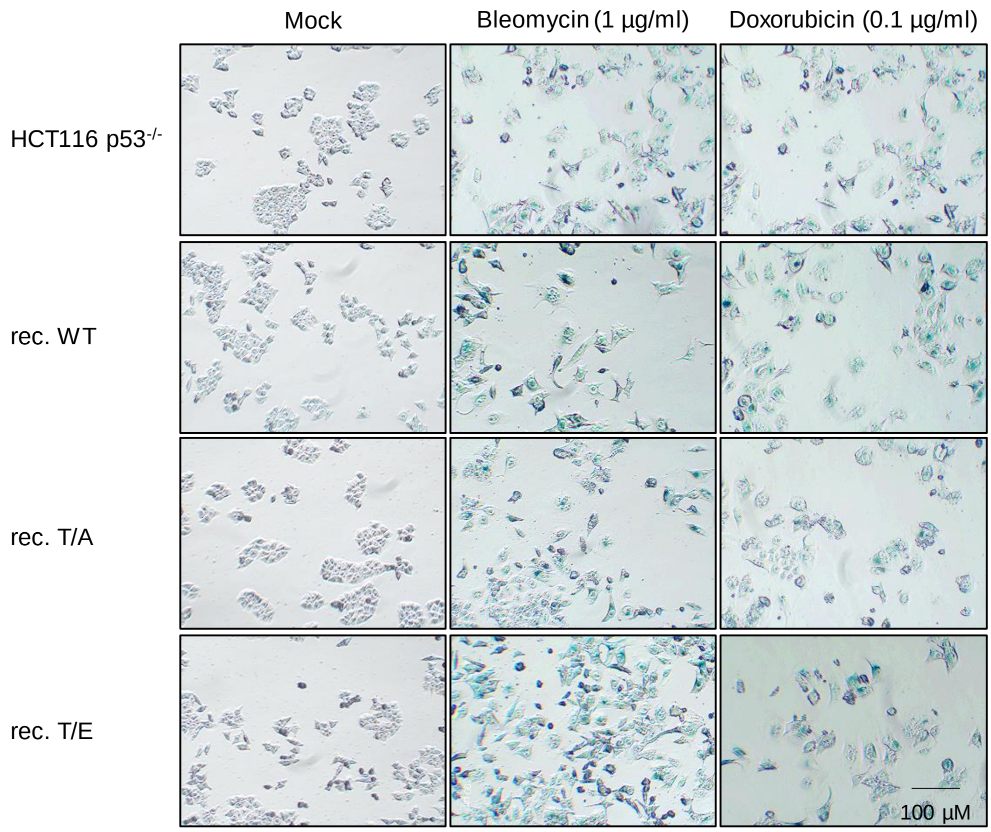

Fig. 19 Impact of pT329 on the p53 dependent senescence. The indicated cells were treated with bleomycin for 4 d or Doxorubicin for 16 h followed by 4 d days of recovery. The cells were incubated with X-gal and analysed for ß-galactosidase activity indicated by blue staining of the cells.

3.8 The role of T329 phosphorylation in the PTM crosstalk of p53

Since several PTM's influences the occurrence of other PTM's [333], the impact of pT329 on p53-activating modifications was addressed. The cells were stimulated with etoposide to induce the phosphorylation of T329, and PTM's were analysed by Western blotting with phospho-specific antibodies. Upon increasing amounts of etoposide, all activating phospho-sites were induced in the rec. WT cells (Fig. 20A). In the rec. T/E cells, the signal for pS46 was decreased compared to the rec. WT cells. The quantification showed that S46 is significantly less phosphorylated (approx. 70 %) in the rec. T/E cells, whereas S15 and S392 showed comparable phosphorylation levels. In the rec. T/A cells, only the phosphorylation of S15 was induced. For S392, only a very weak phospho-signal could be observed, and none for pS46. The quantification revealed that the phosphorylation of S392 and S46 are highly impaired in the rec. T/A cells.

The comparative time curve after UVC radiation confirmed that S392 got less phosphorylated and S46 showed no phosphorylation at all in the rec. T/A cells (Fig. 20B). In summary, the phospho-mutant T329A showed a severe reduction of p53 activating phosphorylations.

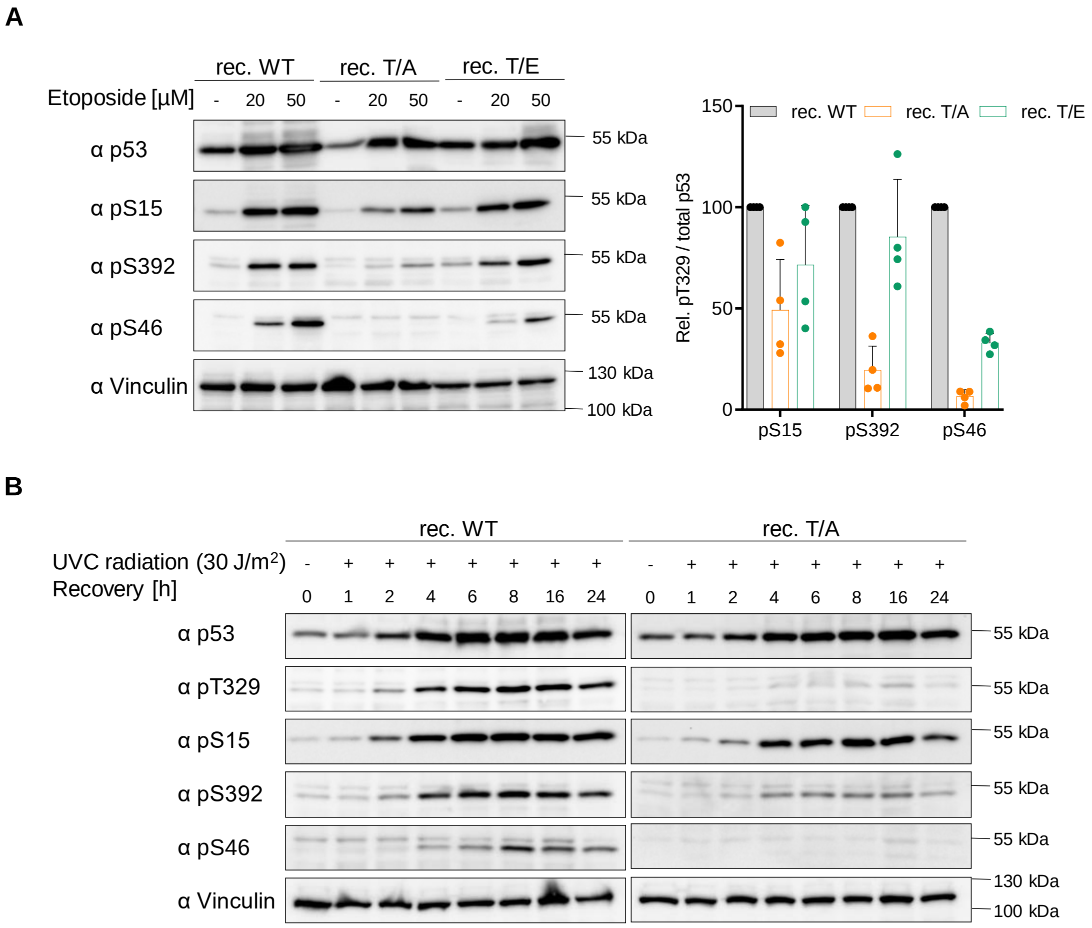

Fig. 20 Influence of pT329 on other p53-activating phospho-sites. A: The cells were treated with etoposide for 16 h. The cells were lysed and analysed by Western blotting. Densitometric analysis was performed normalising the signal of the phospho-specific antibodies to the total p53 signal given by the DO-1 antibody (α p53). The phospho-signal is shown relative to p53 WT. Four replicates are shown with SD. **B:** The cells were treated with UVC radiation and were incubated for the indicated time periods. The cells were lysed and analysed by Western blotting.

3.8.1 The phosphorylation of T329 plays a role in the interaction with HIPK2

S46 gets phosphorylated after severe DNA damage to mediate the induction of apoptosis. Many kinases have been identified to play a role in S46 phosphorylation. One major kinase that is shown to phosphorylate S46 directly is HIPK2 [239]. Knowing that S46 phosphorylation is impaired due to the mutation of T329, the interaction between p53 and HIPK2 was investigated. HA-tagged HIPK2 was transiently expressed in the cells via plasmid transfection. HIPK2 was immunoprecipitated with an α HA antibody. The eluate was analysed by Western blotting for co-precipitation of p53. Only the rec. WT p53 was co-precipitated under DNA damage conditions (Fig. 21A). The p53 T/A protein and the p53 T/E protein showed no or severely less interaction with HIPK2. Hence, it could be concluded that T329 plays a role in the p53 and HIPK2 interaction since both amino acid exchanges prevented proper HIPK2 binding.

3.8.2 Impact of T329 on the acetylation of K373 and K382

The phosphorylation of S46 leads to the acetylation of K373 and K382, which plays an essential role in p53 stabilisation and DNA binding [238–240]. Based on the absent S46 phosphorylation, the acetylation of K373 and K382 was further investigated. The indicated cell lines were stimulated with etoposide to induce the phosphorylation of S46. The cells were lysed and analysed by Western blotting with PTM specific antibodies. Both cell lines with T329 mutations showed less or no acetylation of K373 and K382 (Fig. 21B). This confirmed the important role of T329 in the PTM crosstalk of p53.

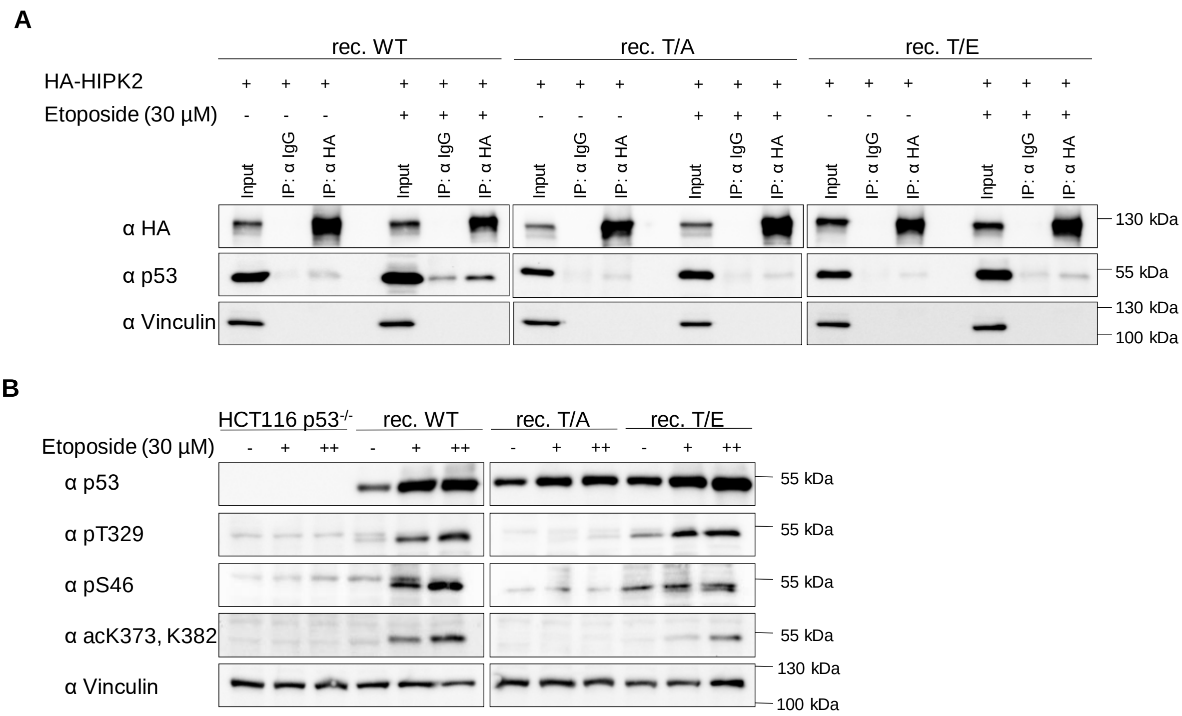

Fig. 21 Influence of pT329 on the interaction with HIPK2 and K373 and K382 acetylation. A: The indicated cells were transfected with HA-HIPK2 and treated for 16 h with etoposide. The cells were lysed and HIPK2 was precipitated with a α HA or control IgG antibody. The input (10 % of the lysate) and the eluate after IP were analysed by Western blotting. **B:** The cells were treated with etoposide for 16 h. The cells were lysed and analysed by Western blotting

3.9 Influence of the inhibition of kinases on the phosphorylation of T329

An inhibitor screening was performed to investigate which kinases might play a role in T329 phosphorylation. Many kinases have already been identified to impact p53 activation upon DNA damage [128]. A selection of these kinases were inhibited with kinase-specific small molecule inhibitors before DNA damage induction. The phosphorylation of T329 was detected after Western blotting and the signal was quantified by normalisation to the total p53 protein. The inhibition of Chk1 and PKC had a reducing effect on the T329 phosphorylation by approx. 30 % (Fig. 22A). The inhibition of the major DNA damage transmitting kinases ATM, ATR and DNA-PK did not affect the T329 phosphorylation. The phosphorylation of S15 occurred independent of kinase inhibition. S392 showed a tendency to be less phosphorylated upon the inhibition of Chk1 and PKC.

Since earlier findings of this study showed that nutlin 3a induced the T329 phosphorylation, the influence of Chk1 and PKC inhibition upon nutlin 3a treatment was investigated. The cells were subsequently treated with kinase inhibitors and CPT or nutlin 3a. The cells were harvested and analysed by Western blotting. The activating phospho-sites of Chk1 (S345) and Chk2 (T68) were stained to ensure that the DNA damage signalling pathway is inactive under nutlin 3a treatment. During CPT treatment. It could be confirmed that Chk1 and PKC inhibition reduced T329, S392 and S46 phosphorylation (Fig 22B). S15 remained phosphorylated. Upon nutlin 3a treatment, only the phosphorylations of T329 and S392 were induced. Both Chk kinases remained inactive. The inhibition of Chk1 did not affect the T329 phosphorylation. In contrast to the DNA damage-induced situation, the inhibition of ATM and Chk1 resulted in increased signals for pT329, pS15, pS392 and pS46 compared to the control without kinase inhibitor. The inhibition of PKC showed a similar reducing impact on the T329 phosphorylation as under DNA damage conditions. Therefore, it is likely that PKC playes a DNA damage-independent role in the phosphorylation of T329.

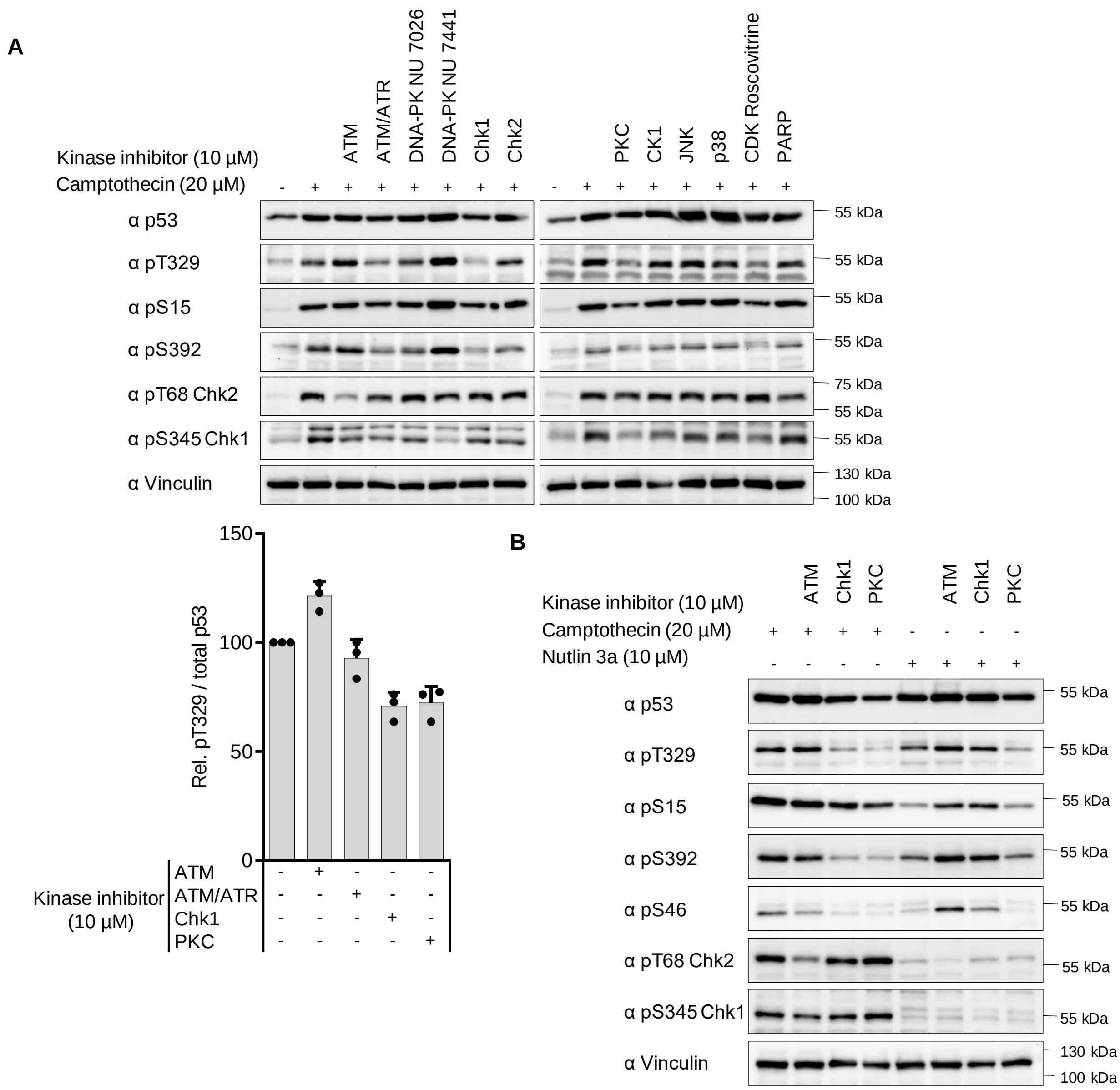

Fig. 22 The inhibition of Chk1 or PKC reduces the pT329 signal. **A:** The cells were incubated for 2 h with the indicated inhibitor. Afterwards the cells were treated with CPT for 16 h. The cells were lysed and analysed by Western blotting. Densitometric analysis was performed normalising the signal of the phospho-specific T329 antibody to the total p53 signal given by the DO-1 antibody (α p53). Three replicates with SD are shown. **B:** HCT116 p53 WT cells were treated with the indicated kinase inhibitor for 2 h followed by a treatment with CPT or 10 µM nutlin 3a for 16 h. The cells were lysed and analysed by Western blotting.

3.9.1 Influence of PKC inhibition on the phosphorylation of T329

To further investigate the PKC kinases' role on the T329 phosphorylation, an inhibitor library was used to characterise further which isoform of PKC is responsible for the T329 phosphorylation. The cells were subsequently treated with PKC inhibitors and CPT to induce DNA damage. The cells were lysed and analysed by Western blotting. Four of the applied inhibitors reduced the T329 phosphorylation (Fig. 23). These inhibitors (Gö6983, LY333531, Rotlerin and B160) have an inhibitory effect on PKCδ, according to the manufacturer's information. Therefore, PKCδ is the PKC isoform most likely to play a role in T329 phosphorylation. Furthermore, p53 is already known to be a substrate for PKCδ phosphorylation [186].

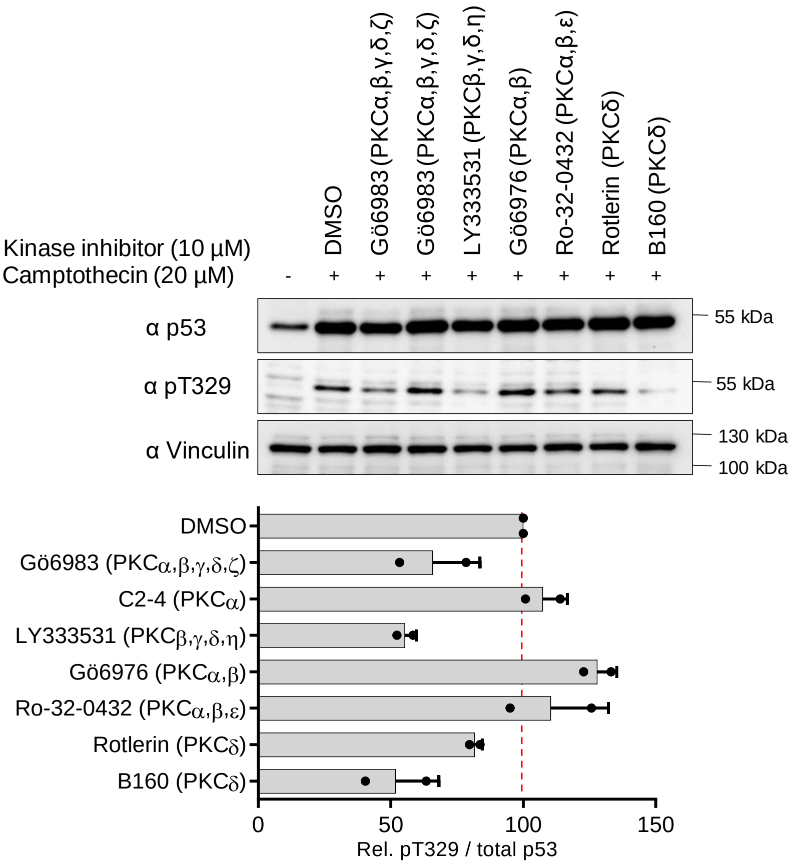

Fig. 23 Influence of PKC inhibition on pT329. **A:** The cells were incubated for 2 h with the indicated inhibitor. Afterwards the cells were treated with CPT for 16 h. The cells were lysed and analysed by Western blotting. Densitometric analysis was performed normalising the signal of the phospho-specific T329 antibody to the total p53 signal given by the DO-1 antibody (α p53). Two replicates with deviation are shown.

3.10 Influence of T329 phosphorylation on the conformation of p53

As the proper conformation of p53 is required for its biological function, the influence of T329 on the conformation of p53 was investigated. In its native conformation, the structure of p53 exposes several parts of the protein to its surrounding, whereas other structures are located inwards. Due to the protein structure, only some motifs for protease cleavage are exposed and accessible. Digestion of native proteins with proteases leads to a conformation-specific cleavage pattern that can be visualised by Western blotting. This cleavage pattern was achieved by a trypsin or thermolysin treatment of a native lysate. Trypsin cuts proteins after arginine or lysine, and thermolysin after hydrophobic amino acids like leucine, isoleucine and phenylalanine. The trypsin treatment resulted in several fragments between 35 – 45 kDa with three prominent p53 fragments (Fig 24A). One of these fragments contained the N-terminal part of p53 and the two others the C-terminal part. This pattern showed no distinct differences in the rec. T/A or rec. T/E p53 protein. The digest with thermolysin resulted in approx. five fragments of p53 with a size of 40 – 55 kDa. The most prominent fragment and one or two smaller ones contained the N-terminal part of p53. The smaller fragments lacked the N-terminal region. Also, this digestion pattern showed no differences between the different p53 mutants. The conformation did not seem to be severely impaired by the mutation of T329.

Since the conformation and its compactness are highly dependent on temperature [51], the thermodynamic influence on the p53 conformation was investigated. To take a closer look at the conformation at different temperatures, conformation-specific antibodies were used. PmAb1620 was used to precipitate p53 in its wild-type conformation. PmAb240, in contrast, precipitates unfolded p53 that lacks its compact conformation [334,335]. The IP was performed at 4 °C and 22 °C to compare the temperature's impact on the conformation of p53. The whole-cell lysate and the precipitated p53 were analysed by Western blotting. Under etoposide treated conditions at 4 °C, the p53 WT protein only showed a precipitated signal after PmAb1620 IP (Fig. 24B). Nearly no p53 protein remained unfolded. At 22 °C p53 showed nearly equal amounts of folded and unfolded protein. In contrast, the conformation defective mutant p53 V143A was only detectable in the unfolded form. At 4 °C, the rec. T/A and the rec. T/E p53 protein was detectable in the correct conformation and showed similar results to the rec. WT p53. At 22 °C, the rec. T/E p53 remained folded and showed only a minor fraction of unfolded p53. In contrast, the rec. T/A protein showed only a tiny fraction of folded protein and a stronger signal for unfolded p53 protein. It can be concluded that the T/A mutation reduces the stability of the p53 conformation at higher temperatures.

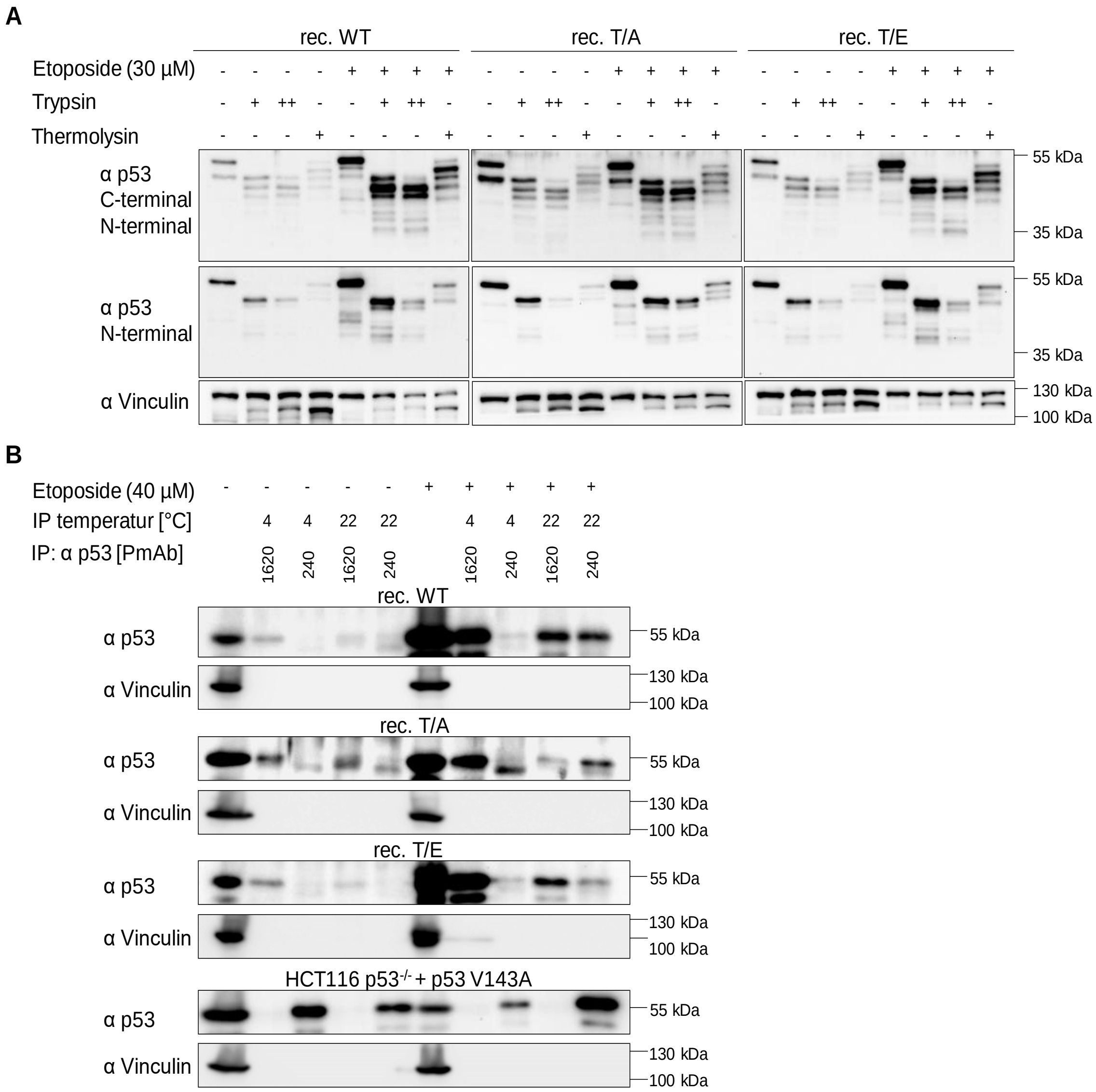

Fig. 24 Impact of pT329 on the p53 WT conformation. A: The indicated cells were treated for 16 h with etoposide. The cells were lysed and parts of the lysate were treated with trypsin (1:6 or 1:12) or thermolysin (5 ng/µl) for 20 min at 37 °C. The lysates were analysed by Western blotting. **B:** The indicated cells were treated with etoposide for 16 h. The cells were lysed and p53 was precipitated with PmAb1620 (WT conformation of p53) or PmAb240 (unfolded p53). The IP was done at 4 °C or RT (22 °C). The input (10 % of the lysate) and the eluate after IP was analysed by Western blotting.

3.11 The pT329 dependent p53 interactome

The pattern of PTM's on p53 is known to influence its interactome and thereby mediates adjustments in the p53 response [187]. To determine the influence of pT329 on the p53 interacting proteins, a mass spectrometry analysis of immunoprecipitated p53 was performed in cooperation with the workgroup of Prof. Dr. Krüger – CECAD - Cologne. The p53 WT and mutated proteins were immunoprecipitated in untreated or etoposide-treated conditions. A quantitative analysis of the co-precipitated proteins was made for biological triplicates and was statistically analysed with an ANOVA approach. 102 proteins showed a differential binding profile with a FDR ≤ 0.1. Proteins with similar binding patterns were displayed in the hierarchical clustering (Fig. 25A).

The fourth cluster contained proteins that were enriched in all α p53 IP’s. The abundance of these common interacting proteins was displayed in the line blot (Fig. 25B).

Cluster 6 contained proteins with preferential binding to the p53 T/A protein. The CCT and TCP proteins belong to the TRiC (T-complex protein ring complex) complex. The line blot revealed that these proteins were enriched in all the α p53 IP’s with a significantly stronger interaction with the p53 T/A protein.

Cluster 10 contained proteins with a preferential interaction with the p53 WT protein under DNA damage conditions. These proteins showed an inducible interaction with p53 WT and did not bind to both mutated p53 proteins. A closer look on these proteins in the line blot revealed the strong interaction of several ribosomal proteins with the p53 WT protein. Additionally, the kinase CK2α (*CSNK2A1*) that is known to phosphorylate p53 and the nuclear protein Nucleolin (NCL) primarily interacted with the p53 WT protein [224].

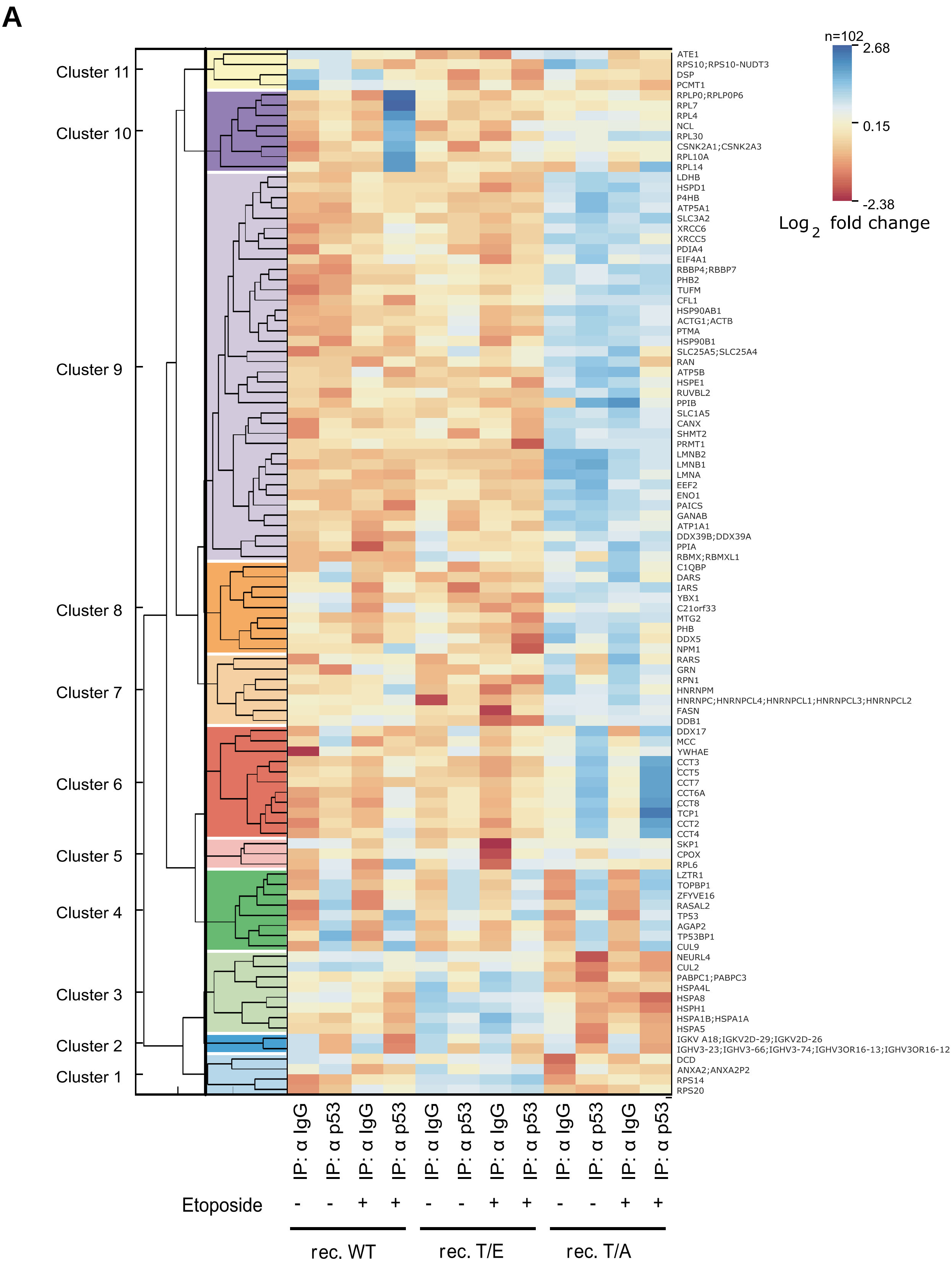
A
Cluster 11
Cluster 10
Cluster 9
Cluster 8
Cluster 7
Cluster 6
Cluster 5
Cluster 4
Cluster 3
Cluster 2
Cluster 1
ATE1
RPS10;RPS10-NUDT3
DSP
PCMT1
RPLP0;RPLP0P6
RPL7
RPL4
NCL
RPL30
CSNK2A1;CSNK2A3
RPL10A
RPL14
LDHB
HSPD1
P4HB
ATP5A1
SLC3A2
XRCC6
XRCC5
PDIA4
EIF4A1
RBBP4;RBBP7
PHB2
TUFM
CFL1
HSP90AB1
ACTG1;ACTB
PTMA
HSP90B1
SLC25A5;SLC25A4
RAN
ATP5B
HSPE1
RUVBL2
PPIB
SLC1A5
CANX
SHMT2
PRMT1
LMNB2
LMNB1
LMNA
EEF2
ENO1
PAICS
GANAB
ATP1A1
DDX39B;DDX39A
PPIA
RBMX;RBMXL1
C1QBP
DARS
IARS
YBX1
C21orf33
MTG2
PHB
DDX5
NPM1
RARS
GRN
RPN1
HNRNPM
HNRNPC;HNRNPCL4;HNRNPCL1;HNRNPCL3;HNRNPCL2
FASN
DDB1
DDX17
MCC
YWHAE
CCT3
CCT5
CCT7
CCT6A
CCT8
TCP1
CCT2
CCT4
SKP1
CPOX
RPL6
LZTR1
TOPBP1
ZFYVE16
RASAL2
TP53
AGAP2
TP53BP1
CUL9
NEURL4
CUL2
PABPC1;PABPC3
HSPA4L
HSPA8
HSPH1
HSPA1B;HSPA1A
HSPA5
IGKV A18;IGKV2D-29;IGKV2D-26
IGHV3-23;IGHV3-66;IGHV3-74;IGHV3OR16-13;IGHV3OR16-12
DCD
ANXA2;ANXA2P2
RPS14
RPS20
n=102
2.68
0.15
-2.38
Log 2 fold change
IP: α IgG
IP: α p53
IP: α IgG
IP: α p53
IP: α IgG
IP: α p53
IP: α IgG
IP: α p53
IP: α IgG
IP: α p53
IP: α IgG
IP: α p53
Etoposide
- - + + - - + + - - + +
rec. WT
rec. T/E
rec. T/A

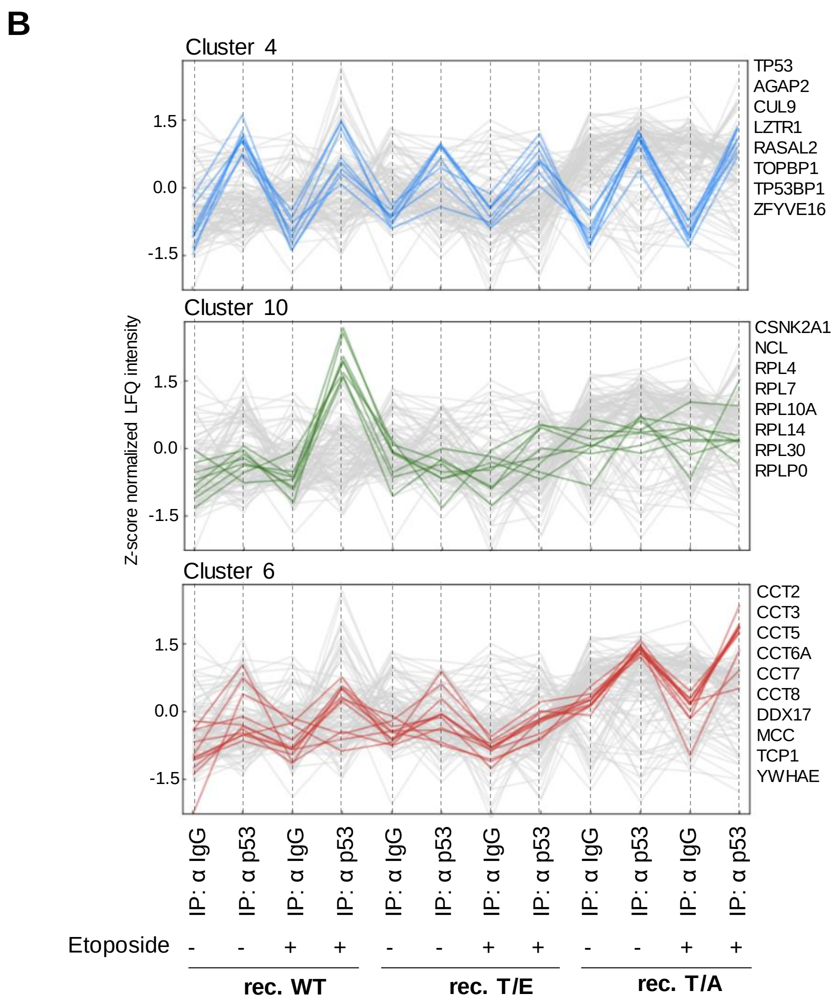

Fig. 25 Cluster analysis of p53 interacting proteins. A: The indicated cell lines were treated with etoposide for 16 h. The cells were lysed and p53 was precipitated by the DO-1 antibody or a control IgG antibody. The precipitated proteins were analysed by mass spectrometry. Shown is a hierarchical clustering of 102 significantly (FDR ≤ 0,1) deregulated proteins after ANOVA analysis. **B:** Displayed are expression profiles of selected cluster after Z-score normalisation of the LFQ intensities. The cluster 4 shows proteins abundant in all p53 IPs and shows common interacting proteins. Cluster 10 displays proteins interacting stronger with the WT p53 under etoposide treatment. Cluster 6 displays proteins, that interact more strongly with the T/A mutant.

To further investigate the differential binding partners of p53 WT and p53 T/A, the amount of all proteins was compared and statistically analysed in unstimulated and etoposide-treated conditions. All abundant proteins were displayed in the volcano blot (Fig. 26A,D). The significant (p-value ≤ 0.05) proteins that primarily interact with p53 T/A ($\log_2$ fold change ≥ 0.5) were marked in orange and the preferred binding partners of p53 WT ($\log_2$ fold change ≤ -0.5) were marked in purple. To highlight already published interactions and further investigate the differential interactome, the interactors were combined with proteins that are only detectable in the corresponding sample and could not be considered in statistical analysis. These sets of proteins were analysed with a STRING analysis. What is worth mentioning was the preferred interaction of NEURL4 with p53 WT since it is known to promote p53 activation (Fig. 26B) [336]. In the p53 T/A interactome the members of the TRiC complex were marked in green (Fig. 26C). Additionally, LMNB1 and LMNB2 showed a high p53 T/A binding specificity. The interaction with PP1B is worth mentioning since it is known to play a role in p53 degradation [337]. Under etoposide-treated conditions, the p53 WT interactome contained ribosomal proteins and the p53 activity supporting proteins CK2α (*CSNK2A1*) and CCAR2 (Fig. 26E). The induction of DNA damage had no severe effect on the p53 T/A interactome. The occupancy with TRiC complex members was still prominent (Fig. 26F).

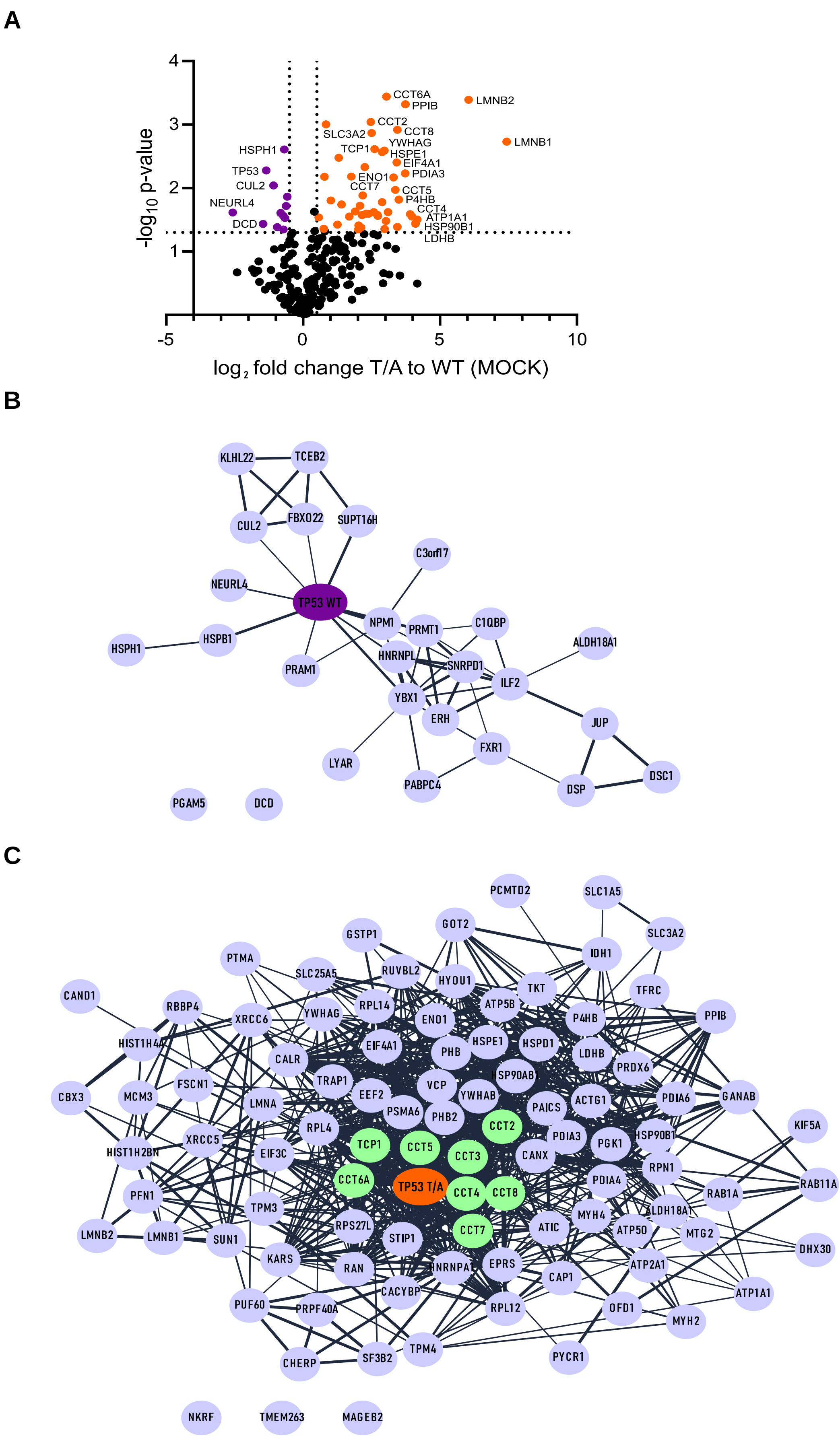
A
4
3
2
1
-5
0
5
10
-log10 p-value
log2 fold change T/A to WT (MOCK)
CCT6A
PPIB
LMNB2
CCT2
CCT8
SLC3A2
YWHAG
LMNB1
TCP1
HSPE1
EIF4A1
HSPH1
TP53
ENO1
PDIA3
CUL2
CCT7
CCT5
P4HB
NEURL4
CCT4
ATP1A1
DCD
HSP90B1
LDHB
B
KLHL22
TCEB2
CUL2
FBXO22
SUPT16H
C3orf17
NEURL4
TP53 WT
NPM1
PRMT1
C1QBP
ALDH18A1
HSPH1
HSPB1
HNRNPL
SNRPD1
PRAM1
ILF2
YBX1
ERH
JUP
FXR1
LYAR
DSC1
PABPC4
DSP
PGAM5
DCD
C
PCMTD2
SLC1A5
GOT2
SLC3A2
GSTP1
IDH1
PTMA
RUVBL2
SLC25A5
HYOU1
CAND1
TKT
TFRC
RBBP4
RPL14
ATP5B
YWHAG
XRCC6
ENO1
P4HB
PPIB
HIST1H4A
EIF4A1
HSPE1
HSPD1
PHB
LDHB
CALR
PRDX6
HSP90AB1
CBX3
MCM3
FSCN1
TRAP1
VCP
EEF2
YWHAB
ACTG1
PDIA6
GANAB
LMNA
PAICS
PSMA6
PHB2
CCT2
KIF5A
RPL4
PDIA3
HSP90B1
XRCC5
TCP1
CCT5
CCT3
PGK1
HIST1H2BN
EIF3C
CANX
RPN1
CCT6A
TP53 T/A
CCT4
CCT8
PDIA4
RAB11A
PFN1
RAB1A
TPM3
ALDH18A1
MYH4
RPS27L
ATIC
LMNB2
LMNB1
SUN1
STIP1
CCT7
ATP5D
MTG2
DHX30
KARS
RAN
HNRNPA1
EPRS
ATP2A1
CAP1
CACYBP
PUF60
RPL12
OFD1
ATP1A1
PRPF40A
MYH2
TPM4
CHERP
SF3B2
PYCR1
NKRF
TMEM263
MAGEB2

D

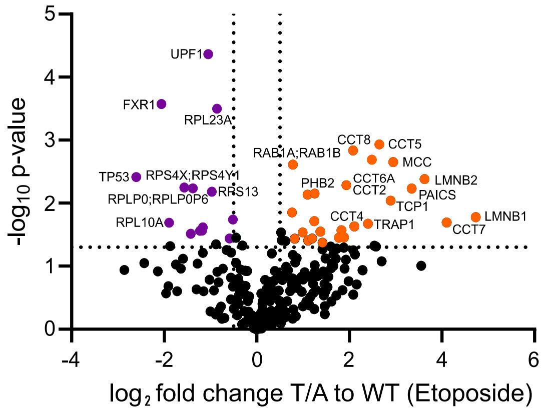

UPF1
FXR1
RPL23A
TP53
RPS4X;RPS4Y1
RPS13
RPLP0;RPLP0P6
RPL10A
CCT8
CCT5
RAB1A;RAB1B
MCC
PHB2
CCT6A
CCT2
LMNB2
PAICS
TCP1
CCT4
TRAP1
LMNB1
CCT7
0
1
2
3
4
5
-4
-2
0
2
4
6
$-\log_{10}$ p-value
$\log_2$ fold change T/A to WT (Etoposide)

E

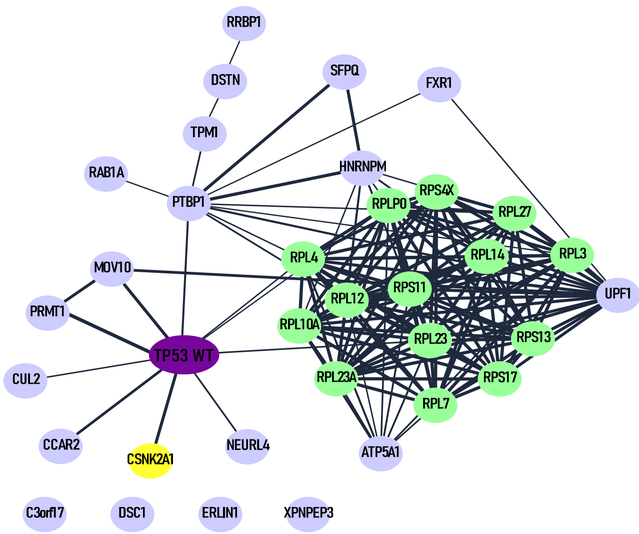

RRBP1
DSTN
SFPQ
FXR1
TPM1
RAB1A
HNRNPM
PTBP1
RPS4X
RPLP0
RPL27
RPL14
RPL3
MOV10
RPL4
RPS11
UPF1
PRMT1
RPL12
RPL10A
RPL23
RPS13
TP53 WT
CUL2
RPL23A
RPS17
RPL7
CCAR2
CSNK2A1
NEURL4
ATP5A1
C3orf17
DSC1
ERLIN1
XPNPEP3

F

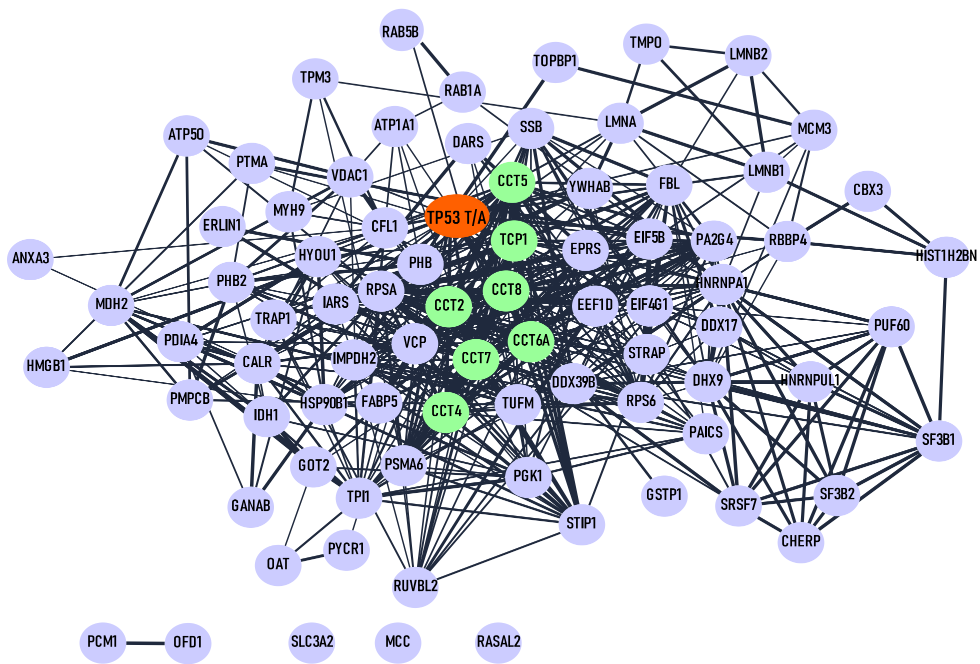

RAB5B
TMPO
TOPBP1
LMNB2
TPM3
RAB1A
ATP1A1
SSB
LMNA
MCM3
ATP50
DARS
PTMA
VDAC1
CCT5
YWHAB
FBL
LMNB1
CBX3
MYH9
ERLIN1
CFL1
TP53 T/A
TCP1
EPRS
EIF5B
PA2G4
RBBP4
HIST1H2BN
ANXA3
HYOU1
PHB
PHB2
RPSA
CCT8
HNRNPA1
MDH2
IARS
CCT2
EEF1D
EIF4G1
DDX17
PUF60
TRAP1
PDIA4
VCP
CCT6A
STRAP
HMGB1
CALR
IMPDH2
CCT7
DDX39B
DHX9
HNRNPUL1
PMPCB
HSP90B1
FABP5
RPS6
IDH1
CCT4
TUFM
PAICS
SF3B1
GOT2
PSMA6
PGK1
GANAB
TPI1
GSTP1
SRSF7
SF3B2
STIP1
CHERP
PYCR1
OAT
RUVBL2
PCM1
OFD1
SLC3A2
MCC
RASAL2

Fig. 26 Network analysis of differential p53 interacting proteins. A: The indicated cell lines were lysed and p53 was precipitated by the DO-1 antibody or a control IgG antibody. The precipitated proteins were analysed by mass spectrometry. The volcano blot shows proteins that are significantly (p-value ≤ 0,05) deregulated comparing the protein abundance of p53 T/A with p53 WT p53. The x axis displays the fold change (fc). Proteins on the left side (marked in purple) are more abundant in p53 WT samples. The orange proteins on the right side are more abundant in T/A samples. **B:** Displayed is the STRING protein interaction profile of p53 WT binding proteins in untreated conditions. The lines indicate already published interactions. **C:** Displayed is the STRING protein interaction profile of p53 T/A binding proteins in untreated conditions. Members of the chaperonin-containing T-complex (TRiC) are marked in green. **D:** The indicated cell lines were treated with etoposide for 16 h. The cells were lysed and p53 was precipitated by the DO-1 antibody or a control IgG antibody. The precipitated proteins were analysed by mass spectrometry. The volcano blot shows proteins that are significantly (p-value ≤ 0,05) deregulated comparing the protein abundance of p53 T/A with WT p53 IP. **E:** Displayed is the STRING protein interaction profile of p53 WT binding proteins upon DNA damage. The ribosome-associated proteins are marked in green**. F:** Displayed is the STRING protein interaction profile of p53 T/A binding proteins upon DNA damage. Members of the chaperonin-containing T-complex (TRiC) are marked in green.

3.11.1 The impact of CK2α on the T329 phosphorylation

CK2α is a p53 interacting kinase that phosphorylates p53 at the activating residue S392 [224]. The differential interactome detected CK2α as a p53 WT-specific interactor under DNA damage conditions. Since this interaction was dependent on T329, this result was confirmed by Co-IP experiments. The cells were transfected with HA-CK2α and an α HA IP was performed. The co-precipitation of p53 was analysed by Western blotting. Only the rec. p53 WT protein showed an interaction with HA-CK2α upon etoposide treatment (Fig 27A). This confirmed the differential interaction. To investigate if CK2α has an impact on T329 phosphorylation, a specific inhibitor was used. The inhibition of the kinase function of CK2α significantly reduced the T329 phosphorylation (Fig. 27B).

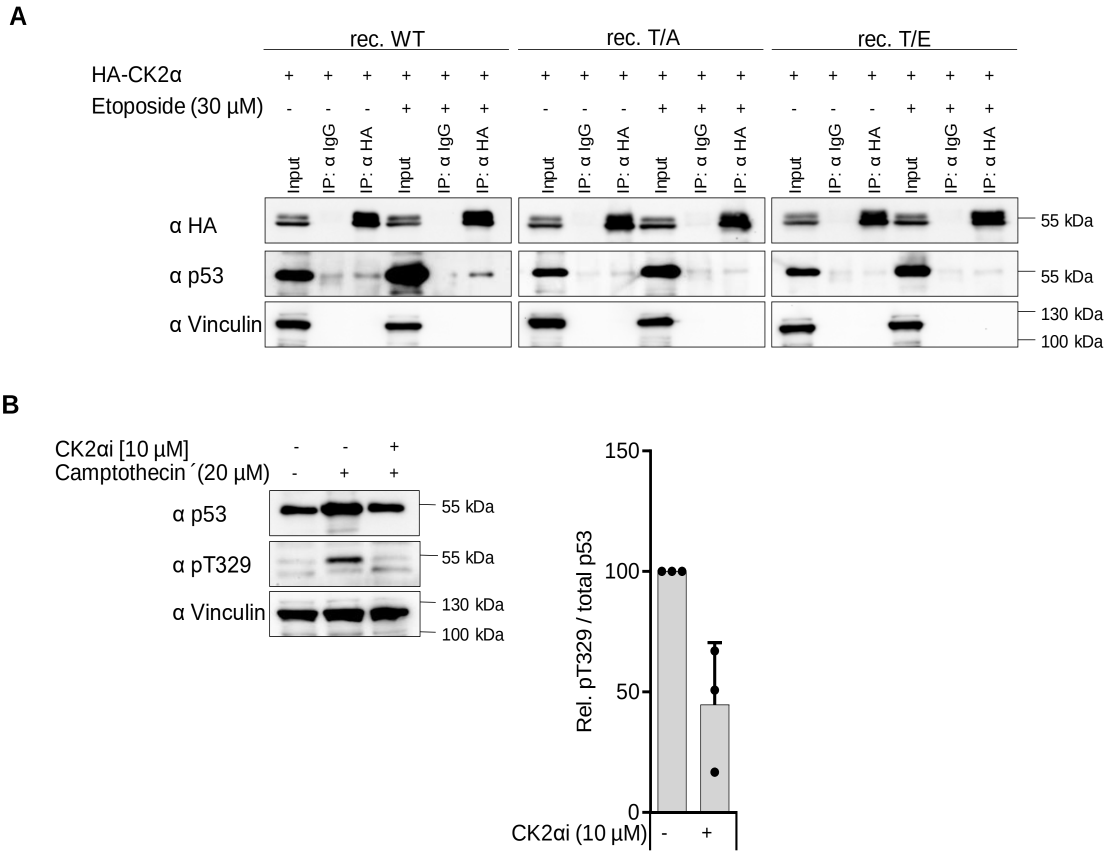

Fig. 27 The role of CK2α in T329 phosphorylation. A: The indicated cells were transfected with HA-CK2α and treated for 16 h with etoposide. The cells were lysed and CK2α was precipitated with a α HA or control IgG antibody. The input (10 % of the lysate) and the eluate after IP was analysed by Western blotting. **B:** HCT116 p53 WT cells were treated with the CK2α inhibitor CX-4945 for 2 h followed by a treatment with CPT for 16 h. The cells were lysed and analysed by Western blotting. Densitometric analysis was performed normalising the signal of the phospho-specific T329 antibody to the total p53 signal given by the DO-1 antibody (α p53). Three replicates with SD are shown.

3.11.2 Impact of CK2α knockdown on p53 functionality

To confirm the impact of CK2α on the phosphorylation of T329, a CK2α knockdown with siRNA against the responsible transcript of *CSNK2A1* was performed. HCT116 p53 WT cells were transfected with siRNA for 48 h. The RNA was isolated and analysed via qPCR. The inhibitor screening revealed an effect of Chk1 and PKCδ inhibition on the T329 phosphorylation. For further characterisation of the impact of these kinases, siRNA against *CHEK1* was used. Unfortunately, no sufficient knockdown of PKCδ could be achieved. The control qPCR showed downregulation of *CSNK2A1* and *CHEK1* to under 10 % remaining transcript (Fig. 28A). The influence of the knockdown of both kinases on pT329 was investigated by Western blotting. The knockdown of Chk1 leaded to a minor reduction of the pT329 signal of approx. 25 %, whereas the knockdown of CK2α resulted in a reduction of approx. 50 %.

The most prominent observation in this study was the loss of induction of DNA binding and transcription activation of p53 in the phospho-mutant p53 T/A cells. To check whether the phosphorylation of T329 depending on CK2α and/or Chk1 is responsible for the p53 activation, the transcriptional activity was investigated under the candidate kinases' knockdown. The transcription of three representative p53 target genes was determined by qPCR. As already described, the rec. T/A cells showed a severely reduced p53 target gene expression upon DNA damage induction compared to the rec. WT cells (Fig. 28B). The knockdown of CK2α resulted in a reduction of p53 target gene expression comparable to the rec. T/A cells. In contrast, the knockdown of Chk1 had no impact on the p53 target gene expression. Thus, the activation of p53-dependent gene transcription was reduced upon the mutation T329A and upon CK2α knockdown. It remains unclear whether CK2α contributes directly or indirectly to the phosphorylation of T329 and the activation of p53.

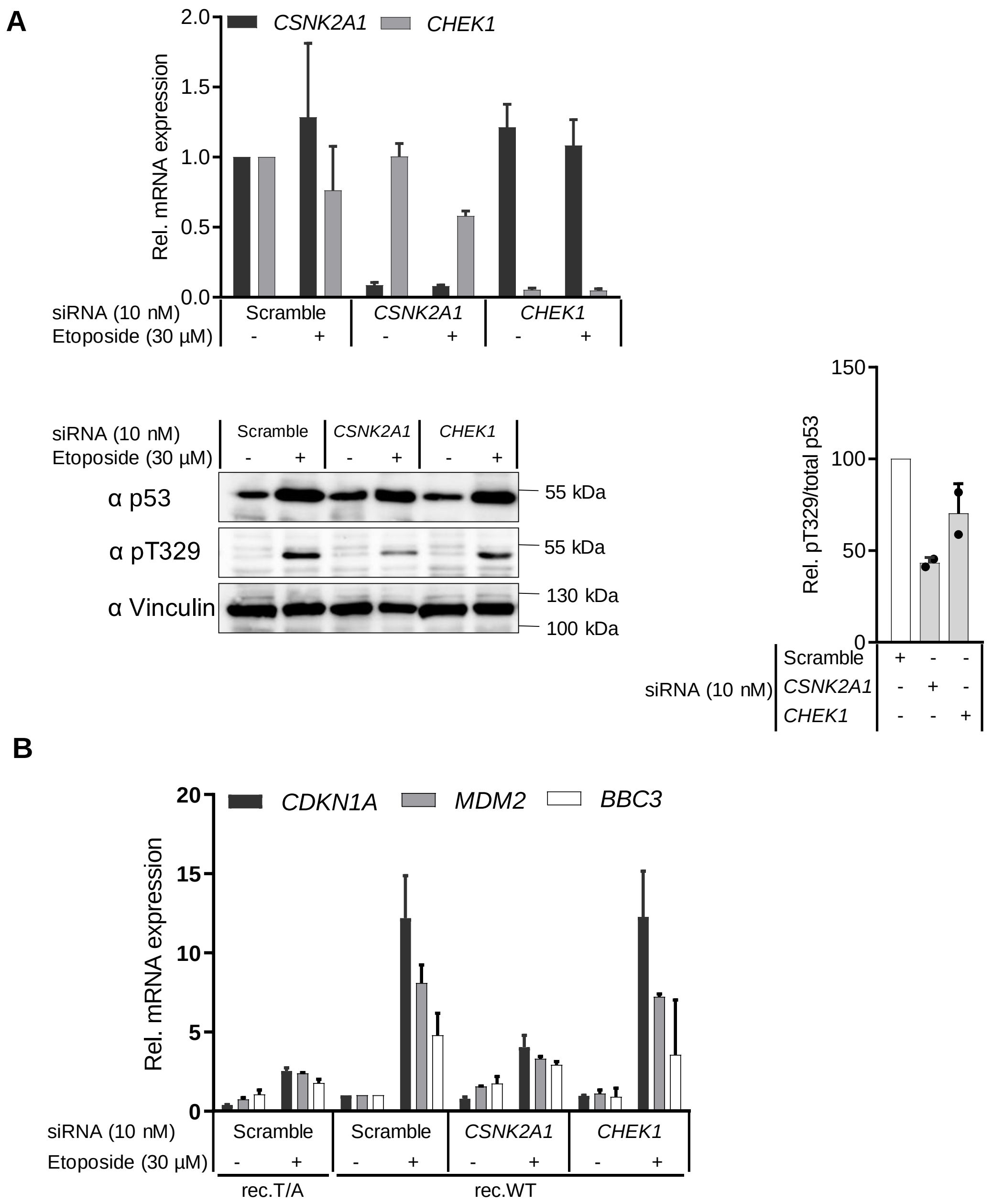

Fig. 28 The role of CK2α and Chk1 in T329-dependent p53 activation. A: The indicated cells were transfected with siRNA targeting *CSNK2A1* or *CHEK1* for 48 h and were treated for 16 h with etoposide. The cells were lysed and analysed by Western blotting. Densitometric analysis was performed normalising the signal of the phospho-specific T329 antibody to the total p53 signal given by the DO-1 antibody (α p53). Two replicates with deviation are shown. The knockdown of *CSNK2A1* and *CHEK1* was confirmed by qPCR. The mean of two replicates are shown with deviation. **B:** The indicated cells were transfected with siRNA targeting *CSNK2A1* or *CHEK1* for 48 h, and were treated for 16 h with etoposide. The total RNA was isolated and the expression of p53 target genes was analysed by qPCR. TPI was used as a housekeeping gene to determine ΔC_T values. The relative expression ($\Delta\Delta C_T$) of the mRNA expression for each gene is shown normalised to the siScramble sample of HCT116 WT. Mean values with SD of two replicates are shown.

4 DISCUSSION

The aim of this study was the identification of phosphorylation patterns of p53 to gain new aspects in the modulation of the p53 response. The residue T329 was identified as a novel phosphorylation site and its function in the p53 response was characterised. This study provides new details on the activation of p53 which pays a major role in prevention and treatment of cancer.

4.1 T329 gets phosphorylated during p53 activation

During the activation of p53 the phosphorylation of specific residues contributes to drive the p53 response towards the most beneficial cell fate. Depending on the damage of the cell this might be the arrest of the cell cycle and the repair of the DNA damage, or the induced apoptosis to prevent uncontrolled cell division [186]. The T329 residue in the TD has not yet been described as being phosphorylated during the p53 response *in vivo* [338,339]. However, *in vitro* kinase assays described Chk1-mediated p53 T329 phosphorylation [340]. Complementing these findings, the present study firstly identified the etoposide-inducible phosphorylation of T329 at the endogenous p53 WT protein *in vivo*. The generation of a phospho-specific antibody was used to further analyse the occurrence of pT329.

Along with other well-characterised activating phosphorylations, the phosphorylation of T329 is stimulated upon exposure to several DNA damaging agents. The time curve reveals that pT329 occurred as an early PTM briefly after pS15, similar to pS392 and earlier than pS46. Along with the kinetics, the intracellular localisation in the cytoplasmic and soluble nuclear fraction also suggests that T329 is an PTM occuring early in the p53 response.

Further, the dissociation of p53 and MDM2, achieved by nutlin 3a treatment, also lead to the phosphorylation of T329. Although the induction of phosphorylations upon nutlin 3a treatment is weaker compared to the induction by DNA damage, it was shown that nutlin 3a induces pS15 and pS392 as well. However, it is unclear whether the compound itself induces a small amount of DNA strand breaks and thereby induces the phosphorylations, or if the increased signal of the phospho-specific antibodies could be explained by the increased amount of p53 itself. The phosphorylations might also be induced by nutlin 3a independently of DNA damage, as already shown by Jones et al in 2008 [341]. The knockdown of MDM2 supports the observation that T329 is phosphorylated even without active DNA damage response. Hence, it is likely that pT329 occurs upon DNA damage and MDM2 dissociation in combination with the phosphorylations of S15 and S392. Therefore, it remains questionable, if T329 gets phosphorylated by a kinase activated by

DNA damage, and/or a constitutively active kinase, which is only able to phosphorylate T329 if p53 dissociates from MDM2.

4.2 The phosphorylation of T329 is required for p53 activation

Previous experiments with the p53 T329A mutant showed that pT329 does not play a critical role in the tetramerisation of the p53 protein. Therefore, this residue was not considered to be important for p53 activation [342]. This study also showed that the accumulation and tetramerisation of p53 after a stimulus is not severely affected by the mutation of T329. Nevertheless, a slight impact of the T329 phosphorylation on the tetramerisation cannot be excluded with the applied methods. Even though it was shown that T329 is not crucial for tetramerisation, it could be demonstrated that the phosphorylation of S392 increases the formation of tetramers [65]. Hence the phosphorylation of S392 is reduced upon the T329A mutation, the T329 phosphorylation might indirectly influence the tetramerisation by influencing pS392. To investigate minimal effects on the formation of tetramers, approaches like gel filtration chromatography should be used to investigate and compare the tetramerisation of T329 mutants with S392 mutants under DNA damage conditions.

However, the present study reveals a great impact of pT329 on the activation of p53, independent of tetramerisation. First if all, the mRNA and the overall protein amount pf p53 was reduced in the T329A mutant. Therefore, a reduced p53 functionality resulting from the reduced protein amount needs to be considered. The reason for the reduced transcription and protein levels remains unclear and needs to be further investigated. All investigated p53 functions (cell cycle arrest in the G1 phase, induction of apoptosis and senescence) were reduced in the T329A mutant. These findings were well-founded on the reduced p53-dependent gene transcription revealed by the RNA-sequencing. Additionally, the ChIP experiment showed that the p53 T329A protein lacked the induction of DNA binding upon DNA damage. Overall the decreased occupancy of p53 T329A and the reduced transcription of p53 target genes suggest that the phosphorylation of T329 is important for proper p53 activation.

The investigation of other PTMs revealed, that T329 impacts the PTM pattern of p53. The reduced amount of S392 phosphorylation might additionally reduce the DNA affinity, as the phosphorylation of S392 has already been described to enhance the DNA binding affinity of p53 [343]. Furthermore, loss of pS46 and the resulting loss of acetylated K373 and K382 are likely to impair the DNA binding activity, given that these PTMs have been shown to increase the DNA affinity of p53 [238–240]. This implicates that the phosphorylation of T329 plays an essential role in the mediation of other activating PTMs.

Since the PTM pattern influences the interactome of p53, changes in the interacting proteins also contributes to the affected p53 functionality of the T329A mutant and will be discussed in 4.5.

4.3 The influence of T329 phosphorylation on the thermodynamic stability of p53

The thermodynamic stability of p53 is often affected by mutations. For instance, the common cancer mutations R248Q, R249S and R175H increase the percentage of unstructured p53 in the cell [344]. Since it was already shown that the mutation T329S decreases the thermodynamic stability of p53, whereas T329I increases its stability [342], it is likely that modification of this residue might influence the stability of the p53 confirmation. The impact of T329 phosphorylation was investigated by the use of conformation-specific antibodies. The phospho-mutant T329A p53 protein showed an elevated percentage of unfolded p53 at RT, whereas the phospho-mimetic T329E protein showed less unfolded p53 than the WT p53 protein. This increase in the thermodynamic stability might be due to a stabilisation of the protein by the negatively charged glutamic acid. This implicates that the phosphorylation of T329 could also increase the stability of p53. Since both T329 mutants were correctly folded at 4 °C it can be assumed that the phosphorylation of T329 does not affect the conformation of p53 at low temperatures, but increases its temperature-dependent stability. Moreover, prior studies have shown that the phosphorylation on S392 increases the thermodynamic stability of p53 [343]. Therefore, pT329 may also indirectly reduce the thermodynamic stability by the reduction of pS392.

4.4 Impact of T329 phosphorylation on p53 degradation

Under unstressed conditions the degradation of p53 is mainly mediated by polyubiquitylation and degradation by the proteasome [192,193]. Within this study the degradation of the p53 mutations by the proteasome could not be evaluated and should be repeated with the corresponding controls. However, it was shown that p53 mutants that destabilise p53, like R175H, are less prone for degradation by the proteasome. Instead, an increased level of the p53 R175H mutant could be observed upon the inhibition of autophagy, indicating autophagic degradation [345]. The mutation T329A lead to an increased amount of unfolded p53 protein and shows a slight tendency to be more affected by authophagic degradation. Therefore, the phosphorylation of T329 might stabilise p53 also by reducing its degradation, resulting in an increased level of activated and folded p53 in the cell. If the phosphorylation of T329 mediates stabilisation by reduction of autophagy needs to be further investigated, since the impact of T329 mutations on the p53 degradation rate is too small to fully explain the reduced p53 protein amount in the p53 T329A cells. It should be further investigated which mechanism is underlying the reduced protein amount, which can be already detected in the p53 mRNA expression. Therefore, it should be investigated if the *de novo* synthesis of new proteins is affected by the mutation of T329.

The differential interactome supports the theory that the p53 T329A mRNA might be less translated, since the p53 WT protein, primary interacts with the ribosomal proteins upon DNA damage. The ribosomal proteins play an important role in regulating the p53 response, mainly by controlling the translation of p53 mRNA [214]. In addition, the ribosomal proteins interact with MDM2 and thereby prevent the polyubiquitylation of p53 [346]. For instance, p53 interacts with RPL27, which was identified in this study as a T329-dependent interactor, in a complex with MDM2. RPL27 and p53 compete for the same binding-site at MDM2. Thereby, RPL27 reduces the interaction of p53 with MDM2 and increases the p53 amount [347]. Similar mechanisms were demonstrated for the proteins RPL5, RPL11 and RPL25. This T329 dependent interaction with ribosomal proteins might explain the reduced p53 T329A expression and should be further investigated.

As the amount of p53 in the cell plays a crucial role in determining the p53 functionality, further analysis of the impact of T329 on the amount of p53 will be necessary [348,349].

4.5 The phosphorylation at T329 influences the p53 interactome

As it was likely that the influence of pT329 on the PTM pattern affects the interactome of p53, interacting proteins were determined by mass spectrometry.

The mass spectrometry revealed several proteins which primarily interact with the p53 WT protein. The ribosomal proteins were detected as differential interactors of the p53 WT proteins as outlined in 4.4. It is likely that the ribosomal proteins are primarily detected under stress conditions, since the rRNA transcription is reduced, and the RPL proteins remain unbound in the cell [350]. This favours the interaction with p53 mRNA and cause the increased p53 expression. Furthermore the PRL proteins interact with p53 and reduce its degradation [351]. The reduced interaction with the RPL might be one explanation for the reduced amount of the p53 T329A protein. Whether or not the p53 WT protein and the ribosomal proteins directly interact with each other or in a complex with MDM2, remains unclear in this study and needs to be further investigated.

Furthermore, Nucleolin was identified as a p53 WT-specific interactor. It is already known that the C-terminal part of the p53 protein interacts with Nucleolin upon DNA damage and thereby transiently mediates the inhibition of replication [352]. Moreover, Nucleolin increases the p53 response by inhibiting MDM2 [353]. Another known interactor of p53's C-terminal region that has been confirmed in this study is NEURL4. This interaction was previously shown to elevate the transcriptional activity of p53 [336]. Since these proteins interact primarily with the p53 WT protein, it can be assumed that pT329 plays a role in these interactions. However, this interaction could not be confirmed with the T329E p53 protein. Therefore, it remains unclear if the threonine is essential to mediate the interaction or if the phosphorylation is needed.

This study revealed many proteins that primarily interact with the p53 T329A protein. For instance, Peptidyl-prolyl cis-trans isomerase B (PPIB, CypB), which is a direct target of p53-dependent gene expression, interacted to a greater extend with the p53 T329A protein. Furthermore, PPIB binds p53 and MDM2 and mediates the degradation of p53 [354]. This mechanism might be counteracted by the phosphorylation on T329, which would further increase the p53 amount. Moreover, Lamin-B1 (LMNB1) and Lamin-B2 (LMNB2) were highly abundant in the T329A interactome. The levels of LMNB1/2 are known to be raised in proliferating cells and downregulated upon p53 activation [337]. Therefore, it could be concluded that the reduced p53 activity in the T329A cells elevated the abundance of LMNB1 and LMNB2.

Additionally, many chaperones were identified as primary interactors of the T329A protein. The chaperone HSP90 is known to interact with mutant p53 and increases the mutant p53 level by preventing its degradation [355]. Furthermore, HSP90 also interacts with WT p53 in order to stabilise the protein at 37 °C and enhance the p21 expression [356]. Additionally, a robust interaction could be determined between p53 T329A and the chaperonin complex TRiC.

It is known and could be confirmed in this study that the TRiC complex interacts besides WT p53, primarily and stronger with mutated p53, like p53 R175H [357]. This complex enforces the correct folding of its client proteins. The knockdown of the TRiC complex results in misfolded p53 proteins [358]. Moreover, loss of the p53/TRiC interaction results in reduced p53-dependent gene transcription, and gain of functional activities of WT p53 similar to tumor-derived mutants [357]. Rivlin *et al*. demonstrated that mutant p53 can gain p53 WT functionality during cell development. The researchers claim that the interaction with the TRiC complex may exhibit this function [359]. This strong interaction of the p53 T329A protein with chaperons might be a mechanism of the cell to counter the instability of the protein and maintain as much p53 functionality as possible.

Nevertheless, most of the p53 WT interacting proteins were not found to also interact with the T329E mutant. Therefore, it remains unclear if simply any mutation of T329 will interfere with p53 WT interactions or if the phosphorylation of T329 specifically contributes to the p53 interactome.

It should be taken into consideration that the interactome could also be affected by an impaired tetramerisation since many proteins do not interact with the TD itself but can only interact with the tetrameric form of p53 [263,360].

It should be mentioned, that the abundant peptides were not normalised to the amount of isolated p53 protein. It should be recommended to re-analyse the data after normalisation to the amount of detected p53 peptides, to get a better understanding about the differential interactome.

4.6 The role of Chk1, PKC and CK2 in the phosphorylation of T329

The inhibition of Chk1 and PKCδ, which are both involved in p53 activation, led to a reduction of pT329. Chk1 is a DNA damage responsive kinase that gets activated by ATR and phosphorylates p53 at several residues [219]. Therefore, it can be expected that its inhibition leads to a reduction in p53 phosphorylation. Since the inhibition of ATM and Chk2 did not affect pT329, this indicates that the phosphorylation of T329 primarily occurs upon the repair process of DNA that exposes ssDNA and thereby activates the ATR/Chk1 pathway. DeHart *et al.* identified T329 as a direct Chk1 target in an *in vitro* kinase assay approach using a p53 peptide array [340]. If Chk1 directly phosphorylates T329 *in vivo* remains ambiguous, as the knockdown or inhibition of Chk1 resulted in residual T329 phosphorylation and unaltered p53 activity. This implicates that additional kinases contribute to the T329 phosphorylation, or that despite the knockdown there is still enough active Chk1 left to phosphorylate T329.

The family of PKC kinases consist of eleven family members divided into the conventional PKCs (α, βI, βII, γ), the novel PKCs (δ, ε, η, μ, θ) and the atypical PKCs (ζ, ι, λ). They get activated by diacylglycerol (DAG) alone or in combination with calcium. Specifically, PKCδ has been identified as a positive regulator of apoptosis upon genotoxic agent induced stress [361]. Moreover, this kinase has been shown to interact with the TD of p53 and to mediate the phosphorylation on S46 [222]. Besides this direct phosphorylation of S46, an indirect effect of PKCδ mainly on the activation of other kinases was demonstrated for the phosphorylations of S15, S20, S33 and T81. Furthermore, different PKC isoforms were identified to phosphorylate residues in the CTD [361]. Similar to Chk1, it remains unclear if PKCδ directly phosphorylates T329.The direct phosphorylation should be investigated with an in vitro kinase approach. Since all kinase inhibitors have inhibitory off-target effects on other kinases, another approach that confirms the impact of PKCδ on pT329 is necessary to validate this observation.

Even though CK2 is not a DNA damage-responsive kinase, it is known to phosphorylate p53 at S392 [224]. In contrast to Chk1 and PKCδ, it is constitutively active and mainly mediates cell growth and survival, counteracting the classic p53 function. It consists of a tetrameric shape with two catalytic α subunits and two regulatory β subunits [362]. Keller *et al.* postulated that the CK2 complex associates with hSPT16 and SSRP1 upon DNA damage, and thereby increases the affinity to p53, leading to the phosphorylation on S392 [363]. The interactome identified CK2 as a T329-dependent interacting protein, which primarily interacts with phosphorylated p53 WT. Therefore, CK2 was further investigated as a possible kinase involved in T329 phosphorylation. Previous experiments revealed, that CK2 is often overexpressed in tumor cells, and that the inhibition or downregulation of the kinase increases the apoptosis. Therefore, it became a target for tumor therapy. It has been demonstrated that the inhibition of CK2 reduces the chemotherapy resistance to DNA damaging drugs [364]. It remains unclear if this reduction of chemotherapy resistance is dependent on the p53 status, as it has been observed in both p53 WT and p53 mutant cells [365,366]. One theory postulates that CK2 triggers the DNA damage repair and thereby the survival of the chemotherapy-treated cell. Apart from p53, CK2 also phosphorylates DNA-PK, Rad51, MDC1, 53BP1 and the XRCC proteins involved in DNA damage repair. The inhibition of CK2 reduced DNA damage repair and increase DNA lesions that further induced apoptosis [362]. As shown by Ravi *et al*., this induction of apoptosis can occur independently of p53 [367]. Moreover, p53 itself counteracts the expression of CK2 and thereby reduces its proliferative function [368]. The contribution of CK2 to the activation of p53 by phosphorylation seems to be inconsistent with the other functions of CK2 and possibly acts as a negative regulator on its own activity. Interestingly, the phosphorylations of S329 and T329 are detectable upon nutlin 3a treatment. Therefore, the contribution of a constitutively active kinase to T329 phosphorylation is likely. The reduced interaction of CK2 and p53 upon the mutation of T329 underlies the direct interaction of CK2 with the C-terminal part of p53 [258]. The necessity of the phosphorylation of T329 for this interaction remains questionable in this study.

Similar to Chk1 and PKCδ, the direct phosphorylation by CK2 at T329 of p53 could not be confirmed in this study.

Even though the kinase consensus motifs of all three kinases show minimal compatibility with the T329 site, they contribute directly or indirectly to the phosphorylation on T329. Further investigations like *in vitro* kinase assays are necessary to identify the direct kinase. Moreover, the reduced activity of p53 upon knockdown or inhibition of these kinases was expected and has already been described. Since all of the investigated kinases are already described to activate p53 by phosphorylation, it is not possible to distinguish between the function of pT329 and the other already described phospho-sites in the used system [186]. Therefore, the function of pT329 may predominantly be its role in the mediation of the p53 PTM network.

4.7 Influence of T329 mutations on the GOF of p53

The functional characterisation of p53 residues is highly dependent on the cell- and expression system. Since one important regulation of the p53 system is mediated by the p53 protein amount, experiments with overexpressed p53 are highly artificial. Nevertheless, most functional studies on mutated p53 variants were performed with plasmid encoded, overexpressed p53. This procedure is justified with the argument that most common cancer mutations of p53 result in high protein amounts in the cell [279]. In recent studies, it was demonstrated that the mutant p53 in non-cancerous cells is not as highly abundant as initially assumed. Indeed, it is often less abundant than the WT p53, due to the destabilisation caused by mutations [369]. The high protein level of p53 mutants cloud be explained by the reduced transcriptional activity of p53 mutants. Therefore, the degradation of p53 is reduced due to the reduced MDM2 expression. This negative feedback loop is often missing in p53 mutant cells, contributing to increased p53 protein levels [370,371]. Comparing mutant p53 cancer cells to p53 knockout cells, some p53 mutants were shown to increase genomic instability, chemotherapy resistance and metastasis. These effects are mediated mainly by the protein-protein interactions of mutant p53. The DBD is often destabilised and the specific DNA binding is impaired. In contrast, the other, unstructured, domains still interact with other proteins like transcription factors. Therefore, the unspecific binding to DNA with the C-terminal part of p53 and the interaction with other transcription-influencing proteins promotes the gain of function activity of p53. As the p53 mutants are linked to progressive cancer, inhibiting this gain of function abilities became an attractive goal in cancer therapy research [279].

The present study demonstrates that the mutation of T329A resulted in a highly altered p53-dependent gene expression and p53-dependent interactome. This could implicate gain of function activities for the T329A mutant. It should be further investigated if the altered gene expression or the primary interactors of the T329A mutant could result in tumor-supporting p53 functionality. Therefore, the T329 phosphorylation might be important to direct the p53 response and prevent GOF *in vivo*. Nevertheless, the reduced p53-dependent gene expression in the T329A mutant states that the major phenotype of the T329A mutant is rather a LOF than a GOF.

It was shown that the high abundance of p53 led to enhanced adherence and cell motility, which, in turn, was linked to increased metastasis [330]. In contrast to other p53 mutants, the changes in p53 functionality in the T329A cells did not increase the cell adherence and motility, which might be explained by the low abundance of the T329A mutant.

Moreover, the T329A cells are as resistant to chemotherapy as the p53 knockout cells. Overall, a contribution of the mutation of T329 to increased metastasis, chemotherapie resistance and therefore tumor progression is unlikely. This might explain why this residue is so rarely mutated as it does not result in tumor beneficial p53 functionality.

4.8 Influence of T329 phosphorylation on cancer therapy

This study demonstrates a significant impact of the p53 T329 phosphorylation on the activation of p53. The role of pT329 in cancer development and progression seems questionable, as mutations of this site occur very rarely *in vivo*. Nevertheless, this study demonstrates that common cancer mutations of p53 reduce the T329 phosphorylation and thereby the subsequent phosphorylations of S392 and S46. An approach to rescue the T329 phosphorylation might therefore restore the p53 functionality. Since Chk1 and CK2 are activated upon cell-intrinsic signalling pathways, they are activated upon most chemotherapy attempts. Additionally, active CK2 is linked to progressive tumor growth and poor prognosis for the patients [362]. Therefore, an artificial induction of their activity to induce pT329 might not be a worthwhile goal for cancer therapy.

Hence the induction of T329 phosphorylation could be achieved by the artificial activation of PKCδ. The drug Ingol-3-angelate (PEP005) is a structural analogue to phorbol ester and activates PKCδ [372]. It induces a G1 cell cycle arrest and apoptosis, which might be mediated by activated p53 upon the phosphorylation of T329 and S46. After the clinical trials, PEP005 was approved for the treatment of actinic keratosis under the name Picato. The toxicities of this drug resulted in an increased risk of skin cancer and Picato was withdrawn from the European market. To reduce the toxicities, a combination with other well-characterised cancer drugs may be used to allow for a reduced dosage of PRP005 and to improve cancer therapy by activating PKCδ [373].

The missing T329 phosphorylation in common cancer mutations of p53 might contribute to the applicability of cyclotherapy. While the mutated p53 lacks T329 phosphorylation and is not fully activated upon exposure to DNA damaging agents, the p53 WT in healthy cells is activated and mediates a cell cycle arrest. Consequently, these cells are not affected by chemotherapy that targets cycling cells. This reduces side effects and allows the treatment with higher and more efficient doses of chemotherapy [374,375].

As the lack of pT329 resulted in reduced folding of p53, the refolding and restoring of the p53 functionality could be an attractive approach in p53 mutations that show impaired T329 phosphorylation. Many compounds like Rita, PRIMA-1^{Met} or CP31398 have been described to refold the denatured p53 protein and increase the activity of mutant p53. Nevertheless, none of these compounds is approved as a drug due to dosage-dependent toxicities [376]. For most compounds, it was demonstrated that they not only specifically activate mutant p53, but also activate WT p53, which results in overall induction of apoptosis and explains the high toxicities [377,378].

This study underlines the importance of the PTM pattern for the full activation of p53. The phosphorylation of T329 plays an essential role as a priming modification that mediates the PTM network and activates p53 to maintain the genomic stability in the cell. This demonstrates that T329, which was claimed to be not crucial for p53 research as it is not mutated in cancer, is indirectly affected by common cancer mutations and may contribute to impaired p53 activation.

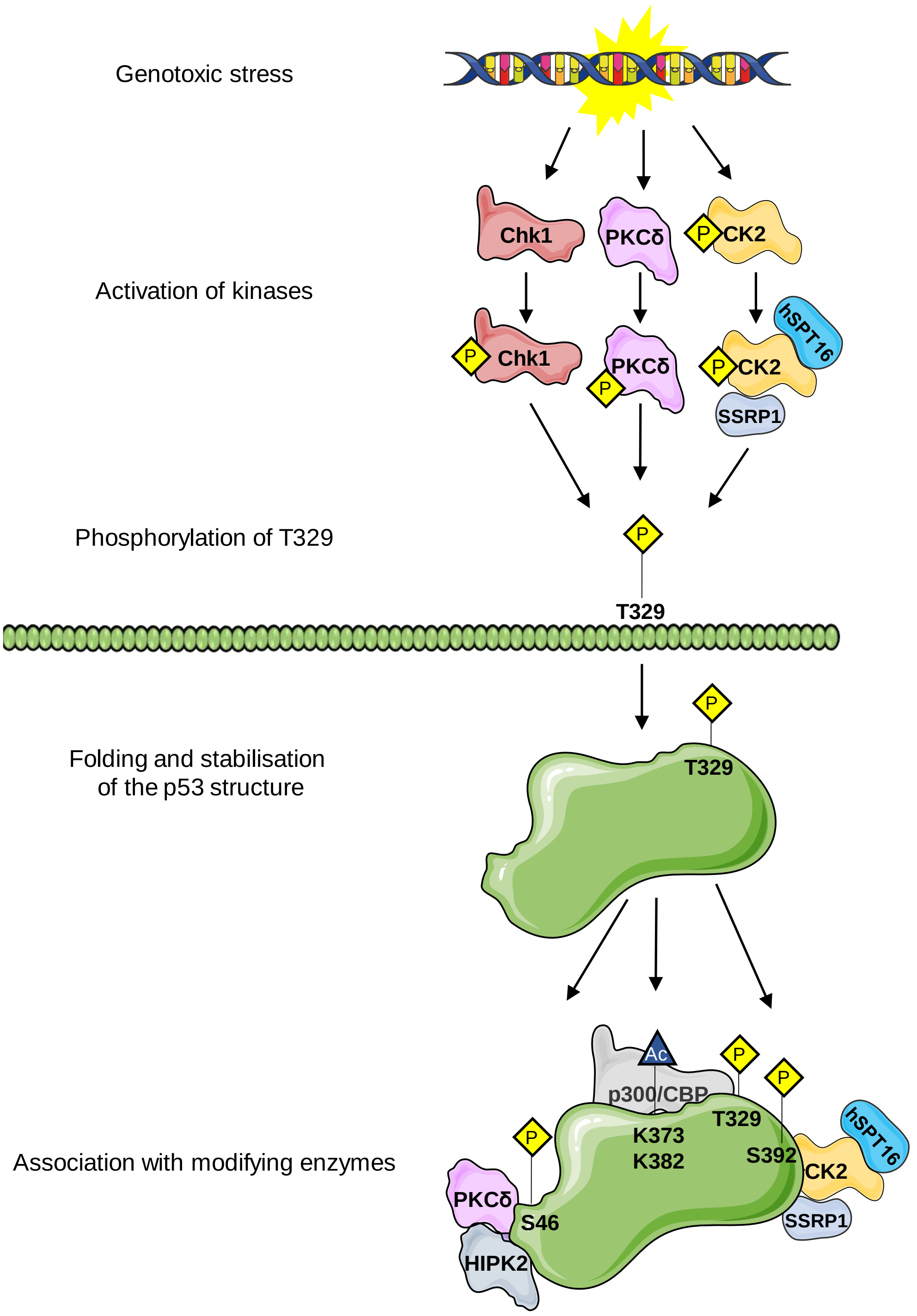

Fig. 29 Model of the p53 activation mediated by T329 phosphorylation. Genotoxic stress activates kinases, which phosphorylate T329. This supports the folding and the stabilisation of the p53 conformation. Other modifying enzymes interact with the folded p53 protein and mediate additional PTMs that fully activate p53.

5 SUMMARY

As a tumor suppressor the transcription factor p53 plays an essential role in maintaining genome stability due to its ability to repair the genome and induce apoptosis upon DNA damage. Phosphorylations play an important role in the activation and regulation of the p53 response. Many PTMs have already been identified as important regulators, such as the phosphorylation at S329 by CK2 and the phosphorylation at S46 by HIPK2 or PKCδ. This study identifies and characterises the phosphorylation of T329 in the tetramerisation domain of p53 as a priming modification, which mediates further PTMs and thus contribute to the p53 activation. Initially, pT329 was identified by mass spectrometry as a result of DNA damage. With a pT329-specific antibody, the phosphorylation under various genotoxic stimulants could be confirmed. To investigate the pT329 functions, HCT116 p53 knockout cells were reconstituted with p53 WT, p53 T329A and p53 T329E in the safe harbour gene locus AAVS1. The T329A mutant represents the non-phosphorylated T329 and the T329E mutant the state of the phosphorylated T329. The T329A mutation leads to a significant reduction in p53-dependent gene expression, which results in impaired G1 cell cycle arrest and reduced induction of apoptosis. Chromatin immunoprecipitation showed that the T329A mutant does not bind inductively to the DNA after stimulation of the p53 response. An examination of the p53 conformation showed that p53 T329A has a lower thermodynamic stability than p53 WT or p53 T329E. The phosphorylation at T329 thus supports the folding and thereby the stability of the p53 protein. As a result, pT329 plays an important role in protein-protein interactions, and thus also in the modification of p53 with PTMs. The interactome confirmed that both mutations of T329 have an evident influence on the association of p53 with other proteins. Thus, the T329A mutant stronger binds chaperones, while ribosomal proteins interact primarily with the p53 WT protein. In addition, the visualisation of other activating PTMs showed that activating modifications such as pS392, pS46 and acK373/K382 are missing or are significantly reduced in p53 T329A. Therefore, pT329 influences the p53 activation probably by stabilising the conformation and the mediation of the activating PTM network. Through kinase inhibitors and knockdown experiments, Chk1, CK2 and PKCδ could be identified as possible kinases for T329 phosphorylation.

In summary, phosphorylation of T329 is a new detail in p53 activation, thus improving the understanding of p53 activation in relation to cancer prevention and therapy.

6 ZUSAMMENFASSUNG

Der Transkriptionsfaktor p53 spielt als Tumorsuppressor eine bedeutende Rolle in der Bewahrung der Stabilität des Genoms, da er in Folge von DNA Schädigungen sowohl die Reparatur des Genoms, als auch die Apoptose einleiten kann. Phosphorylierungen spielen dabei eine bedeutende Rolle in der Aktivierung und Ausrichtung der p53 Antwort. Viele post-translationale Modifikationen (PTMs) wurden bereits als wichtige Regulatoren identifiziert, wie beispielsweise die Phosphorylierung an S329 durch CK2 und die Phosphorylierung an S46 durch HIPK2 und PKCδ. Die vorliegende Studie identifiziert und charakterisiert die Phosphorylierung an T329 in der Tetramerisierungsdomäne von p53 als vorbereitende Modifikation, welche der Vermittlung weiterer PTMs und damit der vollen p53 Aktivierung dient. Initial wurde pT329 mittels Massenspektrometrie in Folge von DNA Schädigungen identifiziert. Durch die Herstellung eines pT329 spezifischen Antikörpers konnte die Phosphorylierung unter verschiedenen genotoxischen Stimulantien bestätigt werden. Für die Untersuchung der pT329 Funktionen wurden HCT116 p53 knockout Zellen im *safe harbour* Genlokus AAVS1 mit p53 WT, p53 T329A und p53 T329E rekonstituiert. Dabei soll die T329A Mutante den Zustand des nicht phosphorylierten T329 darstellen und die T329E Mutante den Zustand des phosphorylierten T329. Die T329A Mutation führt zu einer deutlichen Reduktion der p53 abhängigen Genexpression, welche in eingeschränktem G1 Zellzyklusarrest und verringerter Apoptoseinduktion resultiert. Durch eine Chromatin-Immunoprezipitation konnte gezeigt werden, dass die T329A Mutante nach Stimulation der p53 Antwort nicht verstärkt an die DNA bindet. Eine Untersuchung der p53 Konformation zeigte, dass p53 T329A eine geringere thermodynamische Stabilität aufweist als p53 WT und p53 T329E. Die Phosphorylierung an T329 unterstützt somit die Faltung und damit auch die Stabilität des p53 Proteins. In Folge dessen spielt pT329 eine wichtige Rolle bei Protein-Protein Interaktionen, und damit auch bei der Modifikation von p53 durch PTMs. Das Interaktom konnte bestätigen, dass beide Mutationen von T329 einen deutlichen Einfluss auf die Assoziation von p53 mit anderen Proteinen haben. So bindet die T329A Mutante verstärkt Chaperone, während ribosomale Proteine verstärkt mit dem p53 WT Protein interagieren. Zudem konnte die Untersuchung anderer aktivierender PTMs zeigen, dass aktivierende Modifikationen wie pS392, pS46 und acK373/K382 in p53 T329A fehlen oder deutlich reduziert vorliegen. Der Einfluss von pT329 auf die p53 Aktivierung liegt somit vermutlich in der Stabilisierung der Konformation und der Vermittlung des aktivierenden PTM Netzwerkes. Durch Kinaseinhibitoren und *knockdown* Experimente konnten Chk1, CK2 und PKCδ als mögliche Kinasen für die T329 Phosphorylierung identifiziert werden.

Zusammenfassend stellt die Phosphorylierung von T329 ein neues Detail in der p53-Aktivierung dar, und verbessert somit das Verständnis der p53-Aktivierung im Bezug auf Vorbeugung und Therapie von Krebserkrankungen.

References

1. Mills, A. A. *et al.* p63 is a p53 homologue required for limb and epidermal morphogenesis. *Nature* **398**, 708–713 (1999).
2. Yang, A. *et al.* p63 is essential for regenerative proliferation in limb, craniofacial and epithelial development. *Nature* **398**, 714–718 (1999).
3. Yang, A. & McKeon, F. P63 and P73: P53 mimics, menaces and more. *Nat. Rev. Mol. Cell Biol.* **1**, 199–207 (2000).
4. Collavin, L., Lunardi, A. & Del Sal, G. p53-family proteins and their regulators: hubs and spokes in tumor suppression. *Cell Death Differ.* **17**, 901–911 (2010).
5. Belyi, V. A. *et al.* The Origins and Evolution of the p53 Family of Genes. *Cold Spring Harb. Perspect. Biol.* **2**, a001198 (2010).
6. Yang, A. *et al.* p73-deficient mice have neurological, pheromonal and inflammatory defects but lack spontaneous tumours. *Nature* **404**, 99–103 (2000).
7. Donehower, L. A. *et al.* Mice deficient for p53 are developmentally normal but susceptible to spontaneous tumours. *Nature* **356**, 215–221 (1992).
8. Levine, A. J. & Oren, M. The first 30 years of p53: growing ever more complex. *Nat. Rev. Cancer* **9**, 749–758 (2009).
9. Lane, D. P. & Crawford, L. V. T antigen is bound to a host protein in SY40-transformed cells. *Nature* **278**, 261–263 (1979).
10. Linzer, D. I. & Levine, A. J. Characterization of a 54K dalton cellular SV40 tumor antigen present in SV40-transformed cells and uninfected embryonal carcinoma cells. *Cell* **17**, 43–52 (1979).
11. Rotter, V., Witte, O. N., Coffman, R. & Baltimore, D. Abelson murine leukemia virus-induced tumors elicit antibodies against a host cell protein, P50. *J. Virol.* **36**, 547–555 (1980).

12. Rotter, V. p53, a transformation-related cellular-encoded protein, can be used as a biochemical marker for the detection of primary mouse tumor cells. *Proc. Natl. Acad. Sci. U. S. A.* **80**, 2613–2617 (1983).
13. Linzer, D. I., Maltzman, W. & Levine, A. J. The SV40 A gene product is required for the production of a 54,000 MW cellular tumor antigen. *Virology* **98**, 308–318 (1979).
14. Oren, M. & Levine, A. J. Molecular cloning of a cDNA specific for the murine p53 cellular tumor antigen. *Proc. Natl. Acad. Sci. U. S. A.* **80**, 56–59 (1983).
15. Matlashewski, G. *et al.* Isolation and characterization of a human p53 cDNA clone: expression of the human p53 gene. *EMBO J.* **3**, 3257–3262 (1984).
16. Harlow, E., Williamson, N. M., Ralston, R., Helfman, D. M. & Adams, T. E. Molecular cloning and in vitro expression of a cDNA clone for human cellular tumor antigen p53. *Mol. Cell. Biol.* **5**, 1601–1610 (1985).
17. Pennica, D. *et al.* The amino acid sequence of murine p53 determined from a c-DNA clone. *Virology* **134**, 477–482 (1984).
18. Leppard, K. *et al.* Purification and partial amino acid sequence analysis of the cellular tumour antigen, p53, from mouse SV40-transformed cells. *EMBO J.* **2**, 1993–1999 (1983).
19. Zakut-Houri, R., Bienz-Tadmor, B., Givol, D. & Oren, M. Human p53 cellular tumor antigen: cDNA sequence and expression in COS cells. *EMBO J.* **4**, 1251–1255 (1985).
20. Wolf, D., Harris, N., Goldfinger, N. & Rotter, V. Isolation of a full-length mouse cDNA clone coding for an immunologically distinct p53 molecule. *Mol. Cell. Biol.* **5**, 127–132 (1985).
21. Eliyahu, D., Raz, A., Gruss, P., Givol, D. & Oren, M. Participation of p53 cellular tumour antigen in transformation of normal embryonic cells. *Nature* **312**, 646–649 (1984).
22. Jenkins, J. R., Rudge, K. & Currie, G. A. Cellular immortalization by a cDNA clone encoding the transformation-associated phosphoprotein p53. *Nature* **312**, 651–654 (1984).

23. Parada, L. F., Land, H., Weinberg, R. A., Wolf, D. & Rotter, V. Cooperation between gene encoding p53 tumour antigen and ras in cellular transformation. *Nature* **312**, 649–651 (1984).
24. Eliyahu, D., Michalovitz, D. & Oren, M. Overproduction of p53 antigen makes established cells highly tumorigenic. *Nature* **316**, 158–160 (1985).
25. Eliyahu, D. *et al.* Meth A fibrosarcoma cells express two transforming mutant p53 species. *Oncogene* **3**, 313–321 (1988).
26. Finlay, C. A. *et al.* Activating mutations for transformation by p53 produce a gene product that forms an hsc70-p53 complex with an altered half-life. *Mol. Cell. Biol.* **8**, 531–539 (1988).
27. Eliyahu, D., Michalovitz, D., Eliyahu, S., Pinhasi-Kimhi, O. & Oren, M. Wild-type p53 can inhibit oncogene-mediated focus formation. *Proc. Natl. Acad. Sci. U. S. A.* **86**, 8763–8767 (1989).
28. Finlay, C. A., Hinds, P. W. & Levine, A. J. The p53 proto-oncogene can act as a suppressor of transformation. *Cell* **57**, 1083–1093 (1989).
29. Srivastava, S., Zou, Z. Q., Pirollo, K., Blattner, W. & Chang, E. H. Germ-line transmission of a mutated p53 gene in a cancer-prone family with Li-Fraumeni syndrome. *Nature* **348**, 747–749 (1990).
30. Levine, R. L. & Carroll, M. A common genetic mechanism in malignant bone marrow diseases. *N. Engl. J. Med.* **360**, 2355–2357 (2009).
31. Sakaguchi, K. *et al.* Effect of phosphorylation on tetramerization of the tumor suppressor protein p53. *J. Protein Chem.* **16**, 553–556 (1997).
32. Bell, S., Klein, C., Müller, L., Hansen, S. & Buchner, J. p53 contains large unstructured regions in its native state. *J. Mol. Biol.* **322**, 917–927 (2002).
33. Veprintsev, D. B. *et al.* Core domain interactions in full-length p53 in solution. *Proc. Natl. Acad. Sci. U. S. A.* **103**, 2115–2119 (2006).
34. Fields, S. & Jang, S. K. Presence of a potent transcription activating sequence in the p53 protein. *Science* **249**, 1046–1049 (1990).

35. Walker, K. K. & Levine, A. J. Identification of a novel p53 functional domain that is necessary for efficient growth suppression. *Proc. Natl. Acad. Sci. U. S. A.* **93**, 15335–15340 (1996).

36. Müller-Tiemann, B. F., Halazonetis, T. D. & Elting, J. J. Identification of an additional negative regulatory region for p53 sequence-specific DNA binding. *Proc. Natl. Acad. Sci. U. S. A.* **95**, 6079–6084 (1998).

37. Beckerman, R. & Prives, C. Transcriptional regulation by p53. *Cold Spring Harb. Perspect. Biol.* **2**, a000935 (2010).

38. Cho, Y., Gorina, S., Jeffrey, P. D. & Pavletich, N. P. Crystal structure of a p53 tumor suppressor-DNA complex: understanding tumorigenic mutations. *Science* **265**, 346–355 (1994).

39. el-Deiry, W. S., Kern, S. E., Pietenpol, J. A., Kinzler, K. W. & Vogelstein, B. Definition of a consensus binding site for p53. *Nat. Genet.* **1**, 45–49 (1992).

40. Clore, G. M. *et al.* Refined solution structure of the oligomerization domain of the tumour suppressor p53. *Nat. Struct. Biol.* **2**, 321–333 (1995).

41. Clore, G. M. *et al.* High-resolution structure of the oligomerization domain of p53 by multidimensional NMR. *Science* **265**, 386–391 (1994).

42. Ahn, J. & Prives, C. The C-terminus of p53: the more you learn the less you know. *Nat. Struct. Biol.* **8**, 730–732 (2001).

43. Kussie, P. H. *et al.* Structure of the MDM2 oncoprotein bound to the p53 tumor suppressor transactivation domain. *Science* **274**, 948–953 (1996).

44. Weinberg, R. L., Freund, S. M. V., Veprintsev, D. B., Bycroft, M. & Fersht, A. R. Regulation of DNA binding of p53 by its C-terminal domain. *J. Mol. Biol.* **342**, 801–811 (2004).

45. Dunker, A. K., Cortese, M. S., Romero, P., Iakoucheva, L. M. & Uversky, V. N. Flexible nets. The roles of intrinsic disorder in protein interaction networks. *FEBS J.* **272**, 5129–5148 (2005).

46. Kitayner, M. *et al.* Structural basis of DNA recognition by p53 tetramers. *Mol. Cell* **22**, 741–753 (2006).

47. Gorina, S. & Pavletich, N. P. Structure of the p53 tumor suppressor bound to the ankyrin and SH3 domains of 53BP2. *Science* **274**, 1001–1005 (1996).

48. Derbyshire, D. J. *et al.* Crystal structure of human 53BP1 BRCT domains bound to p53 tumour suppressor. *EMBO J.* **21**, 3863–3872 (2002).

49. Joo, W. S. *et al.* Structure of the 53BP1 BRCT region bound to p53 and its comparison to the Brca1 BRCT structure. *Genes Dev.* **16**, 583–593 (2002).

50. Lavin, M. F. & Gueven, N. The complexity of p53 stabilization and activation. *Cell Death Differ.* **13**, 941–950 (2006).

51. Cañadillas, J. M. P. *et al.* Solution structure of p53 core domain: Structural basis for its instability. *Proc. Natl. Acad. Sci. U. S. A.* **103**, 2109–2114 (2006).

52. Bullock, A. N., Henckel, J. & Fersht, A. R. Quantitative analysis of residual folding and DNA binding in mutant p53 core domain: definition of mutant states for rescue in cancer therapy. *Oncogene* **19**, 1245–1256 (2000).

53. Butler, J. S. & Loh, S. N. Structure, function, and aggregation of the zinc-free form of the p53 DNA binding domain. *Biochemistry* **42**, 2396–2403 (2003).

54. Klein, C. *et al.* NMR spectroscopy reveals the solution dimerization interface of p53 core domains bound to their consensus DNA. *J. Biol. Chem.* **276**, 49020–49027 (2001).

55. Rippin, T. M., Freund, S. M. V., Veprintsev, D. B. & Fersht, A. R. Recognition of DNA by p53 core domain and location of intermolecular contacts of cooperative binding. *J. Mol. Biol.* **319**, 351–358 (2002).

56. Kraiss, S., Quaiser, A., Oren, M. & Montenarh, M. Oligomerization of oncoprotein p53. *J. Virol.* **62**, 4737–4744 (1988).

57. McCormick, F., Clark, R., Harlow, E. & Tjian, R. SV40 T antigen binds specifically to a cellular 53 K protein in vitro. *Nature* **292**, 63–65 (1981).

58. Schmieg, F. I. & Simmons, D. T. Characterization of the in Vitro interaction between SV40 T antigen and p53: Mapping the p53 binding site. *Virology* **164**, 132–140 (1988).

59. Friedman, P. N., Chen, X., Bargonetti, J. & Prives, C. The p53 protein is an unusually shaped tetramer that binds directly to DNA. *Proc. Natl. Acad. Sci.* **90**, 3319–3323 (1993).

60. Stenger, J. E., Mayr, G. A., Mann, K. & Tegtmeyer, P. Formation of stable p53 homotetramers and multiples of tetramers. *Mol. Carcinog.* **5**, 102–106 (1992).

61. Iwabuchi, K., Li, B., Bartel, P. & Fields, S. Use of the two-hybrid system to identify the domain of p53 involved in oligomerization. *Oncogene* **8**, 1693–1696 (1993).

62. Pavletich, N. P., Chambers, K. A. & Pabo, C. O. The DNA-binding domain of p53 contains the four conserved regions and the major mutation hot spots. *Genes Dev.* **7**, 2556–2564 (1993).

63. Stürzbecher, H. W. *et al.* A C-terminal alpha-helix plus basic region motif is the major structural determinant of p53 tetramerization. *Oncogene* **7**, 1513–1523 (1992).

64. Wang, Y. *et al.* p53 domains: identification and characterization of two autonomous DNA-binding regions. *Genes Dev.* **7**, 2575–2586 (1993).

65. Sakaguchi, K. *et al.* Phosphorylation of Serine 392 Stabilizes the Tetramer Formation of Tumor Suppressor Protein p53. *Biochemistry* **36**, 10117–10124 (1997).

66. Jeffrey, P. D., Gorina, S. & Pavletich, N. P. Crystal structure of the tetramerization domain of the p53 tumor suppressor at 1.7 angstroms. *Science* **267**, 1498–1502 (1995).

67. Mittl, P. R., Chène, P. & Grütter, M. G. Crystallization and structure solution of p53 (residues 326-356) by molecular replacement using an NMR model as template. *Acta Crystallogr. D Biol. Crystallogr.* **54**, 86–89 (1998).

68. Joerger, A. C. & Fersht, A. R. Structure–function–rescue: the diverse nature of common p53 cancer mutants. *Oncogene* **26**, 2226–2242 (2007).

69. Chène, P., Mittl, P. & Grütter, M. In vitro structure-function analysis of the β-strand 326-333 of human p5311Edited by A. Fersht. *J. Mol. Biol.* **273**, 873–881 (1997).

70. Mateu, M. G. & Fersht, A. R. Nine hydrophobic side chains are key determinants of the thermodynamic stability and oligomerization status of tumour suppressor p53 tetramerization domain. *EMBO J.* **17**, 2748–2758 (1998).

71. Waterman, J. l., Shenk, J. l. & Halazonetis, T. d. The dihedral symmetry of the p53 tetramerization domain mandates a conformational switch upon DNA binding. *EMBO J.* **14**, 512–519 (1995).

72. Chène, P. & Bechter, E. Cellular characterisation of p53 mutants with a single missense mutation in the β-strand 326–333 and correlation of their cellular activities with in vitro properties11Edited by A. R. Fersht. *J. Mol. Biol.* **288**, 891–897 (1999).

73. Hupp, T. R., Meek, D. W., Midgley, C. A. & Lane, D. P. Regulation of the specific DNA binding function of p53. *Cell* **71**, 875–886 (1992).

74. Hainaut, P. & Milner, J. Redox Modulation of p53 Conformation and Sequence-specific DNA Binding in Vitro. *Cancer Res.* **53**, 4469–4473 (1993).

75. Halazonetis, T. d. & Kandil, A. n. Conformational shifts propagate from the oligomerization domain of p53 to its tetrameric DNA binding domain and restore DNA binding to select p53 mutants. *EMBO J.* **12**, 5057–5064 (1993).

76. Balagurumoorthy, P. *et al.* Four p53 DNA-binding domain peptides bind natural p53-response elements and bend the DNA. *Proc. Natl. Acad. Sci.* **92**, 8591–8595 (1995).

77. Bargonetti, J., Manfredi, J. J., Chen, X., Marshak, D. R. & Prives, C. A proteolytic fragment from the central region of p53 has marked sequence-specific DNA-binding activity when generated from wild-type but not from oncogenic mutant p53 protein. *Genes Dev.* **7**, 2565–2574 (1993).

78. McLure, K. G. & Lee, P. W. K. How p53 binds DNA as a tetramer. *EMBO J.* **17**, 3342–3350 (1998).

79. Nagaich, A. K. *et al.* p53-induced DNA bending and twisting: p53 tetramer binds on the outer side of a DNA loop and increases DNA twisting. *Proc. Natl. Acad. Sci.* **96**, 1875–1880 (1999).

80. Sang, B. C., Chen, J. Y., Minna, J. & Barbosa, M. S. Distinct regions of p53 have a differential role in transcriptional activation and repression functions. *Oncogene* **9**, 853–859 (1994).

81. Shaulian, E., Zauberman, A., Milner, J., Davies, E. a. & Oren, M. Tight DNA binding and oligomerization are dispensable for the ability of p53 to transactivate target genes and suppress transformation. *EMBO J.* **12**, 2789–2797 (1993).

82. Stenger, J. e. *et al.* p53 oligomerization and DNA looping are linked with transcriptional activation. *EMBO J.* **13**, 6011–6020 (1994).

83. Subler, M. A., Martin, D. W. & Deb, S. Overlapping domains on the p53 protein regulate its transcriptional activation and repression functions. *Oncogene* **9**, 1351–1359 (1994).

84. Tarunina, M. & Jenkins, J. R. Human p53 binds DNA as a protein homodimer but monomeric variants retain full transcription transactivation activity. *Oncogene* **8**, 3165–3173 (1993).

85. Zhang, W. *et al.* A temperature-sensitive mutant of human p53. *EMBO J.* **13**, 2535–2544 (1994).

86. Chène, P. The role of tetramerization in p53 function. *Oncogene* **20**, 2611–2617 (2001).

87. Stommel, J. M. *et al.* A leucine-rich nuclear export signal in the p53 tetramerization domain: regulation of subcellular localization and p53 activity by NES masking. *EMBO J.* **18**, 1660–1672 (1999).

88. Tidow, H. *et al.* Quaternary structures of tumor suppressor p53 and a specific p53–DNA complex. *Proc. Natl. Acad. Sci.* **104**, 12324–12329 (2007).

89. Joerger, A. C. & Fersht, A. R. The Tumor Suppressor p53: From Structures to Drug Discovery. *Cold Spring Harb. Perspect. Biol.* **2**, (2010).

90. Ang, H. C., Joerger, A. C., Mayer, S. & Fersht, A. R. Effects of common cancer mutations on stability and DNA binding of full-length p53 compared with isolated core domains. *J. Biol. Chem.* **281**, 21934–21941 (2006).

91. Nikolova, P. V., Henckel, J., Lane, D. P. & Fersht, A. R. Semirational design of active tumor suppressor p53 DNA binding domain with enhanced stability. *Proc. Natl. Acad. Sci.* **95**, 14675–14680 (1998).

92. Cook, A. & Milner, J. Evidence for allosteric variants of wild-type p53, a tumour suppressor protein. *Br. J. Cancer* **61**, 548–552 (1990).

93. Wang, P. L., Sait, F. & Winter, G. The 'wildtype' conformation of p53: epitope mapping using hybrid proteins. *Oncogene* **20**, 2318–2324 (2001).

94. Stephen, C. W. & Lane, D. P. Mutant conformation of p53. Precise epitope mapping using a filamentous phage epitope library. *J. Mol. Biol.* **225**, 577–583 (1992).

95. Horn, H. F. & Vousden, K. H. Coping with stress: multiple ways to activate p53. *Oncogene* **26**, 1306–1316 (2007).

96. Batchelor, E., Mock, C. S., Bhan, I., Loewer, A. & Lahav, G. Recurrent initiation: a mechanism for triggering p53 pulses in response to DNA damage. *Mol. Cell* **30**, 277–289 (2008).

97. Raycroft, L., Wu, H. Y. & Lozano, G. Transcriptional activation by wild-type but not transforming mutants of the p53 anti-oncogene. *Science* **249**, 1049–1051 (1990).

98. Zhu, J., Zhou, W., Jiang, J. & Chen, X. Identification of a novel p53 functional domain that is necessary for mediating apoptosis. *J. Biol. Chem.* **273**, 13030–13036 (1998).

99. Bargonetti, J., Friedman, P. N., Kern, S. E., Vogelstein, B. & Prives, C. Wild-type but not mutant p53 immunopurified proteins bind to sequences adjacent to the SV40 origin of replication. *Cell* **65**, 1083–1091 (1991).

100. Kern, S. E. *et al.* Identification of p53 as a sequence-specific DNA-binding protein. *Science* **252**, 1708–1711 (1991).

101. Funk, W. D., Pak, D. T., Karas, R. H., Wright, W. E. & Shay, J. W. A transcriptionally active DNA-binding site for human p53 protein complexes. *Mol. Cell. Biol.* **12**, 2866–2871 (1992).

102. Zauberman, A., Barak, Y., Ragimov, N., Levy, N. & Oren, M. Sequence-specific DNA binding by p53: identification of target sites and lack of binding to p53 - MDM2 complexes. *EMBO J.* **12**, 2799–2808 (1993).

103. Prives, C. & Manley, J. L. Why is p53 acetylated? *Cell* **107**, 815–818 (2001).

104. Friedler, A., Veprintsev, D. B., Freund, S. M. V., von Glos, K. I. & Fersht, A. R. Modulation of binding of DNA to the C-terminal domain of p53 by acetylation. *Struct. Lond. Engl. 1993* **13**, 629–636 (2005).

105. Qian, H., Wang, T., Naumovski, L., Lopez, C. D. & Brachmann, R. K. Groups of p53 target genes involved in specific p53 downstream effects cluster into different classes of DNA binding sites. *Oncogene* **21**, 7901–7911 (2002).

106. Weinberg, R. L., Veprintsev, D. B., Bycroft, M. & Fersht, A. R. Comparative binding of p53 to its promoter and DNA recognition elements. *J. Mol. Biol.* **348**, 589–596 (2005).

107. el-Deiry, W. S. *et al.* WAF1, a potential mediator of p53 tumor suppression. *Cell* **75**, 817–825 (1993).

108. Kastan, M. B. *et al.* A mammalian cell cycle checkpoint pathway utilizing p53 and GADD45 is defective in ataxia-telangiectasia. *Cell* **71**, 587–597 (1992).

109. Wu, X., Bayle, J. H., Olson, D. & Levine, A. J. The p53-mdm-2 autoregulatory feedback loop. *Genes Dev.* **7**, 1126–1132 (1993).

110. Juven, T., Barak, Y., Zaubermann, A., George, DL:, Oren, M., . Wild type p53 can mediate sequence-specific transactivation of an internal promoter within the mdm2 gene. *Oncogene* **8**, 3411–3416 (1993).

111. Wei, C.-L. *et al.* A global map of p53 transcription-factor binding sites in the human genome. *Cell* **124**, 207–219 (2006).

112. Li, M. *et al.* Distinct regulatory mechanisms and functions for p53-activated and p53-repressed DNA damage response genes in embryonic stem cells. *Mol. Cell* **46**, 30–42 (2012).

113. Fischer, M. Census and evaluation of p53 target genes. *Oncogene* **36**, 3943–3956 (2017).

114. Fischer, M., Steiner, L. & Engeland, K. The transcription factor p53: Not a repressor, solely an activator. *Cell Cycle* **13**, 3037–3058 (2014).

115. Spurgers, K. B. *et al.* Identification of cell cycle regulatory genes as principal targets of p53-mediated transcriptional repression. *J. Biol. Chem.* **281**, 25134–25142 (2006).

116. Branzei, D. & Foiani, M. Regulation of DNA repair throughout the cell cycle. *Nat. Rev. Mol. Cell Biol.* **9**, 297–308 (2008).

117. Vermeulen, K., Van Bockstaele, D. R. & Berneman, Z. N. The cell cycle: a review of regulation, deregulation and therapeutic targets in cancer. *Cell Prolif.* **36**, 131–149 (2003).

118. Branzei, D. & Foiani, M. The Rad53 signal transduction pathway: Replication fork stabilization, DNA repair, and adaptation. *Exp. Cell Res.* **312**, 2654–2659 (2006).

119. Branzei, D. & Foiani, M. Regulation of DNA repair throughout the cell cycle. *Nat. Rev. Mol. Cell Biol.* **9**, 297–308 (2008).

120. Williams, A. B. & Schumacher, B. p53 in the DNA-Damage-Repair Process. *Cold Spring Harb. Perspect. Med.* **6**, (2016).

121. Sancar, A., Lindsey-Boltz, L. A., Unsal-Kaçmaz, K. & Linn, S. Molecular mechanisms of mammalian DNA repair and the DNA damage checkpoints. *Annu. Rev. Biochem.* **73**, 39–85 (2004).

122. Ford, J. M. & Hanawalt, P. C. Expression of Wild-type p53 Is Required for Efficient Global Genomic Nucleotide Excision Repair in UV-irradiated Human Fibroblasts *. *J. Biol. Chem.* **272**, 28073–28080 (1997).

123. Wang, X. W. *et al.* p53 modulation of TFIIH-associated nucleotide excision repair activity. *Nat. Genet.* **10**, 188–195 (1995).

124. Tan, T. & Chu, G. p53 Binds and Activates the Xeroderma Pigmentosum DDB2 Gene in Humans but Not Mice. *Mol. Cell. Biol.* **22**, 3247–3254 (2002).

125. Adimoolam, S. & Ford, J. M. p53 and DNA damage-inducible expression of the xeroderma pigmentosum group C gene. *Proc. Natl. Acad. Sci.* **99**, 12985–12990 (2002).

126. Pâques, F. & Haber, J. E. Multiple pathways of recombination induced by double-strand breaks in Saccharomyces cerevisiae. *Microbiol. Mol. Biol. Rev. MMBR* **63**, 349–404 (1999).

127. Sonoda, E., Hochegger, H., Saberi, A., Taniguchi, Y. & Takeda, S. Differential usage of non-homologous end-joining and homologous recombination in double strand break repair. *DNA Repair* **5**, 1021–1029 (2006).

128. Bartek, J. & Lukas, J. DNA damage checkpoints: from initiation to recovery or adaptation. *Curr. Opin. Cell Biol.* **19**, 238–245 (2007).

129. Falck, J., Coates, J. & Jackson, S. P. Conserved modes of recruitment of ATM, ATR and DNA-PKcs to sites of DNA damage. *Nature* **434**, 605–611 (2005).

130. You, Z., Chahwan, C., Bailis, J., Hunter, T. & Russell, P. ATM Activation and Its Recruitment to Damaged DNA Require Binding to the C Terminus of Nbs1. *Mol. Cell. Biol.* **25**, 5363–5379 (2005).

131. Ira, G. *et al.* DNA end resection, homologous recombination and DNA damage checkpoint activation require CDK1. *Nature* **431**, 1011–1017 (2004).

132. Sung, P. & Klein, H. Mechanism of homologous recombination: mediators and helicases take on regulatory functions. *Nat. Rev. Mol. Cell Biol.* **7**, 739–750 (2006).

133. Mailand, N. *et al.* RNF8 ubiquitylates histones at DNA double-strand breaks and promotes assembly of repair proteins. *Cell* **131**, 887–900 (2007).

134. Linke, S. P. *et al.* p53 interacts with hRAD51 and hRAD54, and directly modulates homologous recombination. *Cancer Res.* **63**, 2596–2605 (2003).

135. Gong, L. *et al.* p53 isoform Δ113p53/Δ133p53 promotes DNA double-strand break repair to protect cell from death and senescence in response to DNA damage. *Cell Res.* **25**, 351–369 (2015).

136. Nurse, P. A long twentieth century of the cell cycle and beyond. *Cell* **100**, 71–78 (2000).

137. Hochegger, H., Takeda, S. & Hunt, T. Cyclin-dependent kinases and cell-cycle transitions: does one fit all? *Nat. Rev. Mol. Cell Biol.* **9**, 910–916 (2008).

138. Pardee, A. B. A restriction point for control of normal animal cell proliferation. *Proc. Natl. Acad. Sci. U. S. A.* **71**, 1286–1290 (1974).

139. Bartek, J., Bartkova, J. & Lukas, J. The retinoblastoma protein pathway and the restriction point. *Curr. Opin. Cell Biol.* **8**, 805–814 (1996).

140. Harbour, J. W. & Dean, D. C. The Rb/E2F pathway: expanding roles and emerging paradigms. *Genes Dev.* **14**, 2393–2409 (2000).

141. Malumbres, M. & Barbacid, M. Mammalian cyclin-dependent kinases. *Trends Biochem. Sci.* **30**, 630–641 (2005).

142. Michalovitz, D., Halevy, O. & Oren, M. Conditional inhibition of transformation and of cell proliferation by a temperature-sensitive mutant of p53. *Cell* **62**, 671–680 (1990).

143. Mercer, W. E. *et al.* Negative growth regulation in a glioblastoma tumor cell line that conditionally expresses human wild-type p53. *Proc. Natl. Acad. Sci. U. S. A.* **87**, 6166–6170 (1990).

144. Baker, S. J., Markowitz, S., Fearon, E. R., Willson, J. K. & Vogelstein, B. Suppression of human colorectal carcinoma cell growth by wild-type p53. *Science* **249**, 912–915 (1990).

145. Diller, L. *et al.* p53 functions as a cell cycle control protein in osteosarcomas. *Mol. Cell. Biol.* **10**, 5772–5781 (1990).

146. Kastan, M. B., Onyekwere, O., Sidransky, D., Vogelstein, B. & Craig, R. W. Participation of p53 protein in the cellular response to DNA damage. *Cancer Res.* **51**, 6304–6311 (1991).

147. el-Deiry, W. S. *et al.* WAF1, a potential mediator of p53 tumor suppression. *Cell* **75**, 817–825 (1993).

148. Harper, J. W., Adami, G. R., Wei, N., Keyomarsi, K. & Elledge, S. J. The p21 Cdk-interacting protein Cip1 is a potent inhibitor of G1 cyclin-dependent kinases. *Cell* **75**, 805–816 (1993).

149. Wang, L., Han, H., Dong, L., Wang, Z. & Qin, Y. Function of p21 and its therapeutic effects in esophageal cancer (Review). *Oncol. Lett.* **21**, 1–1 (2021).

150. Chen, J., Jackson, P. K., Kirschner, M. W. & Dutta, A. Separate domains of p21 involved in the inhibition of Cdk kinase and PCNA. *Nature* **374**, 386–388 (1995).

151. Cho, Y.-J. & Liang, P. S-phase-coupled apoptosis in tumor suppression. *Cell. Mol. Life Sci. CMLS* **68**, 1883–1896 (2011).

152. Giono, L. E. & Manfredi, J. J. The p53 tumor suppressor participates in multiple cell cycle checkpoints. *J. Cell. Physiol.* **209**, 13–20 (2006).

153. Flatt, P. M., Tang, L. J., Scatena, C. D., Szak, S. T. & Pietenpol, J. A. p53 regulation of G(2) checkpoint is retinoblastoma protein dependent. *Mol. Cell. Biol.* **20**, 4210–4223 (2000).

154. Harrington, E. A., Bruce, J. L., Harlow, E. & Dyson, N. pRB plays an essential role in cell cycle arrest induced by DNA damage. *Proc. Natl. Acad. Sci. U. S. A.* **95**, 11945–11950 (1998).

155. St Clair, S. *et al.* DNA damage-induced downregulation of Cdc25C is mediated by p53 via two independent mechanisms: one involves direct binding to the cdc25C promoter. *Mol. Cell* **16**, 725–736 (2004).

156. Chan, T. A., Hermeking, H., Lengauer, C., Kinzler, K. W. & Vogelstein, B. 14-3-3Sigma is required to prevent mitotic catastrophe after DNA damage. *Nature* **401**, 616–620 (1999).

157. Lopez-Girona, A., Kanoh, J. & Russell, P. Nuclear exclusion of Cdc25 is not required for the DNA damage checkpoint in fission yeast. *Curr. Biol.* **11**, 50–54 (2001).

158. Zhan, Q. *et al.* Association with Cdc2 and inhibition of Cdc2/Cyclin B1 kinase activity by the p53-regulated protein Gadd45. *Oncogene* **18**, 2892–2900 (1999).

159. Jin, S. *et al.* GADD45-induced cell cycle G2-M arrest associates with altered subcellular distribution of cyclin B1 and is independent of p38 kinase activity. *Oncogene* **21**, 8696–8704 (2002).

160. Elmore, S. Apoptosis: A Review of Programmed Cell Death. 40 (2007).

161. Locksley, R. M., Killeen, N. & Lenardo, M. J. The TNF and TNF receptor superfamilies: integrating mammalian biology. *Cell* **104**, 487–501 (2001).

162. Kischkel, F. C. *et al.* Cytotoxicity-dependent APO-1 (Fas/CD95)-associated proteins form a death-inducing signaling complex (DISC) with the receptor. *EMBO J.* **14**, 5579–5588 (1995).

163. Saelens, X. *et al.* Toxic proteins released from mitochondria in cell death. *Oncogene* **23**, 2861–2874 (2004).

164. Cory, S. & Adams, J. M. The Bcl2 family: regulators of the cellular life-or-death switch. *Nat. Rev. Cancer* **2**, 647–656 (2002).

165. Bratton, D. L. *et al.* Appearance of phosphatidylserine on apoptotic cells requires calcium-mediated nonspecific flip-flop and is enhanced by loss of the aminophospholipid translocase. *J. Biol. Chem.* **272**, 26159–26165 (1997).

166. van Engeland, M., Nieland, L. J., Ramaekers, F. C., Schutte, B. & Reutelingsperger, C. P. Annexin V-affinity assay: a review on an apoptosis detection system based on phosphatidylserine exposure. *Cytometry* **31**, 1–9 (1998).

167. Yonish-Rouach, E. *et al.* Wild-type p53 induces apoptosis of myeloid leukaemic cells that is inhibited by interleukin-6. *Nature* **352**, 345–347 (1991).

168. Shaw, P. *et al.* Induction of apoptosis by wild-type p53 in a human colon tumor-derived cell line. *Proc. Natl. Acad. Sci. U. S. A.* **89**, 4495–4499 (1992).

169. Sax, J. K. & El-Deiry, W. S. Identification and characterization of the cytoplasmic protein TRAF4 as a p53-regulated proapoptotic gene. *J. Biol. Chem.* **278**, 36435–36444 (2003).

170. Liu, X., Yue, P., Khuri, F. R. & Sun, S.-Y. p53 Upregulates Death Receptor 4 Expression through an Intronic p53 Binding Site. *Cancer Res.* **64**, 5078–5083 (2004).

171. Miyashita, T. & Reed, J. C. Tumor suppressor p53 is a direct transcriptional activator of the human bax gene. *Cell* **80**, 293–299 (1995).

172. Nakano, K. & Vousden, K. H. PUMA, a novel proapoptotic gene, is induced by p53. *Mol. Cell* **7**, 683–694 (2001).

173. Marchenko, N. D., Zaika, A. & Moll, U. M. Death signal-induced localization of p53 protein to mitochondria. A potential role in apoptotic signaling. *J. Biol. Chem.* **275**, 16202–16212 (2000).

174. Wang, Y., Blandino, G., Oren, M. & Givol, D. Induced p53 expression in lung cancer cell line promotes cell senescence and differentially modifies the cytotoxicity of anti-cancer drugs. *Oncogene* **17**, 1923–1930 (1998).

175. Serrano, M., Lin, A. W., McCurrach, M. E., Beach, D. & Lowe, S. W. Oncogenic ras provokes premature cell senescence associated with accumulation of p53 and p16INK4a. *Cell* **88**, 593–602 (1997).

176. Mijit, M., Caracciolo, V., Melillo, A., Amicarelli, F. & Giordano, A. Role of p53 in the Regulation of Cellular Senescence. *Biomolecules* **10**, (2020).

177. Itahana, K., Campisi, J. & Dimri, G. P. Methods to detect biomarkers of cellular senescence: the senescence-associated beta-galactosidase assay. *Methods Mol. Biol. Clifton NJ* **371**, 21–31 (2007).

178. Kruiswijk, F., Labuschagne, C. F. & Vousden, K. H. p53 in survival, death and metabolic health: a lifeguard with a licence to kill. *Nat. Rev. Mol. Cell Biol.* **16**, 393–405 (2015).

179. Tasdemir, E. *et al.* Regulation of autophagy by cytoplasmic p53. *Nat. Cell Biol.* **10**, 676–687 (2008).

180. Crighton, D. *et al.* DRAM, a p53-induced modulator of autophagy, is critical for apoptosis. *Cell* **126**, 121–134 (2006).

181. Kruiswijk, F., Labuschagne, C. F. & Vousden, K. H. p53 in survival, death and metabolic health: a lifeguard with a licence to kill. *Nat. Rev. Mol. Cell Biol.* **16**, 393–405 (2015).

182. Budde, A. & Grummt, I. p53 represses ribosomal gene transcription. *Oncogene* **18**, 1119–1124 (1999).

183. Golomb, L. *et al.* Importin 7 and exportin 1 link c-Myc and p53 to regulation of ribosomal biogenesis. *Mol. Cell* **45**, 222–232 (2012).

184. Budanov, A. V. & Karin, M. p53 target genes sestrin1 and sestrin2 connect genotoxic stress and mTOR signaling. *Cell* **134**, 451–460 (2008).

185. Gao, M. *et al.* Ferroptosis is an autophagic cell death process. *Cell Res.* **26**, 1021–1032 (2016).

186. Kumari, R., Kohli, S. & Das, S. p53 regulation upon genotoxic stress: intricacies and complexities. *Mol. Cell. Oncol.* **1**, e969653 (2014).

187. Braithwaite, A. W., Del Sal, G. & Lu, X. Some p53-binding proteins that can function as arbiters of life and death. *Cell Death Differ.* **13**, 984–993 (2006).

188. Bode, A. M. & Dong, Z. Post-translational modification of p53 in tumorigenesis. *Nat. Rev. Cancer* **4**, 793–805 (2004).

189. Espinosa, J. M., Verdun, R. E. & Emerson, B. M. p53 Functions through Stress- and Promoter-Specific Recruitment of Transcription Initiation Components before and after DNA Damage. *Mol. Cell* **12**, 1015–1027 (2003).

190. Gomes, N. P. & Espinosa, J. M. Disparate chromatin landscapes and kinetics of inactivation impact differential regulation of p53 target genes. *Cell Cycle* **9**, 3428–3437 (2010).

191. Morachis, J. M., Murawsky, C. M. & Emerson, B. M. Regulation of the p53 transcriptional response by structurally diverse core promoters. *Genes Dev.* **24**, 135–147 (2010).

192. Momand, J., Zambetti, G. P., Olson, D. C., George, D. & Levine, A. J. The mdm-2 oncogene product forms a complex with the p53 protein and inhibits p53-mediated transactivation. *Cell* **69**, 1237–1245 (1992).

193. Oliner, J. D. *et al.* Oncoprotein MDM2 conceals the activation domain of tumour suppressor p53. *Nature* **362**, 857–860 (1993).

194. Haupt, Y., Maya, R., Kazaz, A. & Oren, M. Mdm2 promotes the rapid degradation of p53. *Nature* **387**, 296–299 (1997).

195. Honda, R., Tanaka, H. & Yasuda, H. Oncoprotein MDM2 is a ubiquitin ligase E3 for tumor suppressor p53. *FEBS Lett.* **420**, 25–27 (1997).

196. Kubbutat, M. H., Jones, S. N. & Vousden, K. H. Regulation of p53 stability by Mdm2. *Nature* **387**, 299–303 (1997).

197. Shvarts, A. *et al.* MDMX: a novel p53-binding protein with some functional properties of MDM2. *EMBO J.* **15**, 5349–5357 (1996).

198. Kostic, M., Matt, T., Martinez-Yamout, M. A., Dyson, H. J. & Wright, P. E. Solution structure of the Hdm2 C2H2C4 RING, a domain critical for ubiquitination of p53. *J. Mol. Biol.* **363**, 433–450 (2006).

199. Linares, L. K., Hengstermann, A., Ciechanover, A., Müller, S. & Scheffner, M. HdmX stimulates Hdm2-mediated ubiquitination and degradation of p53. *Proc. Natl. Acad. Sci. U. S. A.* **100**, 12009–12014 (2003).

200. Jones, S. N., Roe, A. E., Donehower, L. A. & Bradley, A. Rescue of embryonic lethality in Mdm2-deficient mice by absence of p53. *Nature* **378**, 206–208 (1995).

201. Montes de Oca Luna, R., Wagner, D. S. & Lozano, G. Rescue of early embryonic lethality in mdm2-deficient mice by deletion of p53. *Nature* **378**, 203–206 (1995).

202. Parant, J. *et al.* Rescue of embryonic lethality in Mdm4-null mice by loss of Trp53 suggests a nonoverlapping pathway with MDM2 to regulate p53. *Nat. Genet.* **29**, 92–95 (2001).

203. Bond, G. L. *et al.* A single nucleotide polymorphism in the MDM2 promoter attenuates the p53 tumor suppressor pathway and accelerates tumor formation in humans. *Cell* **119**, 591–602 (2004).

204. Hock, A. K. & Vousden, K. H. The role of ubiquitin modification in the regulation of p53. *Biochim. Biophys. Acta* **1843**, 137–149 (2014).

205. Maki, C. G. Oligomerization Is Required for p53 to be Efficiently Ubiquitinated by MDM2. *J. Biol. Chem.* **274**, 16531–16535 (1999).

206. Kubbutat, M. H. G., Ludwig, R. L., Ashcroft, M. & Vousden, K. H. Regulation of Mdm2-Directed Degradation by the C Terminus of p53. *Mol. Cell. Biol.* **18**, 5690–5698 (1998).

207. Li, M., Brooks, C. L., Kon, N. & Gu, W. A dynamic role of HAUSP in the p53-Mdm2 pathway. *Mol. Cell* **13**, 879–886 (2004).

208. Barak, Y., Juven, T., Haffner, R. & Oren, M. mdm2 expression is induced by wild type p53 activity. *EMBO J.* **12**, 461–468 (1993).

209. Okoshi, R. *et al.* Transcriptional regulation of tumor suppressor p53 by cAMP-responsive element-binding protein/AMP-activated protein kinase complex in response to glucose deprivation. *Genes Cells Devoted Mol. Cell. Mech.* **14**, 1429–1440 (2009).

210. Reisman, D., Elkind, N. B., Roy, B., Beamon, J. & Rotter, V. c-Myc trans-activates the p53 promoter through a required downstream CACGTG motif. *Cell Growth Differ. Mol. Biol. J. Am. Assoc. Cancer Res.* **4**, 57–65 (1993).

211. Deffie, A., Wu, H., Reinke, V. & Lozano, G. The tumor suppressor p53 regulates its own transcription. *Mol. Cell. Biol.* **13**, 3415–3423 (1993).

212. Fu, L. & Benchimol, S. Participation of the human p53 3'UTR in translational repression and activation following gamma-irradiation. *EMBO J.* **16**, 4117–4125 (1997).

213. Mosner, J. *et al.* Negative feedback regulation of wild-type p53 biosynthesis. *EMBO J.* **14**, 4442–4449 (1995).

214. Takagi, M., Absalon, M. J., McLure, K. G. & Kastan, M. B. Regulation of p53 translation and induction after DNA damage by ribosomal protein L26 and nucleolin. *Cell* **123**, 49–63 (2005).

215. Ofir-Rosenfeld, Y., Boggs, K., Michael, D., Kastan, M. B. & Oren, M. Mdm2 regulates p53 mRNA translation through inhibitory interactions with ribosomal protein L26. *Mol. Cell* **32**, 180–189 (2008).

216. Wedeken, L., Singh, P. & Klempnauer, K.-H. Tumor suppressor protein Pdcd4 inhibits translation of p53 mRNA. *J. Biol. Chem.* **286**, 42855–42862 (2011).

217. Samad, A., Anderson, C. W. & Carroll, R. B. Mapping of phosphomonoester and apparent phosphodiester bonds of the oncogene product p53 from simian virus 40-transformed 3T3 cells. *Proc. Natl. Acad. Sci. U. S. A.* **83**, 897–901 (1986).

218. Moll, U. M. & Petrenko, O. The MDM2-p53 interaction. *Mol. Cancer Res. MCR* **1**, 1001–1008 (2003).

219. Shiloh, Y. ATM and related protein kinases: safeguarding genome integrity. *Nat. Rev. Cancer* **3**, 155–168 (2003).

220. Toledo, F. & Wahl, G. M. Regulating the p53 pathway: in vitro hypotheses, in vivo veritas. *Nat. Rev. Cancer* **6**, 909–923 (2006).

221. Higashimoto, Y. *et al.* Human p53 is phosphorylated on serines 6 and 9 in response to DNA damage-inducing agents. *J. Biol. Chem.* **275**, 23199–23203 (2000).

222. Yoshida, K., Liu, H. & Miki, Y. Protein kinase C delta regulates Ser46 phosphorylation of p53 tumor suppressor in the apoptotic response to DNA damage. *J. Biol. Chem.* **281**, 5734–5740 (2006).

223. Mayo, L. D. *et al.* Phosphorylation of Human p53 at Serine 46 Determines Promoter Selection and whether Apoptosis Is Attenuated or Amplified *. *J. Biol. Chem.* **280**, 25953–25959 (2005).

224. Matsumoto, M., Furihata, M. & Ohtsuki, Y. Posttranslational phosphorylation of mutant p53 protein in tumor development. *Med. Mol. Morphol.* **39**, 79–87 (2006).

225. Waterman, M. J., Stavridi, E. S., Waterman, J. L. & Halazonetis, T. D. ATM-dependent activation of p53 involves dephosphorylation and association with 14-3-3 proteins. *Nat. Genet.* **19**, 175–178 (1998).

226. Cai, X. & Liu, X. Inhibition of Thr-55 phosphorylation restores p53 nuclear localization and sensitizes cancer cells to DNA damage. *Proc. Natl. Acad. Sci. U. S. A.* **105**, 16958–16963 (2008).

227. Shieh, S.-Y., Ahn, J., Tamai, K., Taya, Y. & Prives, C. The human homologs of checkpoint kinases Chk1 and Cds1 (Chk2) phosphorylate p53 at multiple DNA damage-inducible sites. *Genes Dev.* **14**, 289–300 (2000).

228. CHENE, P. Fast, qualitative analysis of p53 phosphorylation by protein kinases. *Fast Qual. Anal. P53 Phosphorylation Protein Kinases* **28**, 240–242 (2000).

229. Shang, X. *et al.* Dual-specificity phosphatase 26 is a novel p53 phosphatase and inhibits p53 tumor suppressor functions in human neuroblastoma. *Oncogene* **29**, 4938–4946 (2010).

230. Li, D. W.-C. *et al.* Protein serine/threonine phosphatase-1 dephosphorylates p53 at Ser-15 and Ser-37 to modulate its transcriptional and apoptotic activities. *Oncogene* **25**, 3006–3022 (2006).

231. Mi, J., Bolesta, E., Brautigan, D. L. & Larner, J. M. PP2A regulates ionizing radiation-induced apoptosis through Ser46 phosphorylation of p53. *Mol. Cancer Ther.* **8**, 135–140 (2009).

232. Shaltiel, I. A. *et al.* Distinct phosphatases antagonize the p53 response in different phases of the cell cycle. *Proc. Natl. Acad. Sci. U. S. A.* **111**, 7313–7318 (2014).

233. Han, H.-S. *et al.* The estrogen receptor alpha pathway induces oncogenic Wip1 phosphatase gene expression. *Mol. Cancer Res. MCR* **7**, 713–723 (2009).

234. Lu, X. *et al.* The Wip1 Phosphatase acts as a gatekeeper in the p53-Mdm2 autoregulatory loop. *Cancer Cell* **12**, 342–354 (2007).

235. Shreeram, S. *et al.* Wip1 phosphatase modulates ATM-dependent signaling pathways. *Mol. Cell* **23**, 757–764 (2006).

236. Lu, X. *et al.* The Wip1 Phosphatase Acts as a Gatekeeper in the p53-Mdm2 Autoregulatory Loop. *Cancer Cell* **12**, 342–354 (2007).

237. Gu, W. & Roeder, R. G. Activation of p53 sequence-specific DNA binding by acetylation of the p53 C-terminal domain. *Cell* **90**, 595–606 (1997).

238. D'Orazi, G. *et al.* Homeodomain-interacting protein kinase-2 phosphorylates p53 at Ser 46 and mediates apoptosis. *Nat. Cell Biol.* **4**, 11–19 (2002).

239. Hofmann, T. G. *et al.* Regulation of p53 activity by its interaction with homeodomain-interacting protein kinase-2. *Nat. Cell Biol.* **4**, 1–10 (2002).

240. Puca, R. *et al.* HIPK2 modulates p53 activity towards pro-apoptotic transcription. *Mol. Cancer* **8**, 85 (2009).

241. Chao, C. *et al.* Acetylation of Mouse p53 at Lysine 317 Negatively Regulates p53 Apoptotic Activities after DNA Damage. *Mol. Cell. Biol.* **26**, 6859–6869 (2006).

242. Sykes, S. M. *et al.* Acetylation of the p53 DNA-binding domain regulates apoptosis induction. *Mol. Cell* **24**, 841–851 (2006).

243. Tang, Y., Luo, J., Zhang, W. & Gu, W. Tip60-dependent acetylation of p53 modulates the decision between cell-cycle arrest and apoptosis. *Mol. Cell* **24**, 827–839 (2006).

244. Luo, J. *et al.* Negative control of p53 by Sir2alpha promotes cell survival under stress. *Cell* **107**, 137–148 (2001).

245. Sen, N., Kumari, R., Singh, M. I. & Das, S. HDAC5, a key component in temporal regulation of p53-mediated transactivation in response to genotoxic stress. *Mol. Cell* **52**, 406–420 (2013).

246. Shi, X. *et al.* Modulation of p53 function by SET8-mediated methylation at lysine 382. *Mol. Cell* **27**, 636–646 (2007).

247. Kurash, J. K. *et al.* Methylation of p53 by Set7/9 mediates p53 acetylation and activity in vivo. *Mol. Cell* **29**, 392–400 (2008).

248. Jansson, M. *et al.* Arginine methylation regulates the p53 response. *Nat. Cell Biol.* **10**, 1431–1439 (2008).

249. Momand, J., Wu, H. H. & Dasgupta, G. MDM2--master regulator of the p53 tumor suppressor protein. *Gene* **242**, 15–29 (2000).

250. Marine, J.-C. *et al.* Keeping p53 in check: essential and synergistic functions of Mdm2 and Mdm4. *Cell Death Differ.* **13**, 927–934 (2006).

251. Lu, H. & Levine, A. J. Human TAFII31 protein is a transcriptional coactivator of the p53 protein. *Proc. Natl. Acad. Sci. U. S. A.* **92**, 5154–5158 (1995).

252. Thut, C. J., Chen, J. L., Klemm, R. & Tjian, R. p53 transcriptional activation mediated by coactivators TAFII40 and TAFII60. *Science* **267**, 100–104 (1995).

253. Gu, W., Shi, X. L. & Roeder, R. G. Synergistic activation of transcription by CBP and p53. *Nature* **387**, 819–823 (1997).

254. Grossman, S. R. p300/CBP/p53 interaction and regulation of the p53 response. *Eur. J. Biochem.* **268**, 2773–2778 (2001).

255. Samuels-Lev, Y. *et al.* ASPP proteins specifically stimulate the apoptotic function of p53. *Mol. Cell* **8**, 781–794 (2001).

256. Bergamaschi, D. *et al.* iASPP preferentially binds p53 proline-rich region and modulates apoptotic function of codon 72–polymorphic p53. *Nat. Genet.* **38**, 1133–1141 (2006).

257. Das, S. *et al.* Hzf Determines cell survival upon genotoxic stress by modulating p53 transactivation. *Cell* **130**, 624–637 (2007).

258. Götz, C. *et al.* Protein kinase CK2 interacts with a multi-protein binding domain of p53. *Mol. Cell. Biochem.* **191**, 111–120 (1999).

259. Delphi, C. *et al.* The in Vitro Phosphorylation of P53 by Calcium-Dependent Protein Kinase C. *Eur. J. Biochem.* **245**, 684–692 (1997).

260. Ikeda, A. *et al.* p300/CBP-Dependent and -Independent Transcriptional Interference between NF-κB RelA and p53. *Biochem. Biophys. Res. Commun.* **272**, 375–379 (2000).

261. Dobner, T., Horikoshi, N., Rubenwolf, S. & Shenk, T. Blockage by Adenovirus E4orf6 of Transcriptional Activation by the p53 Tumor Suppressor. *Science* **272**, 1470–1473 (1996).

262. Lin, Y. *et al.* The Transactivation and p53-interacting Functions of Hepatitis B Virus X Protein Are Mutually Interfering but Distinct. *Cancer Res.* **57**, 5137–5142 (1997).

263. Marston, N. J., Jenkins, J. R. & Vousden, K. H. Oligomerisation of full length p53 contributes to the interaction with mdm2 but not HPV E6. *Oncogene* **10**, 1709–1715 (1995).

264. Chen, J., Marechal, V. & Levine, A. J. Mapping of the p53 and mdm-2 interaction domains. *Mol. Cell. Biol.* **13**, 4107–4114 (1993).

265. Massimi, P., Pim, D., Bertoli, C., Bouvard, V. & Banks, L. Interaction between the HPV-16 E2 transcriptional activator and p53. *Oncogene* **18**, 7748–7754 (1999).

266. Nie, Y., Li, H.-H., Bula, C. M. & Liu, X. Stimulation of p53 DNA Binding by c-Abl Requires the p53 C Terminus and Tetramerization. *Mol. Cell. Biol.* **20**, 741–748 (2000).

267. Liu, X., Miller, C. W., Koeffler, P. H. & Berk, A. J. The p53 activation domain binds the TATA box-binding polypeptide in Holo-TFIID, and a neighboring p53 domain inhibits transcription. *Mol. Cell. Biol.* **13**, 3291–3300 (1993).

268. Lomax, M. E., Barnes, D. M., Hupp, T. R., Picksley, S. M. & Camplejohn, R. S. Characterization of p53 oligomerization domain mutations isolated from Li-Fraumeni and Li-Fraumeni like family members. *Oncogene* **17**, 643–649 (1998).

269. Mantovani, F. *et al.* The prolyl isomerase Pin1 orchestrates p53 acetylation and dissociation from the apoptosis inhibitor iASPP. *Nat. Struct. Mol. Biol.* **14**, 912–920 (2007).

270. Shahar, O. D. *et al.* Acetylation of Lysine 382 and Phosphorylation of Serine 392 in p53 Modulate the Interaction between p53 and MDC1 In Vitro. *PLOS ONE* **8**, e78472 (2013).

271. Tian, C. *et al.* KRAB-type zinc-finger protein Apak specifically regulates p53-dependent apoptosis. *Nat. Cell Biol.* **11**, 580–591 (2009).

272. Dehner, A. *et al.* Cooperative binding of p53 to DNA: regulation by protein-protein interactions through a double salt bridge. *Angew. Chem. Int. Ed Engl.* **44**, 5247–5251 (2005).

273. Olivier, M. *et al.* The IARC TP53 database: new online mutation analysis and recommendations to users. *Hum. Mutat.* **19**, 607–614 (2002).

274. Hamroun, D. *et al.* The UMD TP53 database and website: update and revisions. *Hum. Mutat.* **27**, 14–20 (2006).

275. Kato, S. *et al.* Understanding the function-structure and function-mutation relationships of p53 tumor suppressor protein by high-resolution missense mutation analysis. *Proc. Natl. Acad. Sci. U. S. A.* **100**, 8424–8429 (2003).

276. Resnick, M. A. & Inga, A. Functional mutants of the sequence-specific transcription factor p53 and implications for master genes of diversity. *Proc. Natl. Acad. Sci. U. S. A.* **100**, 9934–9939 (2003).

277. Dearth, L. R. *et al.* Inactive full-length p53 mutants lacking dominant wild-type p53 inhibition highlight loss of heterozygosity as an important aspect of p53 status in human cancers. *Carcinogenesis* **28**, 289–298 (2007).

278. Menendez, D., Inga, A. & Resnick, M. A. The Biological Impact of the Human Master Regulator p53 Can Be Altered by Mutations That Change the Spectrum and Expression of Its Target Genes. *Mol. Cell. Biol.* **26**, 2297–2308 (2006).

279. Oren, M. & Rotter, V. Mutant p53 Gain-of-Function in Cancer. *Cold Spring Harb. Perspect. Biol.* **2**, a001107–a001107 (2010).

280. Olivier, M. *et al.* The clinical value of somatic TP53 gene mutations in 1,794 patients with breast cancer. *Clin. Cancer Res. Off. J. Am. Assoc. Cancer Res.* **12**, 1157–1167 (2006).

281. Friedler, A., Veprintsev, D. B., Hansson, L. O. & Fersht, A. R. Kinetic instability of p53 core domain mutants: implications for rescue by small molecules. *J. Biol. Chem.* **278**, 24108–24112 (2003).

282. Liu, G. *et al.* Chromosome stability, in the absence of apoptosis, is critical for suppression of tumorigenesis in Trp53 mutant mice. *Nat. Genet.* **36**, 63–68 (2004).

283. Shiraishi, K. *et al.* Isolation of temperature-sensitive p53 mutations from a comprehensive missense mutation library. *J. Biol. Chem.* **279**, 348–355 (2004).

284. Hainaut, P. & Hollstein, M. p53 and human cancer: the first ten thousand mutations. *Adv. Cancer Res.* **77**, 81–137 (2000).

285. Hollstein, M., Sidransky, D., Vogelstein, B. & Harris, C. C. p53 mutations in human cancers. *Science* **253**, 49–53 (1991).

286. Hollstein, M. *et al.* New approaches to understanding p53 gene tumor mutation spectra. *Mutat. Res. Mol. Mech. Mutagen.* **431**, 199–209 (1999).

287. Soussi, T., Dehouche, K. & Béroud, C. p53 website and analysis of p53 gene mutations in human cancer: forging a link between epidemiology and carcinogenesis. *Hum. Mutat.* **15**, 105–113 (2000).

288. Olivier, M. *et al.* Li-Fraumeni and related syndromes: correlation between tumor type, family structure, and TP53 genotype. *Cancer Res.* **63**, 6643–6650 (2003).

289. Ishioka, C. *et al.* Oligomerization is not essential for growth suppression by p53 in p53-deficient osteosarcoma Saos-2 cells. *Biochem. Biophys. Res. Commun.* **232**, 54–60 (1997).

290. Mateu, M. G. & Fersht, A. R. Mutually compensatory mutations during evolution of the tetramerization domain of tumor suppressor p53 lead to impaired hetero-oligomerization. *Proc. Natl. Acad. Sci. U. S. A.* **96**, 3595–3599 (1999).

291. Chène, P. The role of tetramerization in p53 function. *Oncogene* **20**, 2611–2617 (2001).

292. Kawaguchi, T. *et al.* The relationship among p53 oligomer formation, structure and transcriptional activity using a comprehensive missense mutation library. *Oncogene* **24**, 6976–6981 (2005).

293. Higashimoto, Y. *et al.* Unfolding, aggregation, and amyloid formation by the tetramerization domain from mutant p53 associated with lung cancer. *Biochemistry* **45**, 1608–1619 (2006).

294. Chène, P. & Bechter, E. P53 mutants without a functional tetramerisation domain are not oncogenic11Edited by A. R. Fersht. *J. Mol. Biol.* **286**, 1269–1274 (1999).

295. Frazier, M. W. *et al.* Activation of c-myc gene expression by tumor-derived p53 mutants requires a discrete C-terminal domain. *Mol. Cell. Biol.* **18**, 3735–3743 (1998).

296. Lányi, Á. *et al.* `Gain of function' phenotype of tumor-derived mutant p53 requires the oligomerization/nonsequence-specific nucleic acid-binding domain. *Oncogene* **16**, 3169–3176 (1998).

297. Poon, A., Davis, B. H. & Chao, L. The coupon collector and the suppressor mutation: estimating the number of compensatory mutations by maximum likelihood. *Genetics* **170**, 1323–1332 (2005).

298. Brachmann, R. K., Yu, K., Eby, Y., Pavletich, N. P. & Boeke, J. D. Genetic selection of intragenic suppressor mutations that reverse the effect of common p53 cancer mutations. *EMBO J.* **17**, 1847–1859 (1998).

299. Baroni, T. E. *et al.* A global suppressor motif for p53 cancer mutants. *Proc. Natl. Acad. Sci. U. S. A.* **101**, 4930–4935 (2004).

300. Wieczorek, A. M., Waterman, J. L., Waterman, M. J. & Halazonetis, T. D. Structure-based rescue of common tumor-derived p53 mutants. *Nat. Med.* **2**, 1143–1146 (1996).

301. Peng, Z. Current status of gendicine in China: recombinant human Ad-p53 agent for treatment of cancers. *Hum. Gene Ther.* **16**, 1016–1027 (2005).

302. Senzer, N. & Nemunaitis, J. A review of contusugene ladenovec (Advexin) p53 therapy. *Curr. Opin. Mol. Ther.* **11**, 54–61 (2009).

303. Bykov, V. J. N. *et al.* Restoration of the tumor suppressor function to mutant p53 by a low-molecular-weight compound. *Nat. Med.* **8**, 282–288 (2002).

304. Boeckler, F. M. *et al.* Targeted rescue of a destabilized mutant of p53 by an in silico screened drug. *Proc. Natl. Acad. Sci. U. S. A.* **105**, 10360–10365 (2008).

305. Lambert, J. M. R. *et al.* PRIMA-1 reactivates mutant p53 by covalent binding to the core domain. *Cancer Cell* **15**, 376–388 (2009).

306. Watanabe, F. T. *et al.* Curcumin, but not Prima-1, decreased tumor cell proliferation in the syngeneic murine orthotopic bladder tumor model. *Clin. Sao Paulo Braz.* **66**, 2121–2124 (2011).

307. Deneberg, S. *et al.* An open-label phase I dose-finding study of APR-246 in hematological malignancies. *Blood Cancer J.* **6**, e447 (2016).

308. Blanden, A. R., Yu, X., Loh, S. N., Levine, A. J. & Carpizo, D. R. Reactivating mutant p53 using small molecules as zinc metallochaperones: awakening a sleeping giant in cancer. *Drug Discov. Today* **20**, 1391–1397 (2015).

309. Zeestraten, E. C. M. *et al.* Addition of interferon-α to the p53-SLP® vaccine results in increased production of interferon-γ in vaccinated colorectal cancer patients: A phase I/II clinical trial. *Int. J. Cancer* **132**, 1581–1591 (2013).

310. Ma, C. X. *et al.* Targeting Chk1 in p53-deficient triple-negative breast cancer is therapeutically beneficial in human-in-mouse tumor models. *J. Clin. Invest.* **122**, 1541–1552 (2012).

311. Morandell, S. & Yaffe, M. B. Exploiting synthetic lethal interactions between DNA damage signaling, checkpoint control, and p53 for targeted cancer therapy. *Prog. Mol. Biol. Transl. Sci.* **110**, 289–314 (2012).

312. Friedler, A. *et al.* A peptide that binds and stabilizes p53 core domain: chaperone strategy for rescue of oncogenic mutants. *Proc. Natl. Acad. Sci. U. S. A.* **99**, 937–942 (2002).

313. Aas, T. *et al.* Specific P53 mutations are associated with de novo resistance to doxorubicin in breast cancer patients. *Nat. Med.* **2**, 811–814 (1996).

314. O'Shea, D. *et al.* The presence of TP53 mutation at diagnosis of follicular lymphoma identifies a high-risk group of patients with shortened time to disease progression and poorer overall survival. *Blood* **112**, 3126–3129 (2008).

315. Young, K. H. *et al.* Structural profiles of TP53 gene mutations predict clinical outcome in diffuse large B-cell lymphoma: an international collaborative study. *Blood* **112**, 3088–3098 (2008).

316. Vassilev, L. T. MDM2 inhibitors for cancer therapy. *Trends Mol. Med.* **13**, 23–31 (2007).

317. Vassilev, L. T. *et al.* In vivo activation of the p53 pathway by small-molecule antagonists of MDM2. *Science* **303**, 844–848 (2004).

318. Issaeva, N. *et al.* Small molecule RITA binds to p53, blocks p53-HDM-2 interaction and activates p53 function in tumors. *Nat. Med.* **10**, 1321–1328 (2004).

319. Zhao, Y., Aguilar, A., Bernard, D. & Wang, S. Small-Molecule Inhibitors of the MDM2–p53 Protein–Protein Interaction (MDM2 Inhibitors) in Clinical Trials for Cancer Treatment. *J. Med. Chem.* **58**, 1038–1052 (2015).

320. Andreeff, M. *et al.* Results of the Phase I Trial of RG7112, a Small-Molecule MDM2 Antagonist in Leukemia. *Clin. Cancer Res.* **22**, 868–876 (2016).

321. Rao, B., Lain, S. & Thompson, A. M. p53-Based cyclotherapy: exploiting the 'guardian of the genome' to protect normal cells from cytotoxic therapy. *Br. J. Cancer* **109**, 2954–2958 (2013).

322. Cheok, C. F. & Lane, D. P. Exploiting the p53 Pathway for Therapy. *Cold Spring Harb. Perspect. Med.* **7**, a026310 (2017).

323. Cox, J. & Mann, M. MaxQuant enables high peptide identification rates, individualized p.p.b.-range mass accuracies and proteome-wide protein quantification. *Nat. Biotechnol.* **26**, 1367–1372 (2008).

324. Cox, J. *et al.* Andromeda: A Peptide Search Engine Integrated into the MaxQuant Environment. *J. Proteome Res.* **10**, 1794–1805 (2011).

325. Nolte, H., MacVicar, T. D., Tellkamp, F. & Krüger, M. Instant Clue: A Software Suite for Interactive Data Visualization and Analysis. *Sci. Rep.* **8**, 12648 (2018).

326. Ashcroft, M., Kubbutat, M. H. G. & Vousden, K. H. Regulation of p53 Function and Stability by Phosphorylation. *Mol. Cell. Biol.* **19**, 1751–1758 (1999).

327. Węsierska-Gądek, J., Schloffer, D., Kotala, V. & Horky, M. Escape of p53 protein from E6-mediated degradation in HeLa cells after cisplatin therapy. *Int. J. Cancer* **101**, 128–136 (2002).

328. Thakur, B. K. *et al.* Inhibition of NAMPT pathway by FK866 activates the function of p53 in HEK293T cells. *Biochem. Biophys. Res. Commun.* **424**, 371–377 (2012).

329. Kawaguchi, T. *et al.* The relationship among p53 oligomer formation, structure and transcriptional activity using a comprehensive missense mutation library. *Oncogene* **24**, 6976–6981 (2005).

330. Yeudall, W. A., Wrighton, K. H. & Deb, S. Mutant p53 in Cell Adhesion and Motility. *P53 Protoc.* 135–146 (2013) doi:10.1007/978-1-62703-236-0_11.

331. Lee, J.-G., Ahn, J.-H., Jin Kim, T., Ho Lee, J. & Choi, J.-H. Mutant p53 promotes ovarian cancer cell adhesion to mesothelial cells via integrin β4 and Akt signals. *Sci. Rep.* **5**, 12642 (2015).

332. Dimri, G. P. *et al.* A biomarker that identifies senescent human cells in culture and in aging skin in vivo. *Proc. Natl. Acad. Sci. U. S. A.* **92**, 9363–9367 (1995).

333. Gu, B. & Zhu, W.-G. Surf the Post-translational Modification Network of p53 Regulation. *Int. J. Biol. Sci.* **8**, 672–684 (2012).

334. Cook, A. & Milner, J. Evidence for allosteric variants of wild-type p53, a tumour suppressor protein. *Br. J. Cancer* **61**, 548–552 (1990).

335. Stephen, C. W. & Lane, D. P. Mutant conformation of p53. Precise epitope mapping using a filamentous phage epitope library. *J. Mol. Biol.* **225**, 577–583 (1992).

336. Cubillos-Rojas, M., Schneider, T., Bartrons, R., Ventura, F. & Rosa, J. L. NEURL4 regulates the transcriptional activity of tumor suppressor protein p53 by modulating its oligomerization. *Oncotarget* **8**, 61824–61836 (2017).

337. Wu, R. T. Y. & Cheng, W.-H. Chapter 21 - Selenium and Senescence: Centering on Genome Maintenance. in *Foods and Dietary Supplements in the Prevention and Treatment of Disease in Older Adults* (ed. Watson, R. R.) 211–229 (Academic Press, 2015). doi:10.1016/B978-0-12-418680-4.00021-X.

338. Appella, E. & Anderson, C. W. Signaling to p53: breaking the posttranslational modification code. *Pathol. Biol. (Paris)* **48**, 227–245 (2000).

339. Meek, D. W. Mechanisms of switching on p53: a role for covalent modification? *Oncogene* **18**, 7666–7675 (1999).

340. DeHart, C. J. *et al.* A multi-modal proteomics strategy for characterizing posttranslational modifications of tumor suppressor p53 reveals many sites but few modified forms. *bioRxiv* 455527 (2018) doi:10.1101/455527.

341. Jones, R. J. *et al.* Inhibition of the p53 E3 Ligase HDM-2 Induces Apoptosis and DNA Damage–Independent p53 Phosphorylation in Mantle Cell Lymphoma. *Clin. Cancer Res.* **14**, 5416–5425 (2008).

342. Kamada, R., Nomura, T., Anderson, C. W. & Sakaguchi, K. Cancer-associated p53 Tetramerization Domain Mutants. *J. Biol. Chem.* **286**, 252–258 (2011).

343. Nichols, N. M. & Matthews, K. S. Human p53 Phosphorylation Mimic, S392E, Increases Nonspecific DNA Affinity and Thermal Stability [†]. *Biochemistry* **41**, 170–178 (2002).

344. Bullock, A. N. *et al.* Thermodynamic stability of wild-type and mutant p53 core domain. *Proc. Natl. Acad. Sci.* **94**, 14338–14342 (1997).

345. Choudhury, S., Kolukula, V. K., Preet, A., Albanese, C. & Avantaggiati, M. L. Dissecting the pathways that destabilize mutant p53. *Cell Cycle* **12**, 1022–1029 (2013).

346. Russo, A. & Russo, G. Ribosomal Proteins Control or Bypass p53 during Nucleolar Stress. *Int. J. Mol. Sci.* **18**, 140 (2017).

347. Xiong, X., Zhao, Y., He, H. & Sun, Y. Ribosomal protein S27-like and S27 interplay with p53-MDM2 axis as a target, a substrate and a regulator. *Oncogene* **30**, 1798–1811 (2011).

348. Atz, J., Wagner, P. & Roemer, K. Function, oligomerization, and conformation of tumor-associated p53 proteins with mutated C-terminus. *J. Cell. Biochem.* **76**, 572–584 (2000).

349. Rollenhagen, C. & Chène, P. Characterization of p53 mutants identified in human tumors with a missense mutation in the tetramerization domain. *Int. J. Cancer* **78**, 372–376 (1998).

350. Signaling to p53: Ribosomal Proteins Find Their Way | Elsevier Enhanced Reader. https://reader.elsevier.com/reader/sd/pii/S1535610809003353?token=E675ECC8F4E498B821A28E98C6AD18DE8FBE20C952BA51D364C56767915F256D487871542BAFE82D7D1FF23FF43DF27D&originRegion=eu-west-1&originCreation=20220303100908 doi:10.1016/j.ccr.2009.09.024.

351. Dai, M.-S. & Lu, H. Inhibition of MDM2-mediated p53 Ubiquitination and Degradation by Ribosomal Protein L5 *. *J. Biol. Chem.* **279**, 44475–44482 (2004).

352. Daniely, Y., Dimitrova, D. D. & Borowiec, J. A. Stress-Dependent Nucleolin Mobilization Mediated by p53-Nucleolin Complex Formation. *Mol. Cell. Biol.* **22**, 6014–6022 (2002).

353. Saxena, A., Rorie, C. J., Dimitrova, D., Daniely, Y. & Borowiec, J. A. Nucleolin inhibits Hdm2 by multiple pathways leading to p53 stabilization. *Oncogene* **25**, 7274–7288 (2006).

354. Choi, T. G. *et al.* Cyclophilin B induces chemoresistance by degrading wild-type p53 via interaction with MDM2 in colorectal cancer: Cyclophilin B in CRC chemoresistance. *J. Pathol.* **246**, 115–126 (2018).

355. Peng, Y., Chen, L., Li, C., Lu, W. & Chen, J. Inhibition of MDM2 by hsp90 Contributes to Mutant p53 Stabilization *. *J. Biol. Chem.* **276**, 40583–40590 (2001).

356. Walerych, D. *et al.* Hsp90 chaperones wild-type p53 tumor suppressor protein. *J. Biol. Chem.* **279**, 48836–48845 (2004).

357. Trinidad, A. G. *et al.* Interaction of p53 with the CCT Complex Promotes Protein Folding and Wild-Type p53 Activity. *Mol. Cell* **50**, 805–817 (2013).

358. Monteith, J. p53: The TRiC Is Knowing When to Fold 'Em. 2.

359. Rivlin, N. *et al.* Rescue of embryonic stem cells from cellular transformation by proteomic stabilization of mutant p53 and conversion into WT conformation. *Proc. Natl. Acad. Sci.* (2014) doi:10.1073/pnas.1320428111.

360. Lomax, M. E., Barnes, D. M., Hupp, T. R., Picksley, S. M. & Camplejohn, R. S. Characterization of p53 oligomerization domain mutations isolated from Li–Fraumeni and Li–Fraumeni like family members. *Oncogene* **17**, 643–649 (1998).

361. Dashzeveg, N. & Yoshida, K. Crosstalk between tumor suppressors p53 and PKCδ: Execution of the intrinsic apoptotic pathways. *Cancer Lett.* **377**, 158–163 (2016).

362. Borgo, C. & Ruzzene, M. Role of protein kinase CK2 in antitumor drug resistance. *J. Exp. Clin. Cancer Res.* **38**, 287 (2019).

363. Keller, D. M. & Lu, H. p53 serine 392 phosphorylation increases after UV through induction of the assembly of the CK2.hSPT16.SSRP1 complex. *J. Biol. Chem.* **277**, 50206–50213 (2002).

364. Siddiqui-Jain, A. *et al.* CK2 Inhibitor CX-4945 Suppresses DNA Repair Response Triggered by DNA-Targeted Anticancer Drugs and Augments Efficacy: Mechanistic Rationale for Drug Combination Therapy. *Mol. Cancer Ther.* **11**, 994–1005 (2012).

365. Quotti Tubi, L. *et al.* Inhibition of protein kinase CK2 with the clinical-grade small ATP-competitive compound CX-4945 or by RNA interference unveils its role in acute myeloid leukemia cell survival, p53-dependent apoptosis and daunorubicin-induced cytotoxicity. *J. Hematol. Oncol.J Hematol Oncol* **6**, 78 (2013).

366. Dubois, N. *et al.* Constitutive activation of casein kinase 2 in glioblastomas: Absence of class restriction and broad therapeutic potential. *Int. J. Oncol.* **48**, 2445–2452 (2016).

367. Ravi, R. & Bedi, A. Sensitization of Tumor Cells to Apo2 Ligand/TRAIL-induced Apoptosis by Inhibition of Casein Kinase II. *Cancer Res.* **62**, 4180–4185 (2002).

368. Schuster, N. *et al.* Wild-type p53 inhibits protein kinase CK2 activity. *J. Cell. Biochem.* **81**, 172–183 (2001).

369. Yin, Y., Tainsky, M. A., Bischoff, F. Z., Strong, L. C. & Wahl, G. M. Wild-type p53 restores cell cycle control and inhibits gene amplification in cells with mutant p53 alleles. *Cell* **70**, 937–948 (1992).

370. Lang, G. A. *et al.* Gain of function of a p53 hot spot mutation in a mouse model of Li-Fraumeni syndrome. *Cell* **119**, 861–872 (2004).

371. Terzian, T. *et al.* The inherent instability of mutant p53 is alleviated by Mdm2 or p16INK4a loss. *Genes Dev.* **22**, 1337–1344 (2008).

372. Hampson, P. *et al.* PEP005, a selective small-molecule activator of protein kinase C, has potent antileukemic activity mediated via the delta isoform of PKC. *Blood* **106**, 1362–1368 (2005).

373. Marengo, B. *et al.* Protein Kinase C: An Attractive Target for Cancer Therapy. *Cancers* **3**, 531–567 (2011).

374. Carvajal, D. *et al.* Activation of p53 by MDM2 antagonists can protect proliferating cells from mitotic inhibitors. *Cancer Res.* **65**, 1918–1924 (2005).

375. Kranz, D. & Dobbelstein, M. Nongenotoxic p53 activation protects cells against S-phase-specific chemotherapy. *Cancer Res.* **66**, 10274–10280 (2006).

376. Lane, D. P., Cheok, C. F. & Lain, S. p53-based Cancer Therapy. *Cold Spring Harb. Perspect. Biol.* **2**, a001222 (2010).

377. Luu, Y., Bush, J., Cheung, K.-J. & Li, G. The p53 stabilizing compound CP-31398 induces apoptosis by activating the intrinsic Bax/mitochondrial/caspase-9 pathway. *Exp. Cell Res.* **276**, 214–222 (2002).

378. Wang, W., Takimoto, R., Rastinejad, F. & El-Deiry, W. S. Stabilization of p53 by CP-31398 inhibits ubiquitination without altering phosphorylation at serine 15 or 20 or MDM2 binding. *Mol. Cell. Biol.* **23**, 2171–2181 (2003).

Danksagung

Im Besonderen möchte ich mich bei Herrn Prof. Dr. Lienhard Schmitz für die Möglichkeit bedanken, meine Doktorarbeit in seiner Arbeitsgruppe auf diesem spannenden Thema anfertigen zu dürfen. Vielen Dank für Deine Unterstützung und das kollegiale Miteinander in den letzten Jahren. Dein Vertrauen in mich hat mich zu der selbstbewussten Wissenschaftlerin werden lassen die ich heute bin.

Bei Herrn Prof. Dr. Michael Martin möchte ich mich für eine fantastische Studienzeit bedanken, welche den Grundstein für mein medizinisch-wissenschaftliches Interesse gelegt hat. Auch nach dem Studium haben Sie mich die weiteren Jahre immer unterstützt und standen jederzeit als Ansprechpartner zur Verfügung. Danke für Alles!

Auch bei Frau Prof. Dr. Sandra Hake und Herrn Prof. Dr. Reinhard Dammann möchte ich mich für die Bereitschaft bedanken, mich und meine Arbeit zu prüfen.

Im Laufe dieser Arbeit durfte ich zahlreiche tolle Menschen kennenlernen, deren Freundschaft und wissenschaftliche Expertise die letzten Jahre zu einer sehr schönen Zeit gemacht haben. Thank you Ratnal you were the best colleague I could have wished for. You always motivated and cheered me up. Because of you, I always had the feeling that I wasn't alone. Your friendship means a lot to me and I am sure all of your plans and wishes will come true. Danke Ulli dass du nie eine wissenschaftliche Diskussion gescheut hast und mich jeden Tag daran erinnert hast warum ich diesen Weg eingeschlagen habe. Du hast aus mir eine bessere Wissenschaftlerin und das Labor zu einem zu Hause gemacht. Ich bin froh Dich weiter als Freundin auf Deinem beeindruckenden Weg begleiten zu dürfen. Auch bei Jan und Max möchte ich mich bedanken. Eure Gesellschaft in den letzten Monaten hat mir viel bedeutet. Danke dass Ihr meine schlechte Laune in dieser stressigen Zeit ausgehalten habt und immer wusstet wie Ihr mich aufheitern könnt. Ich wünsche Euch beiden alles Gute für eine private und berufliche Zukunft als Wissenschaftler.

Ich bedanke mich bei meiner Mama dafür, dass sie mir immer den Rücken freihält und unterstützt bei allem was ich tue. Danke Ina für dein Verständnis in den letzten Jahren. Du hast mir immer wieder gezeigt, dass ich mich auf Dich verlassen kann. Danke Paulin für deine Freundschaft und gute Laune die mich so oft aufgemuntert hat.

Danke Alex dafür, dass du immer für mich da bist. Du bist meine größte Unterstützung und mein Ruhepol. Ohne die Sicherheit die Du mir gibst, wäre ich heute nicht da wo ich jetzt bin.